Performance evaluation in indoor sport climbing

Politecnico di Torino
Master of Science Course in Biomedical Engineering

Supervisors:
Prof. Daniela Maffiodo
Prof. Raffaella Sesana

Candidate:
Matteo Donno

24 March 2020

Abstract

Performance evaluation in indoor sport climbing

Sport climbing has shown an exponential growth in popularity in recent years which lead to the scientific community interest. This is has been confirmed and accentuated by the discipline introduction in the next 2020 Tokyo Olympic Games program.

Researcher attention was focused on scientific parameters examination that can objectively explain the climbing ability, which unquestionably depends on training status.

A great parameters number was investigated but, in order to achieve previous goal, development and implementation of devices able to detect interest physical entities was necessary.

The entire thesis work conducted was feasible thanks to an "intelligent" indoor climbing wall equipped whit three holds able to measure forces exchanged in space by the climber.
It was subdivided in a first phase of literature searching about conducted studies focusing on those concerning analysis of indexes able to explain climbing performance evaluation.
Later, after a wall calibration step, we moved on to the practical phase of data collection during which two subjects performed a standardized exercise.
Then, matlab scripts were implemented to actually calculate indexes founded during first phase. Specifically: *Hausdorff dimension* as force signal entropy estimation, *smoothness factor* in order to distinguish an efficient climbing style from an inefficient one, and *friction coefficient* to evaluate each force component trend in space.
Finally, a GUI (Graphical User Interface) able to visualize data recorded for each holds, was implemented using Python object-oriented language.

A mamma e papà,
per i loro immensi sacrifici.

Contents

List of Figures

List of Tables

Chapter 1

Introduction

An introduction about sport climbing will be conducted n this first chapter, explaining specific terms and basic concepts in such a way as to present this discipline to those who do not yet know it and who want to appreciate it, given the growing interest in world of sports.
The discipline history will be illustrated, starting from the birth and coming to the diffusion and the development.
The federations and committees that regulate the discipline and the competitions worldwide will be appointed with a particular reference to the debut of sport climbing in the next olympic games.
Furthermore, the characteristics and identifying aspects about the various disciplines in which this sport activity can be divided and the relative classification scales will be illustrated.

1.1 History

The large popularity during the last decades, in which an explosive growth about both indoor and outdoor climbing celebrity was observed, could let think that this sport, in both its variants, has its birth more than a hundred years ago. Before being performed even in indoor mode, climbing discipline was executed in outdoor locations only. Its large-scale turning point in its nowadays concept coincides with the late 1800s when, starting from mountaineering, alpinists began to climb rock as a new technique to improve their training method [1].

But, the first ever documented mission concerning a rock climbing in a concept very close to the current one dates back at 1492 [2]. This is the first noted technical ascent of a mountain and it was carried out by Antoine de Ville on June, 26 of that year. With the use of ladder and ropes and the help of a dozen men he reached the summit of Mont Aiguille (fig 1.1) where they remained for six days. After that epic shipping, the ascent was repeated again in 1834. Three century later, specifically on 8 August 1786, the Mont Blanc ascent, led by Michael Gabriel Paccard and Jacques Balmat, sets the foundation to modern rock climbing, which will began to spread widely a century later [3].

Figure 1.1: View of Mont Aiguille.

During the following two centuries, mountaineering and rock climbing continued to be increasingly popular, especially in Europe, although the goal of the epoc's climbers was still to reach the summit and not to focus on climbing the rocky walls. The change in the concept of climbing came to an end at the end of the 1800s, when mountaineering effectively broke, giving rise to the discipline of rock climbing. The growing interest of researchers increasingly engaged in the development of safer and more effective equipment has made climbing a real sport in the early 1900s.The birth can therefore be geolocated in Europe, but following the spread in the United States, the practice has acquired enormous interest all over the world, clearly distinguishing itself from mountaineering.

The 50s of 1900 represent the moment of outdoor discipline maximum diffusion. Hence the need for practice discipline in an indoor locations. In fact, during the

1960s the first indoor climbing wall was installed at the Ullswater School (fig 1.2), definitively changing this sport. However, this installation offered an experience too distant from what climbers actually lived in nature. To overcome this limitation, a new concept of wall was produced in 1964. This was equipped with extrusions that made it possible to simulate climbing in nature more faithfully. This new concept has paved the way for the commercialization of interior walls which has further increased the interest and the spread of the discipline. Although in this same period the climbing had a moment of high diffusion and of enormous interest in the American sporting community, it is only in 1987 that the indoor climbing walls were exported to the United States from Europe.

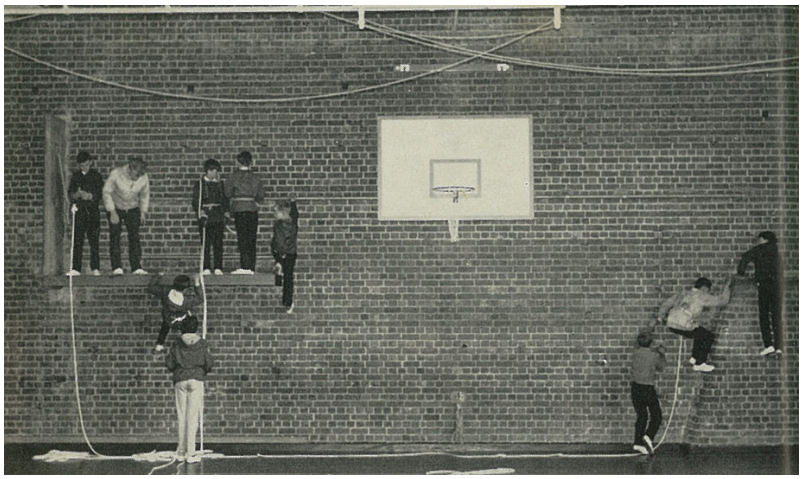

Figure 1.2: First climbing wall at Ullswater school.

Those years can be considered as the starting point for sport climbing. Indeed, 1985 represent the year of the first sport rock climbing competition in history held in Bardonecchia and named "Sportroccia", which has been performed outdoor on rock and not on artificial walls. That was the first of the countless competitions, performed on natural rocks firstly and on artificial wall later, that were subsequently held in different parts of the world, up to the present day when we expect the debut of sport climbing as an Olympic discipline in the 2020 Tokyo Olympics.

1.2 Sport Climbing

1.2.1 Technical Definitions and Statistics

After having outlined the history of sport climbing, a quick overview of some technical definitions, involving outdoor and indoor disciplines, is now introduced. According to definition reported on F.A.S.I. (Federazione Arrampicata Sportiva Italiana) web site [4]: "Sport Climbing is defined as natural climbing (i.e. without the aid of artificial means managed for progression) for competitive, amateur and physical education purposes, carried out both on natural or artificial walls along routes controlled by the base, and on suitably equipped blocks". In general the physical effort made in climbing is discontinuous and requires good maximum strength and resistance to stress, besides agility. These are the fundamental characteristics for an efficient sport climber. The goal of sports climbers is to overcome routes

with increasing difficulty, with the help of special but contained equipment such as: climbing harnesses for belayer and climber, quickdraws, a dynamic rope and a belay device. Furthermore, climbing shoes and chalk bag are costumary used even if not necessary.

As reported by statistical evaluation the number of athletes attracted by discipline are constantly increasing. Climber community is a large and fast growing worlwide group: 44.5 million people are climbing regularly and in the last 10 years, since its foundation, the number of IFSC Member Federations has increased by 25%. In 2019 are 2160 the professional sport climbing athletes licensed all over the word. They come from all the five continents and represent 65 countries. Confirming this large number also the number of worldwide event during the 2019: 21 world competitions they were held around the world, one which about paraclimbing. This area has also developed in a parallel manner allowing disabled athletes to try their hand at climbing. For the last Paraclimb World Championship held in France, 158 was the athletes enrolled and they represent 24 countries with an increase of 24% about the number of partecipants from the 2018 edition [5].

1.2.2 Disciplines

Climbing competitions on artifical walls are regulated, directed, developed and promoted by the International Federation of Sport Climbing (IFSC) with headquarters located in Turin and recognized by the International Olympic Committee (IOC). Three was the different categories in which sport climbing was divided until its introduction in Olympic game: lead, bouldering and speed. To those is added the Olympic combined, specially created for the 2020 Tokyo Olympic Game.

Figure 1.3: IFSC Logo.

Lead Climbing

The specialty of difficulty, commonly called lead, consists in carrying out a climb on ways that gradually increase in difficulty until reaching levels of difficulty at the limit of human abilities.

Shall take place on walls at least 15 meters long and the goal is to reach the highest possible point of the track in the maximum time of 6 minutes. When the competitor no longer has body parts resting on the ground, the time counting starts.

The classification during the competitions is drawn up on the basis of the last hold taken. During the climb the athletes must pass the rope inside the protection points, fast opening carabiners, respecting the progressive order in which they are placed and without skipping any. To determine the rankings, the last hold on which the climber managed to maintain a stable position is considered valid. The sockets counted are only those made with the hands [6].

Figure 1.4: IFSC Lead World Cup.

Each socket is assigned a progressive score and has 2 values: "controlled" if it is gripped; "used" if after gripping, a movement is started which does not allow the next hold to be reached. The maximum score is to insert the rope in the last safety carabiner (the "TOP") or to arrive with both hands in the last grip if the safety rope is used from above. In this case, a "TOP" ranking is assigned to the competitor. It is the first discipline of sports climbing and is inspired by the stairs on a cliff in a natural environment [7].

Bouldering

The specialty called bouldering consists in climbing on low routes, which are maximum 5 meters long, of different difficulty without the use of a harness. The athlete safety is ensured by mattresses placed on the ground. It requires a short but at maximum intensity effort and involves a limited series of movements, that on average are 7/8.

The competition starts with all 4 limbs resting on obligatory "starting holds" for both hands and both feet which shall not include blank or unbounded parts of the Climbing Surface. The Starting Holds should not be marked with specific positions for the hands. Proceedeth on the "Zone hold", selected by the Route-Setter on every boulder for scoring purposes and have to culminates with a "Top" which can be a marked hold ("Top hold"), that must be held by the athlete in order to demonstrate his own stability, or a standing position over the boulder top.

Every athlete has an unlimited number of attempts for reaching the "top" in a given time period which is generally 4 or 5 minutes. Moreover, if an athlete can't reach the "Top" position, but manages to reaches an intermediate outlet called "zone", an additional score is assigned to him/her [6]. Ranking is based, in descending order, on the number of: completed boulders, zone points gained, attempts to complete boulders and attempts to get zone points.

It originates from Bouldering, or climbing on large boulders.

Figure 1.5: IFSC Bouldering World Cup.

Speed Climbing

The speed specialty, commonly known as speed, consists in completing a route in the shortest possible time. Climbing wall where competition can be held was approved in 2007 by the IFSC. It is a 15 metres height long wall with standardized inclination and a sockets layout validate by the IFSC and identical all over the world.

The competition route is equipped with a timing system that allows athletes to stop time. The route is climbed with a rope from the top, with the help of "automatic insurers", so that the athlete can concentrate only on the ascent time.

All competitions start with a sound signal and follow a common starting protocol. After that each competitor have to take position with one foot and both hands on their preferred starting holds and one foot on the starting pad.In order to complete the route contestants have to struck the timing pad with their hand and in this way stop the timer located on the top .

After a qualifying round, in which the best time is considered in two attempts, the best 16 compete in knockout tests as long as the four athletes remain who will compete for the Podium.

Olympic Combined

As previously mentioned, sport climbing will debut in 2020 Tokyo Olympic game. For the entry of this discipline the IOC has decided to assign only one medal and the IFSC, in order not to discriminate any of the three official disciplines, has introduced the Olympic combination in which each athlete will have to test himself/herself in each of the three disciplines. In order, athlete starts with speed climbing, proceeds with bouldering and closes with lead climbing. For the first one a couple of climbers challenge their self on a 15 meters height long wall with the same fixed route. For the boulder, competitor has to climb fixed routes within a fixed time and on four metres height walls. In the last step, athlete have to reach the higher as possible height on a 15 metres height wall and in a pre-established time interval. The final result will be a combination about the three competitions scores [8].

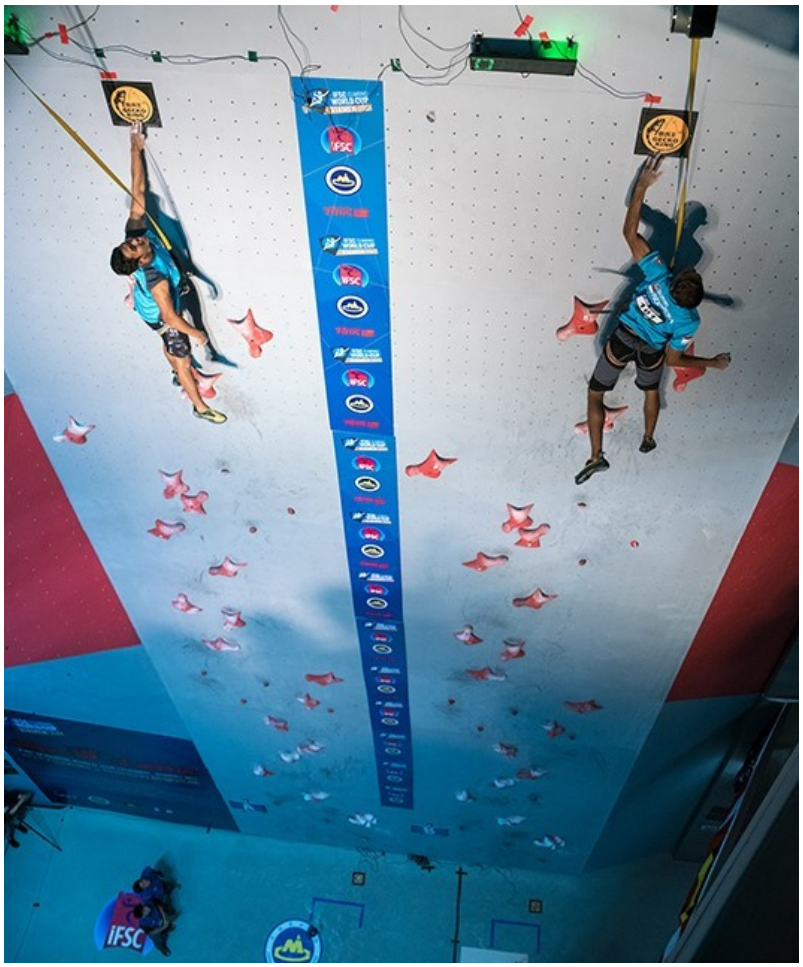

Figure 1.6: IFSC Speed World Cup.

1.3 Grading Scale

There are different measurement scales to classify the difficulty of a climbing route and this is due to a parallel origin of sport in different areas of the world. The assignment of a level to a given climb path is a process that can be defined as being subjective. The classification of a not yet executed route is carried out by the first athlete who performs it and is eventually reviewed by the subsequent climbers who perform it. The classification systems, besides being different in the various geographical areas, are clearly distinguished between the different disciplines. They are divided into the group related to sport climbing and the one related specifically to bouldering, whether they are practiced on rock or on an artificial wall.

1.3.1 Sport Climbing Grades

The five main grading systems for free climbing will now be reported and a table of mutual comparison will be showed.

French Numerical Grades

The French system is the climbing specific one. It turns out to be the most widely used among European countries and in International competitions outer USA. It is

an open ended system and consists of an up to three digits code: the first one is a number starting from 1, the second one is a letter (*a,b* or *c*) which divides each numerical level in four sub-levels and an optional "+" may be added for differentiate the difficulty even more (e.g.: 4c+) [9].

UIAA

The UIAA system is used among Italian, French and Italian climbers. It is an open ended scale and use ascending order Roman symbols to classify difficult route combined with the sign "+" or "-" to more differentiate difficulty degree (e.g.: III+) [10].

Yosemite Decimal System

This grading system is adopted in the United States, where was introduced in 1937. An YDS grade is made up of 3 segment symbol (e.g.: 5.13b). The first number is referred to "Class" and suggests the route technical difficulty: 1 to 4 stand for walks of increasing difficulty and slope while 5 concerned to a rock wall climbing. The class 5 routes are vertical path and required ropes to perform the climbing. Only the fifth class is broken up into sub-classes which are marked by the code second number.Starting from 5.10 and going on, an other partition is made adding the *a,b,c* or *d* letters [11].

British

The UK system is made up of two subsystem: an adjective grade and a technical grade. The first communicates the climb general difficulty degree. It is an open system and in present-days it goes from Easy to E11 ("Extremely Severe"). Along the way, and in ascending order, are Moderate (M), Difficult (D), Hard Diff (HD), Very Difficult (VD), Hard Very Difficult (HVD), Severe (S), Hard Severe (HS), Very Severe (VS), Hard Very Severe (HVS). The Extremely Severe grade is splitting into sub-grades numerated from 1 to 11.
The technical grade indicates the complexity level of the most critical move that can be found during the execution of the path and used numbers and letters as the French system [12].

Ewbank Grading System

The Australian Climbing Grading System is the most clear and intuitive of all. It was created by John Ewbank in 1960s. It only adopts Arabic number starting from 1. It is used in Australia and New Zealand and adopted in South Africa, although little variations [13].

Comparison Table

From what is stated in the previous paragraphs, all the climbing classification systems are not limited above. However, the following table is limited to the hardest route ever climbed. It is located in Flatanger, Norway and is called "*Silence*". It is the only route in the word classificated as 9c in French Scale and it was completed by Adam Ondra in September 3, 2017.

UIAA	French	YDS	British		Australian
			Tech.	*Adj.*	
I	1	3-4	1	M	1-2
		5.0			3-4
II	2	5.1	2		5-6
		5.2		D	7-8
III	3	5.3	3		8-9
IV	4a	5.4		VD	10-11
IV+	4b	5.5	4a	S	11-12
V	4c	5.6	4b	HS	13
V+	5a	5.7	4c	VS	14-15
VI-	5b	5.8		HVS	15-16
VI	5c	5.9	5a		17
VI+	6a	5.10a		E1	18
VII-	6a+	5.10b	5b		19
VII	6b	5.10c		E2	20
VII+	6b+	5.10d	5c		
		5.11a		E3	21
VIII-	6c	5.11b			22
	6c+	5.11c	6a	E4	23
VIII	7a	5.11d			24
VIII+	7a+	5.12a		E5	25
	7b	5.12b			26
IX-	7b+	5.12c	6b	E6	27
IX	7c	5.12d			28
IX+	7c+	5.13a		E7	29
	8a	5.13b	6c		
X-	8a+	5.13c		E8	30
X	8b	5.13d		E9	31
X+	8b+	5.14a	7a	E10	32
	8c	5.14b			33
XI-	8c+	5.14c	7b	E11	34
XI-	9a	5.14d			35
XI+	9a+	5.15a			36
XI+/XIII-	9b	5.15b			37
XIII-	9b+	5.15c			38
XIII	9c	5.15d			

Table 1.1: Comparison of the most common free climbing grading systems [14].

1.3.2 Bouldering Grades

The routes related to the boulder discipline are classified according to different grading systems from those analyzed above and these also differ between the different geographical areas. The two most common systems in bouldering will be explained below.

V-Scale

The V-Scale was created in the 1980s in Texas by boulderer John Sherman, whose nickname was "Verm" or "Vernim" and hence the scale name. It has spread throughout the United States, where it currently appears to be the bouldering reference scale along with the rest of North America. It is an open-ended scale and the difficulty level grows up with the increasing trend of the numbering. It starts at V0 and now reach the maximum level of V17. There is also an additional level VB (where "B" stands for "beginner") below the V0 level. The classification is further subdivided with the addition of the "+" or "-" symbols but only for the low levels scale [15].

Font Grades

The Fontainebleau Scale is the reference scale in the Bouldering European world. The complexity degree increases as the number increases. It is also a scale with no upper limit. It starts at level 0 even if, actually, there are no levels below level 3. Beginning from level 6 suffixes ("A","B" or "C") are added to classify even more detail [16].

Comparison Table

In the table shown on the following page a comparison between the previous two boulder climbing grades will be conducted. Even for boulder field all the grading systems are opened-end but the table is restricted to the two hardest boulder problems: "*Burden of Dreams*" made by Nalle Hukkataival in October 2016 marking it as the first V17 boulder and "*No Kpote Only*" executed by Charles Albert in December 2018 [17].

Fontainebleau	Hueco
3	VB
4-	V0-
4	V0
4+	V0+
5	V1
5+	V2
6A	V3
6A+	
6B	V4
6B+	
6C	V5
6C+	
7A	V6
7A+	V7
7B	V8
7B+	
7C	V9
7C+	V10
8A	V11
8A+	V12
8B	V13
8B+	V14
8C	V15
8C+	V16
9A	V17

Table 1.2: Comparison of the most common Bouldering grading systems [14].

Chapter 2

Human body in sport climbing

The chapter is intended as a report with the aim to illustrate the state of the art concerning sport rock climbing studies. It starts with a research conducted with the aim of better understand rock climbing biomechanics with a focus on static equilibrium process related to climber's adaptation to external disturbance. It continues examining discipline physiological bases with a particular regard to high level performers and their energy expenditure in indoor and outdoor sport climbing. Furthermore, some relevant results concerning hormonal changes on performance influence are explained. The following subchapter conducts a medical examination and highlights particular critical issues related to discipline, especially showing the critical influence of some grip techniques on finger tendons and pulleys. Chapter ends with a quick and short explanation about performance evaluations proposed and about new technological climbing walls developed in order to better understand and mining some discipline scientific conclusions.

2.1 Biomechanical analysis

Sport rock climbing is characterized by an upright movement and by the upper body predominance role that distinguish it from all the other land-based sporting practices. To understand and analyze its biomechanical aspects it is indispensable studying forces exchanged between athlete and hold because they are indicative of the performed activity. In this way, among the many searches that can be performed, the climber's adaptation to external perturbations can be understood.

The climber balance at rest on a wall is allowed by the horizontal supporting forces. If an intentional hold release occurs, an unequal distribution among vertical and horizontal forces arise: both increase on the controlateral holds while on the ipsilateral hold the horizontal one tends to zero and the vertical one remains constant. These changes represent the voluntary release starter point in order to counterbalance the resulted perturbations[18].

These conclusions were carried out analyzing reaction forces exchanged between a climber in quadrupedal position and compared to the values recorded in tripedal static equilibrium. For the study an elementary climbing wall with four holds, one for left hand (LH), one for right hand (RH), one for left foot (LF) and one for right foot (RF), were adopted. A device representation is shown in figure 2.1.

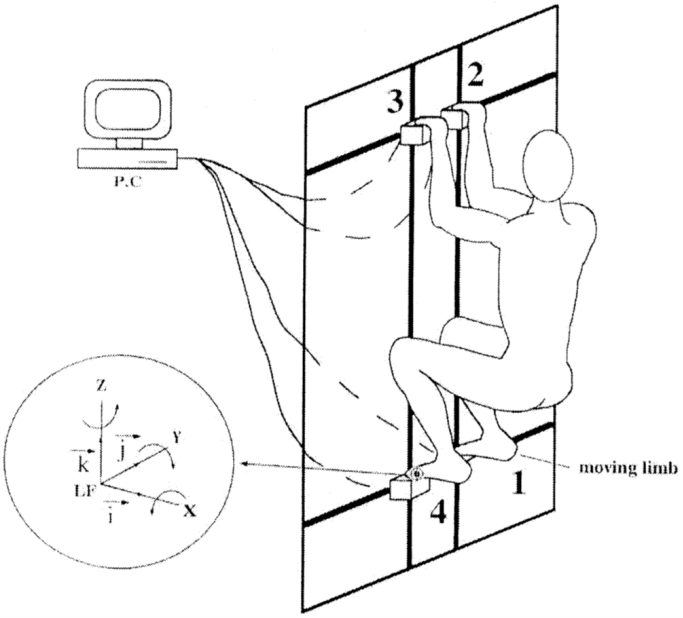

Figure 2.1: Experimental device. Each support is equipped with strain and gauges (3-D). The three components of the force applied to each hold are recorded with respect to the reference system (LF, i, j, k) [18].

Measuring procedures started by placing hold "2" and hold "3" at equal climber shoulders distance and adapting upper and lower holds positions while the subject stands with his arms and his thighs horizontal. In order to standardize the initial forces distribution on the four holds, the climber body weight must be shared equally among holds. When a quarter of body weight was checked on each hold, an audio alarm advises the correct positioning. At that moment, the subject was asked which grip to release keeping the respective limb 2 cm above the hold. Following this, audio alarm stops and subject was on a tripedal position. Lastly, subject were asked to

perform five right foot and five left hand movement in a random sequence, in order to prevent movement prediction and adaptation.

What distinguishes climbing is forearm and finger muscles overuse and therefore the higher force level generated from a climber's hand when compared to a non climber one. No differences between elite and beginner climbers were observed in terms of generated forces but firsts seems to have a more proportional distribution between right and left hand with respect to non climber subjects [19].

During the quadrupedal starting stance, the RH hold recorded a positive horizontal force on the lateral axis and negative on the antero-posterior axis. The RF hold registered an horizontal reaction opposite to the RH one. The same relations were found between LH and LF. Climber weight was equal to vertical reaction forces summation upon the four holds.

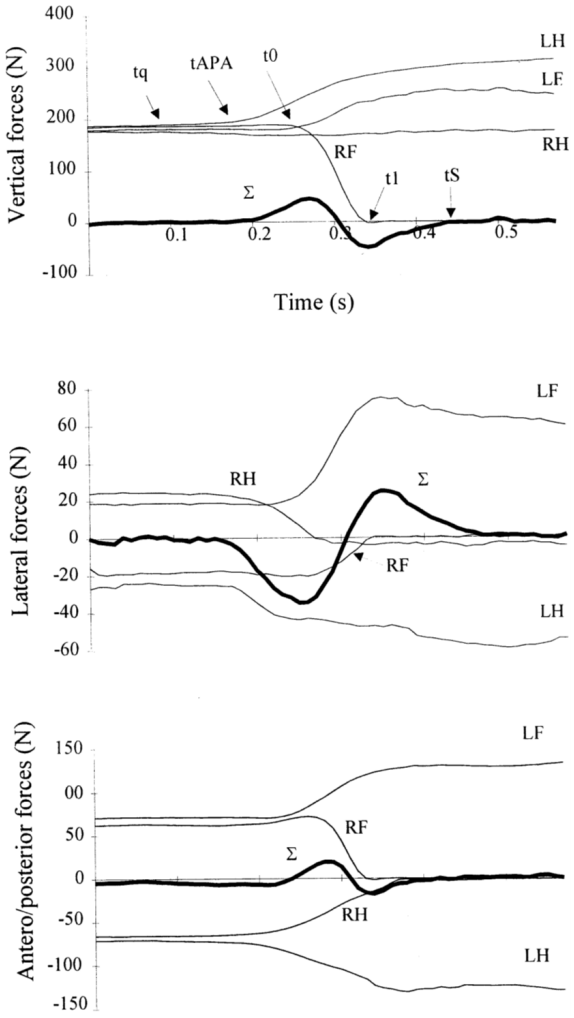

Figure 2.2: Forces variations for one trial. tQ, tAPA, t0, t1 and tS are respectively the time of quadrupedal stabilization, of first force change, the onset of right foot release, the time of take-off and the time of tripedal stabilization [18].

The quadrupedal to tripedal step was marked by force variations on each axes as shown in figure 2.2. A changing in resultant force was observed after the the release starter point (t0) without statistical differences between the axes. Each force variation preceded the beginning of the coluntary RF release because each latency was negative. It emerges that the force changes observed at LH occurred

statistically previously than the force changes observed at LF and RH. No statistical difference was observed between the latencies at LF and RH. During the tripedal state, horizontal and vertical forces on LH and LF show a marked increase. Non significant variation was observed on the RH vertical force but a reduction until zero on the horizontal forces.

2.1.1 Counter-movements features in sport climbing

Sport climbing tasks necessitate specific movement with the aim to balance the center of gravity of the whole body against the route and to decrease muscle fatigue. One of the basic movements is counter-movement: a basic task of moving such that the lower extremity is in the opposite side than direction of movement, counterbalancing the upper extremity reaching. Movement differences between expert and beginner climbers were evaluated analyzing nine expert climbers with at least one year of experience compared to nine beginner climber with less than 5 ascent. The motion tasks include, besides counter movement actually, its previous and next phase as represented in figure 2.3. In detail:

- Phase 1: Moment before left foot leaves
- Phase 2: Moment before left hand detachment from hold
- Phase 3: Left hand grips next hold
- Phase 4: Right hand away from hold
- Phase 5: Right hand grips next hold

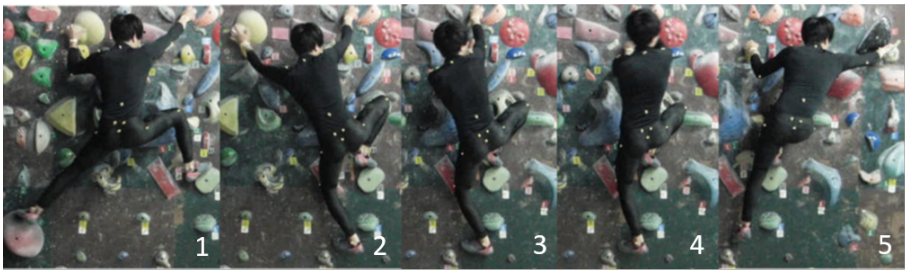

Figure 2.3: Motion task execution [20].

In order to analyze the movement a marker-based motion tracking system was used. Markers were placed on the middle of the dorsal wrist, on the posterior superior iliac spine, end portion of the rib, both acromion and olecranon sides, greater trochanter, femoral lateral epicondyle, lateral malleolus. Finally three markers were put on C7, L3 and S2 vertebrae. In the next phase the angles of flexion between the marked body segments and involved in the movement were worked out.

The study detailed objective was to analyze and to compare various joint angles of interests between the two groups. A substantial difference in the first execution phase was found during which expert climber demonstrates a right shoulder greater flexion and a right elbow and right knee smaller flexions. Furthermore, a right side trunk higher flexion characterized the group. On the fourth phase, expert climber group was marked by a right elbow less smaller flexion and by a right hip higher

flexion and abduction. Lastly, a right elbow enhanced flexion was observed on the climbers group. Regarding horizontal movement width , it was sharply wider in expert group compared to beginner. From the research conducted and the results obtained it has been shown that expert climbers efficiently use lower limbs and trunk in order to implements an upper limbs overload reduction strategy targets [20].

2.1.2 Slope inclination and climbing skill effects on vertical force loading

Among studies conducted, physiological responses and involved forces trends were evaluated at different wall slope in order to analyze vertical load variation and its influence on climbing ability. Five beginner (5.4 - 5.7 on YDS, table 1.1) and six intermediate (5.10b - 5.12a on YDS, table 1.1) climbers have carried out a climbing path on a 7.2 meters high wall with three different slope conditions: 85°, 90° and 98°. Vertical reaction force detection was made by an insole data acquisition, while a spiroergometer for cardiopulmonary exercise testing was adopted to measure minute ventilation, oxygen uptake and carbon dioxide production. Heart rate was checked by an heart rate monitor. Conclusions show that no relevant difference were identified among subjects with different age within and across the two climber groups. Even these investigations come to conclude that beginner climber exercise a lower vertical load on holds used by foot with compared with expert climber and, as a consequence, the first ones show an enhanced physiological response with respect to the second ones. Consequently a good climb in terms of efficiency and energy optimization is characterized by a stronger use of lower limbs that lead to a physiological response lowering. This last lowering was a constant in every study wall slopes. Besides, a lesser heart rate and energy cost is synonyms of a stronger vertical load. During the descent phase, vertical force on holds grasped by foot has proved to be lower than the ascent phase for all the three wall inclination. Force-time integral results to be less on 98° condition and greater on 85° condition [21].

2.2 Physiology of sport rock climbing

Rock climbing physiological aspects are totally different from those with which other sports are characterized. From a muscular viewpoint, forearm represents the most solicited muscle because of its high and discontinuous isometric contractions. Practice execution requests the whole body aerobic strategies use. As difficulty rise, a great heart rate increase and a blood lactate production occur related to oxygen use [22]. This different trend between oxygen consumption and heart rate can be explained by muscle metaboreflex [1], responsible for stimulating chemical afferents thanks to repetitive static contractions. An other clarification can be a supporting reason to this difference: the climber, during ascent, is forced to keep his upper limbs over his heart position for most of the time and this is associated with an heart rate increase. Furthermore, anxiety about falling can explain an heart rhythm rise.

[1] Muscle metaboreflex elicits a sympathetically mediated pressor response consisting of increased heart rate, ventricular performance, central blood volume mobilisation and cardiac output, vasoconstriction in renal and inactive skeletal muscle vasculatures, and increased systemic arterial pressure [23]

2.2.1 Performance analysis in high level climbing

During the lasts three decades, researchers wondered if a standard about climber anthropometric features can be establish. The primary idea about a climber is made by a mesomorph and stately body size, but it is totally replaced by studies conducted. Effectively, a great height allows a wider elongation but carries out to biomechanical disadvantages: an higher body weight needs surely a stronger force to keep holds contact. Last three decades researching concludes that a climber is an individual with:

- small stature and low FM (Fat mass);
- high upper body strength to body weight ratio;
- low sums of skinfolds;
- high handgrip to mass ratio.

These conclusions were formulated from Watts et al., who conducted the last bigger study with 90 subjects [24]. For a more detailed idea take a look to table in figure 2.4.

Table 2 Means (SD) for selected anthropometric variables of the sample

Variable	Controls (n=45)	Climbers (n=90)	Male climbers (n=52)	Female climbers (n=38)
Height (cm)	167.1 (14.0)	158.5 (15.2)*	162.2 (15.6)	151.3 (11.9)
Height percentile	79.3 (25.3)	50.0 (28.7)*	44.8 (26.0)	54.4 (31.3)
Mass (kg)	54.1 (15.0)	47.8 (13.4)*	51.5 (13.6)	40.6 (9.6)
Mass percentile	57.8 (25.6)	39.4 (23.5)*	40.8 (23.6)	39.8 (24.6)
Height/mass ratio	3.28 (0.78)	3.51 (0.74)†	3.33 (0.73)	3.86 (0.64)
BMI	19.0 (3.2)	18.6 (2.3)	19.1 (2.2)	17.5 (2.1)
BMI percentile	38.7 (29.7)	32.7 (21.5)	36.9 (21.3)	29.2 (21.6)
Ape index	0.95 (0.15)	1.01 (0.02)*	1.02 (0.02)	1.01 (0.02)
Biliocrist/biacrom ratio	0.74 (0.05)	0.86 (0.08)*	0.87 (0.08)	0.86 (0.08)
Σ7 skinfolds (mm)	76.7 (33.4)	50.4 (14.5)*	45.3 (13.0)	56.0 (14.5)
Σ9 skinfolds (mm)	101.3 (45.2)	66.5 (20.5)*	59.3 (19.2)	74.3 (19.6)
%Fat Jackson-Pollock	11.3 (6.6)	7.8 (4.4)*	4.4 (2.2)	12.2 (2.6)
%Fat Slaughter	18.7 (6.9)	13.0 (3.7)*	11.0 (2.8)	15.9 (2.9)
Forearm volume (ml)	824.7 (266.6)	828.8 (370.1)	903.9 (254.8)	671.7 (190.6)
Forearm+hand volume (ml)	1148.9 (426.8)	1116.4 (344.9)	1234.4 (326.8)	902.0 (235.3)
Average HG (kg)	30.7 (13.4)	32.8 (12.8)	36.5 (12.9)	25.1 (6.8)
HG/mass ratio	0.55 (0.13)	0.67 (0.12)*	0.70 (0.13)	0.62 (0.08)

*Significantly different from controls ($p<0.01$).
†Significantly different from controls ($p<0.05$).
BMI, Body mass index; HG, handgrip.

Figure 2.4: Mean and standard deviations for the analysis variables [24]

An other research brench concerns aerobic power analyzing and monitoring. The maximum aerobic power (VO_2MAX) is equivalent to the maximum amount of oxygen that can be used in the unit of time by an individual, during a physical activity. This is the maximal intensity a subject can tolerate for about ten minutes. Studies reveal a VO_2 averages between 20 and 30 $ml*kg^{-1}*min^{-1}$ during climbing. These values are close to 10 $kcal*min^{-1}$ in terms of energy expenditure [25].

Blood lactate levels were examined, founding that its increasing trend during a climbing performance is due to hand-grip resistance decreasing and it is not due to hand-grip force reduction [19]. Data, collects from blood samples of climbing competitors within 1 minute of a world competition, reports a BL (Blood lactate) mean concentration of 6.7(1.1) $mmol*l^{-1}$ for a 13.2(4.9)m long path ascent executed in 4.2(1.8) min [26]. Such low values cames out from the small muscle mass portion use for the climbing practice, contrary to the high muscle mass used in other disciplines.

2.2.2 Change on hormonal, cardiovascular, neuromuscular, sleep and fatigue status and their influence on performance [27]

The referring study aim is to investigate some hormonal trends with the purpose of detect, in sport climber, an overreaching condition characterized by a T/C [2] and HR-S-L [3] reduction and by a d-cortisol increasing [28].

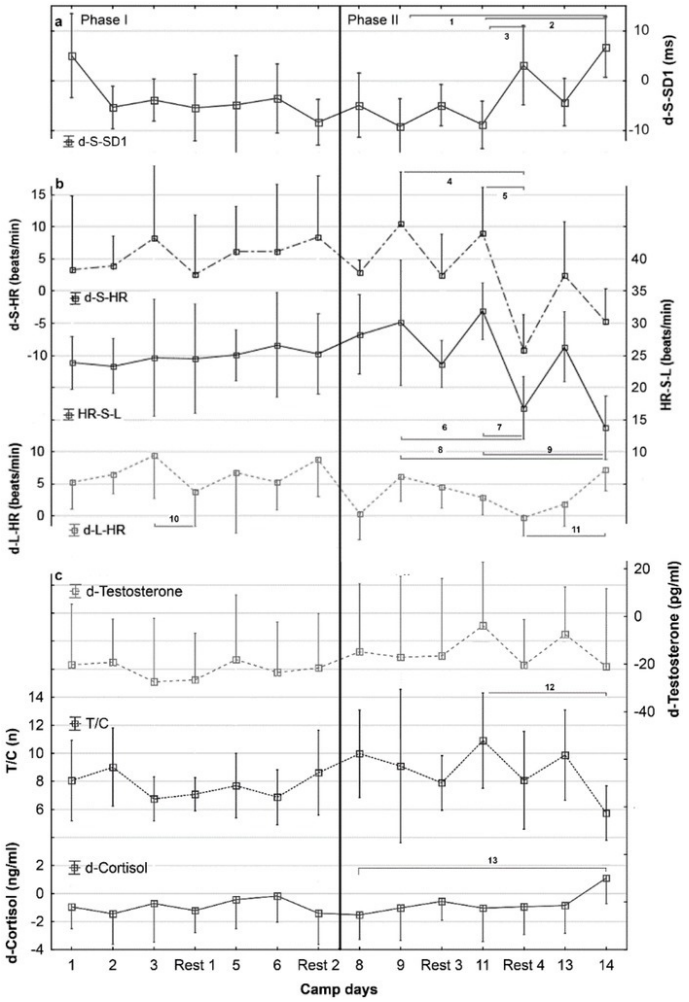

Figure 2.5: Study variables trends. [27]

The two weeks evaluation period was composed by 4 rest days and 10 climbing days, with increasing difficulty ascent path. It was subdivided into phase I (firsts 7 days) and phase II (seconds 7 days) and every participant performed a number of climb approximately equal to 50.

During the first period, a supine heart rate (L-HR) positive growth combined with a parasympathetic activation (dL-SD1) reduction and a cortisol and testosterone decrease were observed. Excluding cortisol, these variations weren't observed during second period. The morning fatigue experienced in the second phase of the investigation caused a sharp drop in T/C and HR-SL (figure 2.5.

[2] T/C: testosterone/cortisone ratio

[3] HR-S-L: difference in S-HR (standing position heart rate) and L-HR (supine position heart rate).

Furthermore, there was a positive correlation between d-cortisol and difficulty and this is in support of the conclusion formulated by Papacosta and Nassis [29], according to which physical activity that exceeds maximum aerobic power by 60% or that lasts at least 20-30 minutes determines a significant change in the salivary concentration of cortisol. The latter turns out to be the main protagonist of catabolic processes.

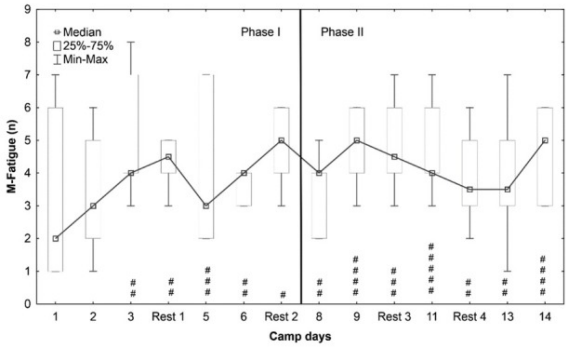

(a) Muscular fatigue.

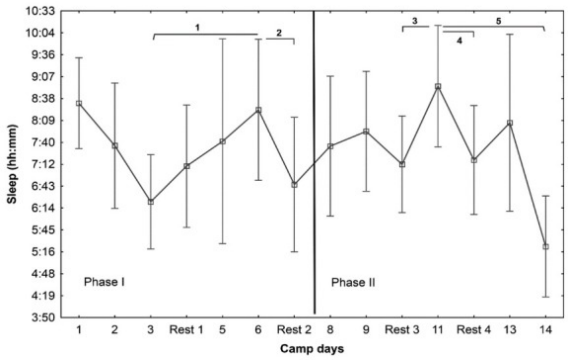

(b) Sleep duration time.

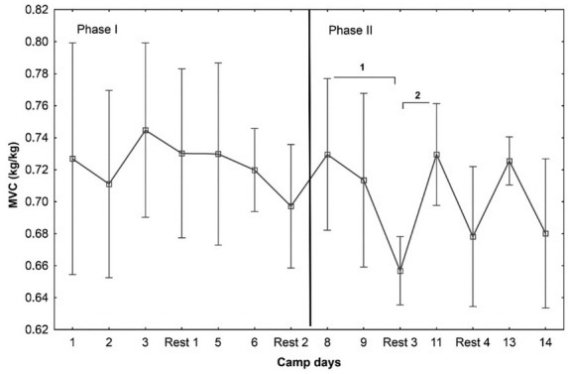

(c) Maximal hand grip strength.

Figure 2.6: Investigation parameters changes subdivided in the two study phases [27].

The study shows a prevalence of the catabolic process following the increase in muscle fatigue (figure 2.6a) combined with a reduction in the T/C ratio. A negative correlation was found between sleep duration and average difficulty (figure 2.6b) and between d-cortisol and sleep. Nonetheless, the authors came to the conclusion that a longer sleep duration was due to a more dynamic secretion of cortisol, that is, to an increase in the secretion of cortisol in the 30 minutes following awakening. This is because the measurements on the athletes were made daily immediately after their

awakening. Finally, a negative correlation was found between HR-S-L and difficulty and this appears to be in contrast with research carried out previously, according to which higher levels of performance would have with lower HR-SL, L-HR and SHR [30]. The large increase in the concentration of cortisol and the drastic reduction in T / C on the last day of the camp confirms the entry of climbers into a state of overreaching.

2.2.3 Energy cost evaluation

Returning to analyze and evaluate aspects related to energy metabolism, the data obtained by evaluating the energy expenditure associated with the execution of the practice in an indoor and outdoor condition are reported in current chapter.

The indoor study reveals, from the regression model performed, a linear increase in both heart rate and VO_2 with climbing velocity, as reported in figure 2.7a .

The outdoor study output is illustrated in figure 2.7b. It is clear that the outdoor practice needed a considerably high oxygen consumption and that heart rate trend reaches immediately a plateau during time. The great energetic expenditure, despite of small muscle groups involved, it can be clarified by the upper limbs isometric contraction widely extended over time [31]. Moreover, because of this isometric contraction highly repeated over time, a blood lactate rise occurs and, consequently, an anaerobic energy contribution predominance.

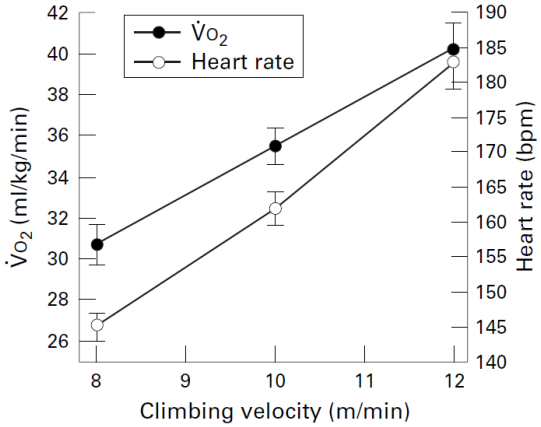

(a) Indoor execution [31].

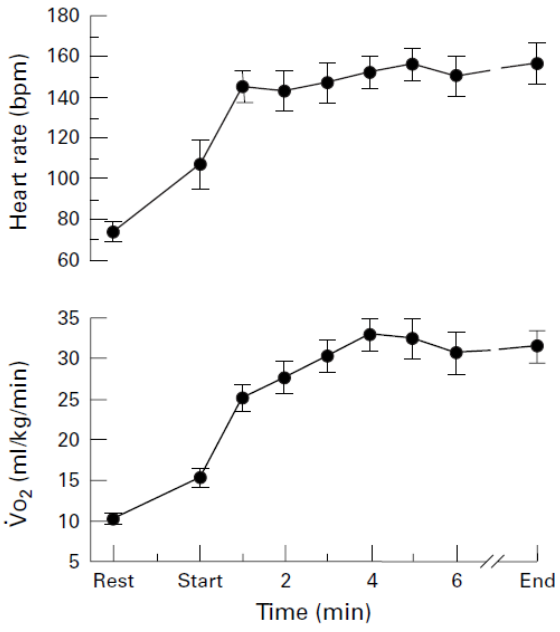

(b) Outdoor execution [31].

Bertuzzi and Franchini, on their studies, confirm that aerobic and anaerobic alactac systems represent the two most energetic system used during sport climbing [32]. Besides, their study supports that an upper body power, training and path difficult are irrelevant on energy sistems. The data are shown in the figure 2.8 in confirmation of the above.

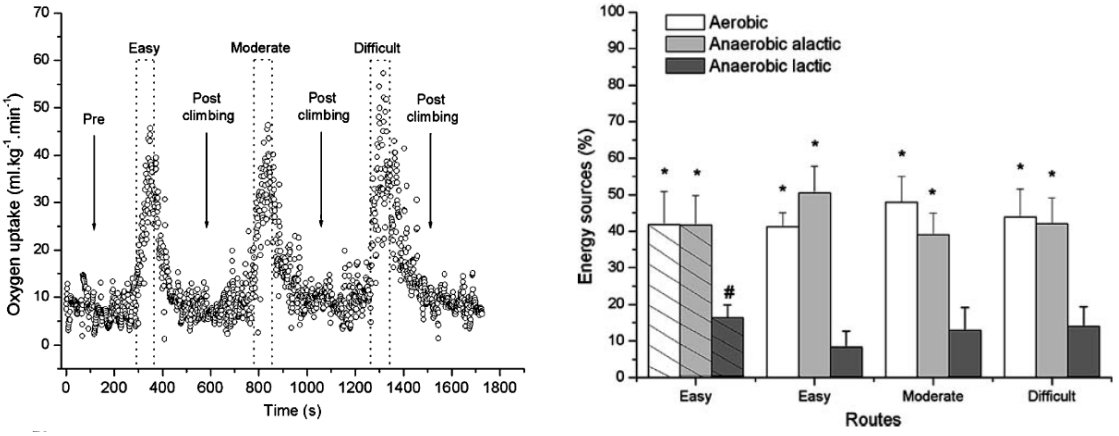

Figure 2.8: Oxygen uptake and energy system comparison among different difficult levels. Adapted from [32].

2.2.4 Forearm muscle oxygenation

The lasts research concerning climbing performance evaluation [33], contrarily to those reported in previous subchapter (2.2.3), which goals were to characterized anaerobic and aerobic metabolism, aims to study forearms hemodynamic since they represent the dominant muscles used in climbing.

Using near-infrared spectroscopy, oxygenation trend was monitored on preponderance arm FDP (Flexor digitorum profundus). Exactly device location on forearm was setted according to guided lines proposed by Schweizer and Hudek [34], as different muscle sections has distinct deoxygenation reactions. Tissue saturation index (TSI) was computed following equation 2.1 and oxydative capacity index was established as TSI half-time (O_2HTR). Saturation time interval was 5 minutes long and was settled starting from 3-5 minutes after a brachial artery occlusion.

$$TSI = \left(\frac{O_2HB}{O_2HB + HHB} \right) * 100 \tag{2.1}$$

Where:

- O_2HB stands for oxyhemoglobin concentration;
- HHB stands for deoxyhemoglobin.

It was confirmed, as suggest Fryer et al [35], that FDP endurance is related to its oxidative capacity, i. e. its oxygen expenditure optimization. In fact, oxydative capacity index can be used as sport climbers training measure because of its improvement is associated with a red-point ability level [4] [33], as shown on figure2.9.

[4]Red-point ability level corresponds to the highest performance grade achieved with physical practice. While on-sight ability level stands for highest performance without prior physical practice.

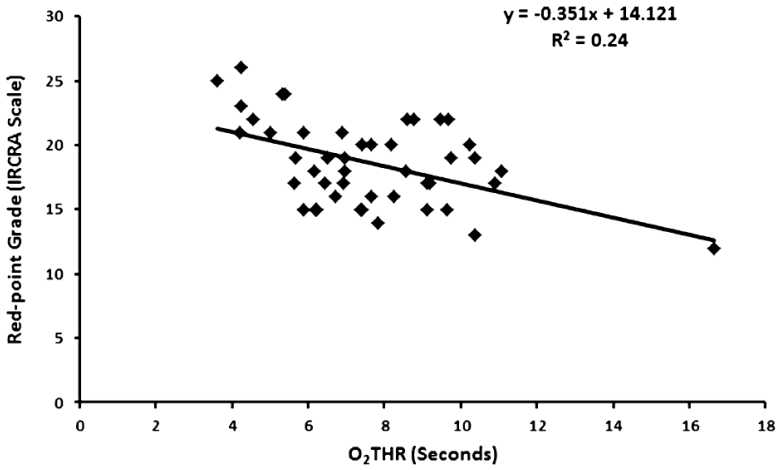

Figure 2.9: Regression line [33]. IRCRA stands for International Rock Climbing Research Association grade scale

2.3 Sport climbing from a medical viewpoint

This chapter contains some analyzes and some statistics related to medical aspects and accidents connected to climbing world. Contrary to traditional rock climbing and mountaineering, which are particularly dangerous practices because of the potential rock falls or abscence of falling protection, sport climbing and boulder are not as risky as commonly thinked. Accident rates has been estimated as 0.079 episodes on 1000 indoor performing hours, 0.2 episodes on 1000 sport climbing hours, 0.6 episodes on 1000 mountaineering hours and 4.2 accidents on 1000 rock climbing hours. These numbers turn out to be wider low compared to motorcycling (13.5 episodes within 1000 practice hours) and football (31 episodes within 1000 practice hours) [36].

Concerning sport climbing, shoulder results the human body segment most subjected to injury. The same goes for bouldering, where finger and shoulder are the most interested. The lower limbs injuries are more probably usual in traditional climbing, if performed with low quality equipment.

Because of crimp grip position (figure 2.10.a), which corresponds to the most adopted grip in 90% of case, damages on finger tendons and pulleys are the most common and they are explained on the next subchapter.

Now damages related to grip situation, shows in figure 2.10.b, will be described. The indicated situation involves the total load over just a finger while the other ones are completely unloaded and inflected over the hand palm. As a consequence tendons of flexor digitorum profundus [5] assume an unnatural conformation which involves their shift each other in different directions. This arrangement can carrys out to muscle strains.

Let's now analyze any accidents deriving from a crimp grip of the type shown in the figure 2.10.d. In this situation, the fingers appear to assume warped positions which, although they may be harmless in normal conditions, can provoke harmful consequences in the case of feet adherence loss. In this case, in fact, fractures, joint

[5]Flexor digitorum profundus muscle is located in the forearm and with its action it flexes the distal and proximal interphalangeal joints from the second to the fifth finger and intervenes in the adduction of the index, ring and little fingers and in the flexion of the wrist.

dislocations or ligaments lacerations may occur due to the sudden torsional forces to which fingers are subjected.

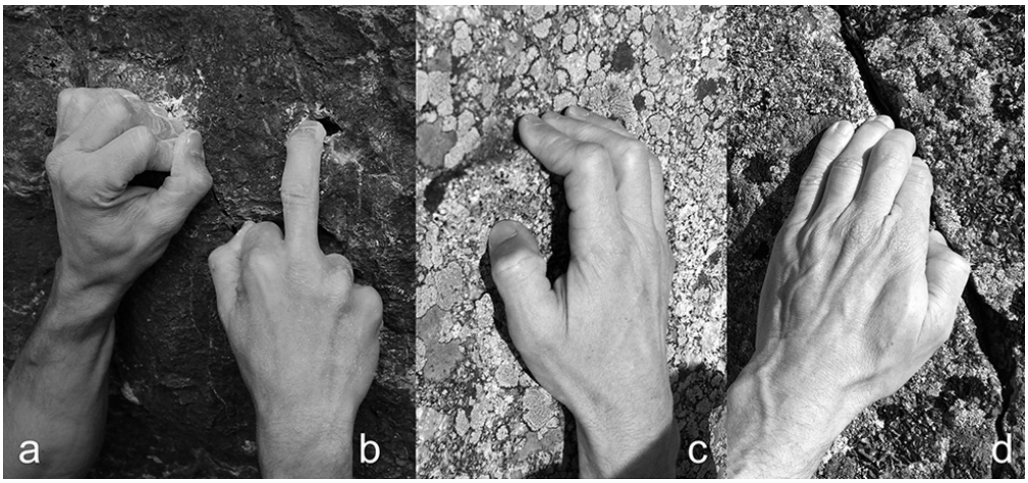

Figure 2.10: Main crimp techniques [36].

As the popularity of sport progressed, questions were raised about the possibility that discipline practice could be correlated with the onset of degenerative arthritis. Analyzing a sample group, consisting of 31 climbers with an average age of 20 years and with a maximum climbing difficulty level equal to X on the UIAA scale (table 1.1), it was found the presence of osteophytes with an incidence equal to 84% in the PIP[6] joints and equal to 68% in the DIP[7] joints. They were more pronunced observing later radiography images, contrarily to an antero-posterior view. Moreover, 19% of subjects show marked osteoarthritis evidence, compared with a same age non climbing subjects group [37]. Since the sport scientific community interests on sport climbing are relatively recent, practice long-term effects are not well known. However some common guidelines were proposed as suggestion to prevent long-term damage: DIP joints should be flexed at 5° - 15° and PIP joints should not be flexed at angles greater than 80° - 90°, because of 85° represents the maximum bending torque produced.

Neurological analysis reveal nerve compression diseases like carpal tunnel syndrome or radial tunnel syndrome, that induce to wrist and finger extensors weakness. In addition to the symptoms deriving from previous pathologies that generate also elbow disturbances, epitrocleitis and epicondylitis affect climbers.

A further muscle group frequently subjected to trauma while climbing is that of the shoulder. In this regard, the greatest incidence pathology is the lesion of the rotator cuff or subacromial bursitis due to a biceps affected by tendinitis.

In addition to the previously reported muscle groups, for which climbing tends to generate damage and injuries, the positive influence that climbing generates on the back lumbar section of the back is to be reported. In fact, a great number of physiotherapists adopt moderate climbing paths to treat low back pain, improve position and strengthen trunk muscles.

[6]PIP: Proximal inter-phalangeal joint.
[7]DIP: Distal inter-phalangeal joint.

2.3.1 Grip techniques impact on finger tendons and pulleys

As previously mentioned, the damage concerning the flexor tendon is the most common among climbers. This is a consequence of traditional crimp technique, reported on figure 2.10.a. This gripping technique consists by a PIP joint angle greater than 90° and by a DIP joint hyperextension. This leads to an overload of the pulleys of the sheath of the flexor tendon which is approximately equal to 3-4 times the load to which the fingertip is subjected. The finger most frequently affected by this pathology is the ring finger, while A2 is the pulley most involved [38]. In figure 2.11 a finger pulley system representation is shown.

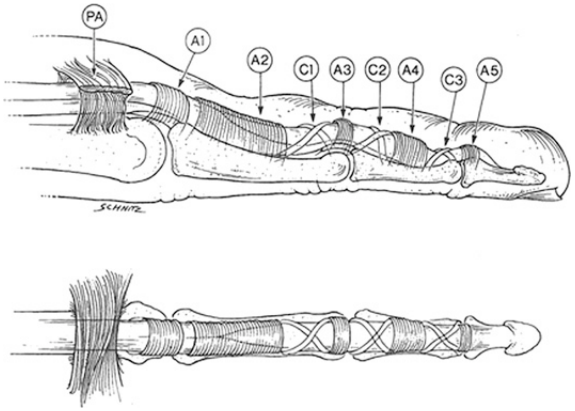

Figure 2.11: Finger annular and crusader pulleys system.

The crimp technique was tested and monitored at different angles (figure 2.12) of the PIP joint. The crimp technique was tested and monitored at different angles of the PIP joint. A variation of the vertical forces was detected in the three conditions studied and it emerged that they are lower at low angles and greater at large angles [39]. It can be deduced that the adoption of one of the illustrated techniques depends solely on an fingers interaction optimization and not on biomechanical aspects. A different positioning of the forearm is also noted. In the situation shown in figure 2.12.a, the hand is arranged vertically with a consequent greater extension of the wrist in order to optimize the contact between fingers and grip. In the grip shown in figure 2.12.c both the hand and the forearm are more inclined and therefore the wrist is more stable. This leads to greater ease for the climber to maintain the body position.

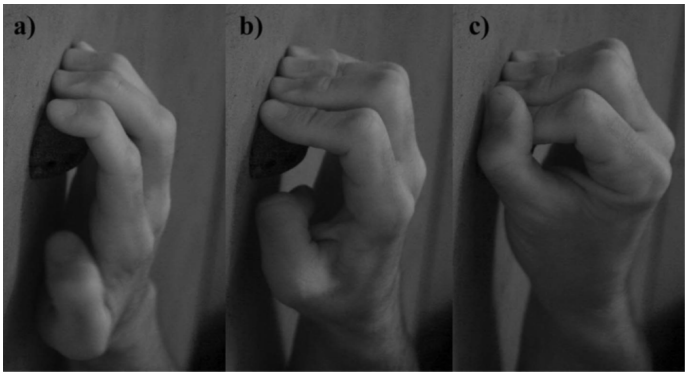

Figure 2.12: Crimp technique studied [39].

2.4 Sport climbing performance evaluations

The huge popularity that sport climbing has achieved during the last year turned this practice from a recreational one to a competitive one, so much so that it will be debut on 2020 Tokyo Olympic games as previously described in 1.2.2. This transition was follow by proper scientific researches in order to find physical or practice principles correlated to climber performance evaluation as well discover and understand which factors may be critical on performance efficiency. In this context this thesis work and all the innovative climbing walls developed are representing a step beyond. The lasts, through "smart" holds able to withdraw and record exchanged forces between athlete and socket, represents the starter point to perform and carrying on these kind of researches.

2.4.1 Parameters identification for performance analysis

Researches related to identification of factors affecting performance represent a growing field, because of the discipline recent large diffusion. It emerges that a good climbing movement background, risk management as well as a good physical preparation and a well climbing route planning represent some of crucial parameters. Efficiency, actually, depends by a combination of climber anthropometric features and those related to path itself [40]. Effort management was a highly interconnected feature with the climbing strategy development. What differentiates the success of a high-level climbing route is the automatic processing of decisions and strategies to be applied by the climber. So a good repertoire of moves to perform, which is intrinsically associated with a good level of strength, would seem to be the winning key to a good performance. It has been deduced that the route preview allows athletes to select path crucial points in order to preserve energy and have a good chance of success.Studies in this direction are only at an early stage and there are many aspects and details to be investigated.

2.4.2 Jerk estimation as motion fluidity

Among all researches taken during the lasts few decades a great number of devices were used. The majority of these were carried out adopting complex instruments, therefore not suitable for all climbers level. On the contrary, thanks to a light ear wearable device (figure 2.13) based on BSN [8] with 3 accelerometers (one for each axis), a better climbing performance was monitored.

Figure 2.13: e-AR device [41]

[8] A BDS (Body Sensor Network) is made up of small devices which, placed on the human body, can provide information on the health of the person, on his way of moving and interacting with the environment

Since an efficient and successful climbing performance is characterized by an high motion fluidity and by a great application force smoothness, an exhaustive index useful in good performance evaluation is jerk (or jolt). It is defined as the third derivative of the position and estimates the motion fluidity [41]. So, a good and successful climbing style is marked by low jerk values. Moreover, on a route repeated subsequently, an increasing jerk is synonymous of physical fatigue as shown in figure 2.14.

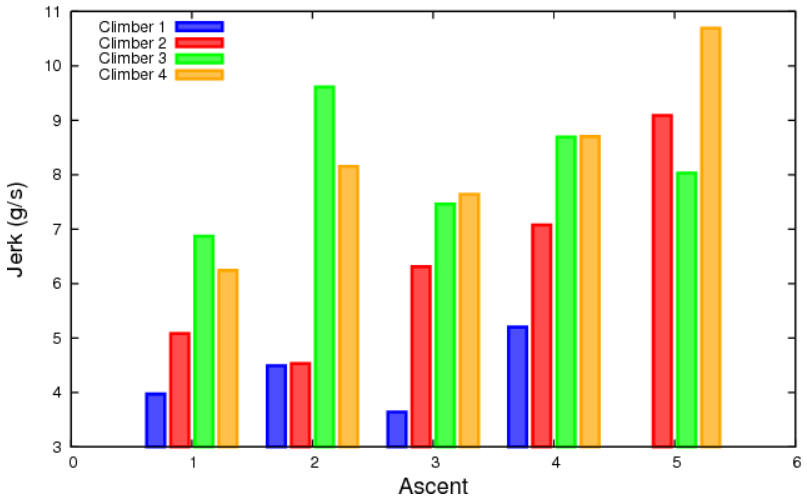

Figure 2.14: Average jerk estimated on the same ascent performed 5 times [41].

2.4.3 Geometric path entropy

Thanks to the use of strain gauges it is possible to detect forces exchanged between athlete and hold in space. After calculating resulting force, dividing it by the gravity acceleration, it is possible to obtain the acceleration to which the climber is subjected. The latter, integrated two times, allows to calculate the athlete characteristic position vector.

Alternatively, trajectory of the climber's center of mass can be calculated using a marker-based monitoring systems. Once known, its geometric disorder can be estimated. A calculation model about it has been proposed and it is useful for assessing the route geometric entropy and it could be adopted in a future step of current study, provided that an acceleration accurate integration is obtained and therefore an highly precise calculation of the climber COM trajectory. A concept graphic representation is shown in figure 2.15 and can be calculated using the following formula [42]:

$$H = ln\left(\frac{2 * LP}{c}\right) \tag{2.2}$$

Where:

- LP corresponds to the actual length of trajectory traveled by the center of mass;
- c corresponds to the perimeter of the convex hull that encloses LP.

This parameter is a performance efficiency indication. In particular, the greater this value, the less efficient the athlete will be in climbing. Therefore a quality climber is the one who reduces this index to a minimum.

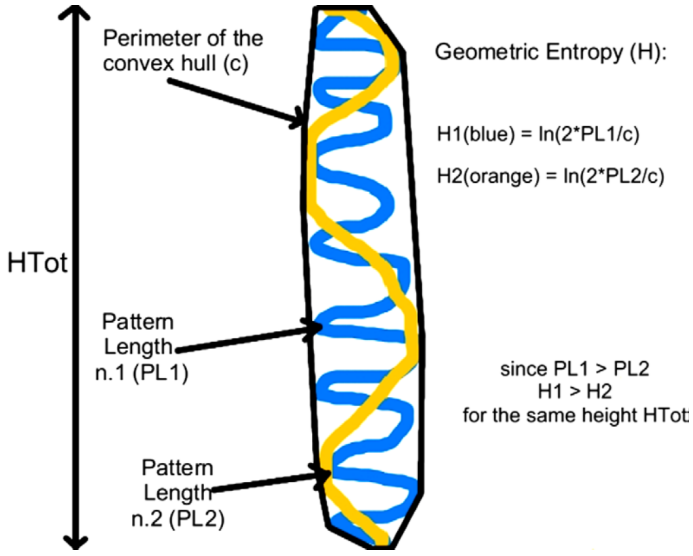

Figure 2.15: Entropy concept graphic explanation [42].

Another aspect can be assessed by calculating the proposed index. It can be considered a path learning factor: if a climber repeats the same ascent path this index should show a decreasing trend as a synonym of learning. It also allows to distinguish between [43]:

1. Agility dominant climber: low acceleration and force levels with predominance of equilibrium control, hence lower entropy;

2. Force dominant climber: high acceleration and force levels, thus greater entropy.

2.4.4 Force signal chaos estimation

Forces detected can be used to measure geometric complexity of force in time signal, thus to perform an entropy estimation. This was proposed by Fuss and Niegl [44] [45], whom in their studies defined features for describing an efficient climbing style and which are reported below:

- Short contact time: greater is the time the climber grabs a hold, first he reaches a muscular fatigue status;

- Small force: bigger is the force exerted, first muscle get tired;

- High smoothness value: an expert climber grasps the grip with low values of jerks, holds and releases the hold gradually.

The researchers adopted *Hausdorff Dimension* as signal entropy measure because it results to be a good summary in order to identify an efficient climbing style, collapsing all the previous features into just one control variable. The *Hausdorff dimension* increases with contact time and force applied and decreases with

smoothness, as a result small values correspond to an efficient climbing style. The referring studies compute Hausdorff dimension on scatter plot reporting the vertical component of the force on abscissa and total force on ordinate (figure 2.16).

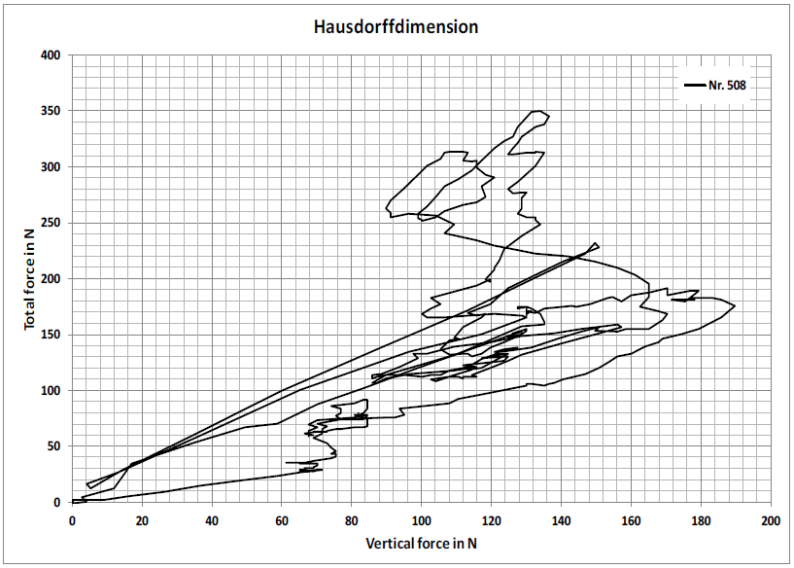

Figure 2.16: Scatter plot [45]

Hausdorff dimension was calculated by the *Box counting method*, particularly with the following reported formula:

$$D = \lim_{R \to 0} \frac{logN}{logR} \tag{2.3}$$

Where N is the number of boxes of size R to cover completely the graph. With reference to the figure reffig: HD, a box corresponds to a tiny single square on reference grid.

In the researchers first analysis [44], it was proposed to normalised it to the mean resultant force of each hold, with the aim of evaluate the single hold performance and difficulty, and to the average of the mean forces of total holds, in view of a mean performance and difficulty estimation. Higher normalised values in beginner climbers than expert ones have been obtained and a clear distinction between feet and hands holds has been observed: the first ones were smaller than second ones. The latter can be explained as the resultant force applied by the foot is commonly stronger than those applied by hands. Hence, considering "D" of a similar order between feet and hands holds, dividing it for an higher resultant force value, it results a smaller normalised value.

2.4.5 Smoothnesss Factor

Since an efficient climbing style is distinguished by a grasp of the grip as smooth as possible, the force-time signal was compared to a parabolic curve of the same impulse which approximates an ideal application force and which equation is reported below:

$$F_{\mathrm{t}} = \left[\frac{t}{T} - \left(\frac{t}{T} \right)^2 \right] \left(\frac{6J}{T} \right) \tag{2.4}$$

Where:

- T is the contact time;
- J is the impulse of the actual force-time signal.

The absolute difference (c curve on figure 2.17) between original force-time signal (a curve on figure 2.17) and parabolic curve (b curve on figure 2.17) were computed and its mean value was determined (d constant straight line on figure 2.17).

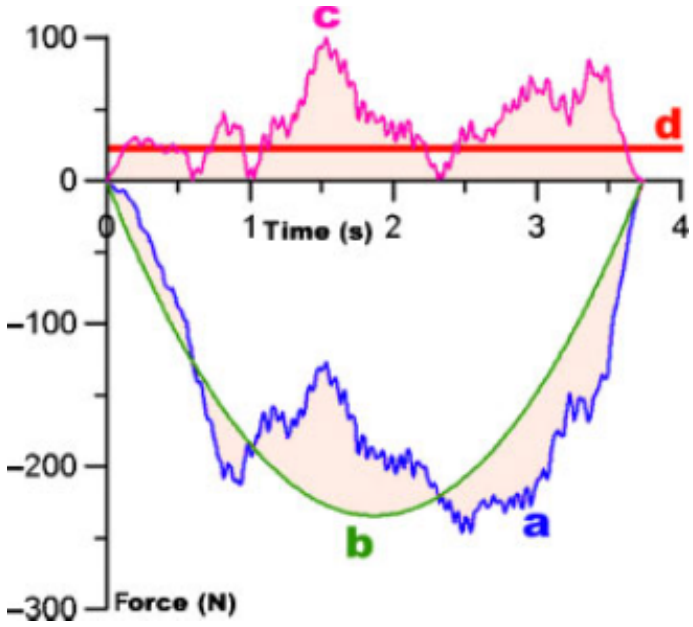

Figure 2.17: Smoothness factor steps calculation [45].

Finally, the smoother factor was estimated dividing climber body weight by the mean of the absolute difference between original signal and parabolic curve.

It is explicit that the larger smoothness factor, the smoother the force application. Thus, expert climber has elevated smoothness factor.

2.4.6 Friction Coefficient

Knowledge of the three components of force in space leads to calculate a parameter called *Friction coefficient* [45]. It is defined as the tangential force normalized to normal force and it is equivalent to an estimate of forces trends in two directions: one useful for performing ascent, i.e. tangential to the climbing wall, contrarily to the normal one, which is on the orthogonal direction to the climbing wall. It results that an efficient climbing style has high friction coefficient values.

In addition, the more away the body centre of mass is from the climbing wall, the more friction force is required at the hands. The more weight is moved from the upper limbs to the feet, the smaller is the friction force at the hands and the closer is the climber to the point of impending slippage. An expert climber has the friction coefficient close to the point of impending slippage [46].

Chapter 3

Sensorized wall

The following pages goal is to present and describe testing wall adopted for the present study.
In the introductory section, the various devices that have been used by the different research groups are quickly reported and then we focus on tested wall which are equiped with holds patented following MACLoC patent [47]: a sensorized grip device for sport climbing equipped with triaxial force sensor, developed and patented in partenership between "Politecnico di Torino" and "Politecnico di Milano".
In order to reach the chapter objective, a theoretical description of the physical principles that regulate the operation of devices capable of measuring a force is first made.
The individual components that make up these devices are then analyzed and explained to then describe what is called the intelligent socket that corresponds to the main protagonist and without which the analyzes conducted would not have been possible.
Finally, the structure of the wall used is described and the hardware and software components that allow to obtain the file on which the measurements are recorded are illustrated without going into too much detail.

3.1 Introduction

A large number of devices typologies and a vast amount of physical quantities have been tested over the years search for in order to quantify climbing from a scientific viewpoint and lay the foundation for any research. Every researching branch and apparatus adopted have advantages and limitations. Throughout recent study years some preexisting systems, which were before employed in different application fields, were used and some new instruments were developed combining different technologies and physical concepts existing yet.

Marker-based motion capture systems represent, for example, an efficient measurement system since allow to record and accurately detect the human body center of mass, by contrast to a force measuring hold where it must be extrapolating from a force measurement. This calculation, in fact, could generate inaccurate kinematic quantities estimations. By the contrast, a motion system is limited as regards the extension of the monitored wall because a great number of cameras are necessary to cover a climber path over an high climbing wall and consequently a great economic expenditure derives. To remedy this problem systems endowed of a single camera in motion with athlete are been developed. Who knows if in the future follow-me drones typology, used in current time by surfer, would be adopted for these purposes.

IMU (Inertial measurement unit) sensors were also used because of their lightweighted and their high wearable features, in addition to directly measuring a kinematic quantity. They are extremely useful in outdoor climbing or in any case where a wide extension has to be covered, but they have highly difficult calibration processes and sophisticated algorithms for noise removal.

Specific devices have also been used to collect surface EMG signal at the level of the muscle groups most commonly used in climbing, i.e. by applying the electrodes on the forearms, but they are not very suitable systems since they hinder the movement of the athletes.

In some cases, however, it is necessary to evaluate and measure forces that athlete exchanges with the wall during his climbing route. To this end, it was thought to create intelligent holds for indoor climbing walls, able to extract forces exchanged by the athlete in space. They represent an optimum solution able to a successful biomechanical analysis with the advantage of being low-cost and sufficiently accurate. The device used in this thesis work is of this type [47].

Furthermore, the possibility of creating a system consisting by the combination of a motion tracking system and a force measurement one has been demonstrated and they were implemented [48].

3.2 Force measurement

From a theoretical point of view, force measurement is permitted by a load cell: device able to convert a force into an electric signal that can be quantified. It is composed by a metallic spring element on which sensing elements are apposed.

Most of the time, metallic body material is aluminium or steel. They are highly strong and this could be in opposition with elasticity concept but they are capable of deforming, even if with small extensions, and returning to assume the initial conformation.

Strain gauges represent the sensor side of the structure. They are electric conductor arranged in a zigzag pattern inside a film, which elongation and shortening cause a resistance variations and a following voltage modification on the relative conditioning circuit (figure 3.4). Once measured, the latter is able to trace a force measure.

3.2.1 Smart hold

In the following section the patented hold [47] functioning will be explained. In this way an application example of the load cell theoretical concept will be shown. Thus, will be face up to basic idea and a more detailed explanation of patented device layout in order to better understand the components of which this smart hold is composed, as well as the composition of adopted materials.

Configuration and structure

Basically, the core idea behind the device is to allocate force transducer directly on hold frame. This has been achieved by using a metallic hollow component, on which hold is connected, instead of being directly connected to the wall by a screw. By this way, previous cited metallic element becomes the device support with sensing capabilities.

It should be underlined that the device has been developed in order to use any common indoor climbing hold on the market. This is further confirmation of the not excessive cost.

To understand and try to have a schematic overview of the above, the figure 3.1 shows a section of the hold anchored on the wall.

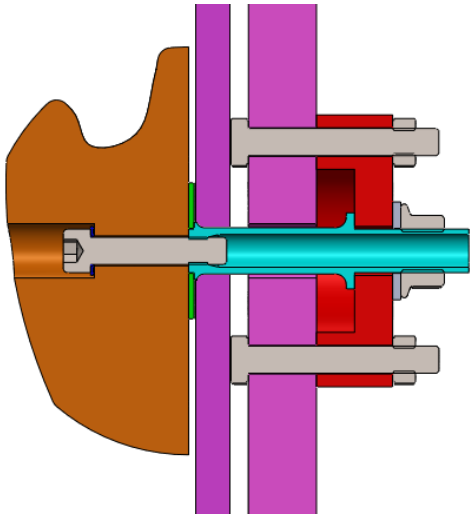

Figure 3.1: Sectioned device illustration [49].

The socket exploded view is also shown below (figure 3.2) in order to illustrate, in greater detail, every single element.

Referring to the figure 3.2, elements are:

- a supporting disc (1): it has 6 holes that allow to constraints the device to the climbing wall rear layer (3) through the use of M10 screws (9) e the respective M10 nuts (10);

- a metallic hollow element (2): it provides mechanical support when climber clings to the handle and generate forces. On this elements are placed the transducers for the forces measurement, whose positioning is described in previous sections (sections 3.2.4 and 3.2.5). This element act as a beam and its extremities are threaded for securing it to the climbing hold (5) and to the supporting disc (1);
- a washer (4);
- a climbing wall front layer (6);
- a lock nut (12): screwed on one end of the beam element (2) by a washer (8) interposition , it locks all the components;
- a common climbing hold (5).

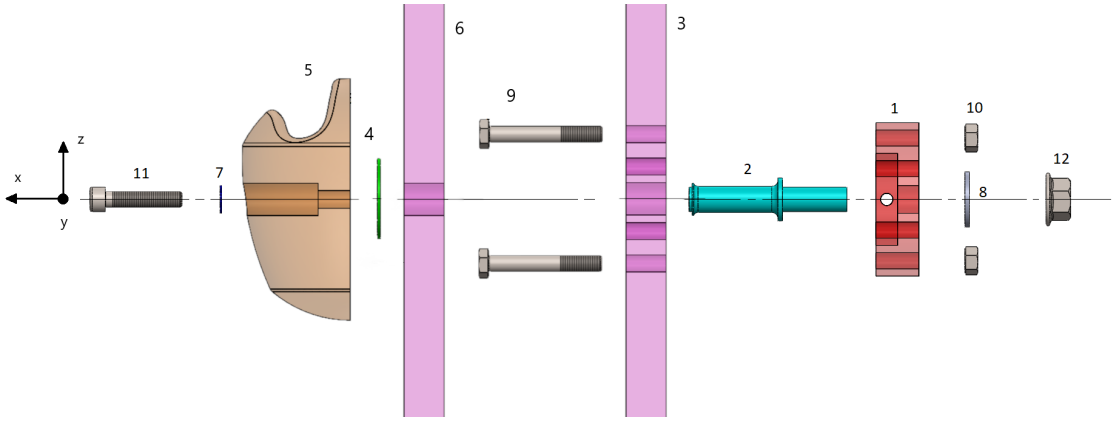

Figure 3.2: Exploded of the sectioned device [49].

All the elements described are made of steel, except for the hold, which is made of polyester resin. Specifically, 42CrMo4 is the chosen steel for the hollow beam element, because of its good stiffness, avoiding excessive strain.

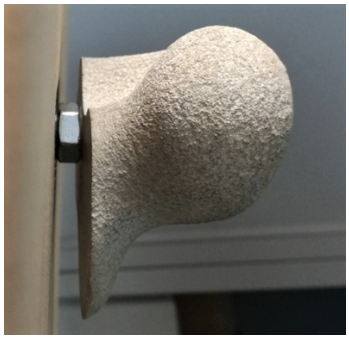

Figure 3.3: Study configuration.

However, the configuration used for acquisitions result to be different from that reported on figure 3.2. It was observed an improvement on accuracy and a measurements homogeneity by temporarily placing a nut between climbing hold (marked by 5 in figure 3.2) and the wall (marked by 3 in figure 3.2). A photo of described situation is shown on figure 3.3. It is noted that this addition turns out to be temporary and may not be necessary for future acquisitions.

During set-up phase, before performing calibration process, an improvement in consistency of acquired data was noted by placing a bolt between the climbing hold and the wall. This inaccuracy could be due to the strain gauges location too close to terminal thread. This accentuated deformation could lead the sensors to resistance values not suitable for the applied load.

3.2.2 Load cell

In the previous chapter it was described how the patented device [47] is composed. At the moment, let's focus on the metallic hollow element (element "2" on figure 3.2), on which strain gauges are applied. It represents a so called load cell.

Basically, a load cell is a device composed by a main metallic element on which sensing components, explained below and called strain gauges, are apposed. Contrarily to a simple cantilever, where deformation strongly depends on the point of application, a load cell is a metal structure optimized for force measurements with reduced sensitivity from the force point of application.

This device must have a simple geometry, which must to be studied, thought and optimized on force it wants to measure.

3.2.3 Deformation sensor

Now a more detailed explanation about strain gauge will be done, analyzing its mechanical and electrical properties.

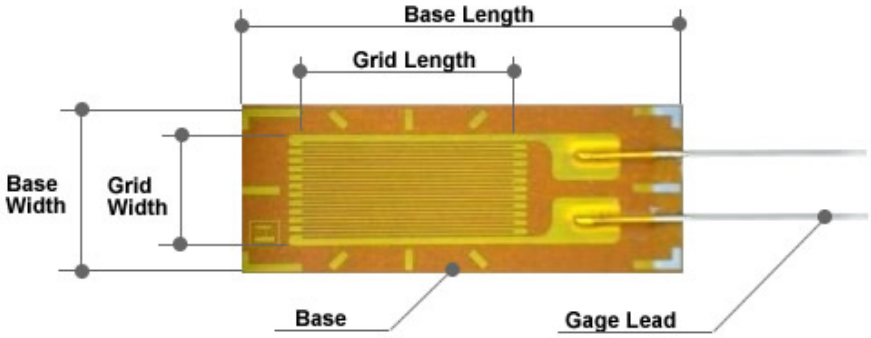

Figure 3.4: Strain gauge representation.

It is a transducer, therefore it detects dimensional deformations due to mechanical and thermal stresses. Thus, knowing the specific physical and mechanical characteristics of the material, it is possible to obtain the material loads which it is subjected by measuring the deformations. This is possible thanks to Hooke's law (equation 3.1) which describe elastic material behavior.

$$\sigma = E\varepsilon \tag{3.1}$$

Multiplying strain measurement by the material Young's modulus (E) can be obtain stress and then the forces which causes it (σ).

An electric strain gauges is characterized by the Gauge factor, which correspond to sensibility understood as the ratio between change in measured value, i.e. resistance, and variation of the real value of the quantity considered, i.e strain.

Going into more detail, starting conductor resistance value is:

$$R_0 = \rho \left(\frac{L}{A} \right) \tag{3.2}$$

Resistance variation using propagation of uncertainties rule, is:

$$\frac{\Delta R}{R_0} = \frac{\Delta \rho}{\rho} + \frac{\Delta L}{L} - \frac{\Delta A}{A} \tag{3.3}$$

Where:

- Section variation can be expressed as follow, where t correspond to conductor diameter :
$$\frac{\Delta A}{A} = 2 \left(\frac{\Delta t}{t} \right) = -2\nu - \varepsilon \tag{3.4}$$

- Poisson ratio, material dependent, is:
$$\nu = \frac{-\varepsilon_{\mathrm{t}}}{\varepsilon} = \frac{-\frac{\Delta t}{t}}{\frac{\Delta L}{L}} \tag{3.5}$$

- Piezoresistive effect, which depends on the volume variation, is:
$$\frac{\Delta \rho}{\rho} = C \left(\frac{\Delta V}{V} \right) = K\varepsilon \tag{3.6}$$

- At last, strain is:
$$\frac{\Delta L}{L} = \varepsilon \tag{3.7}$$

Overall, combining the previous relationships, equation 3.3 becomes:

$$\frac{\Delta R}{R_0} = K\varepsilon + \varepsilon - 2\nu\varepsilon = G\varepsilon \tag{3.8}$$

Finally, the variation in resistance due to strain is:

$$R = R_0 + \Delta R = R_0 \left(\frac{\Delta R}{R_0} \right) = R_0(1 + G\varepsilon) \tag{3.9}$$

Where G is the *Gauge factor*. It is material dependent and it is equal to 2 if ρ is constant and the material keeps the volume constant. Furthermor it is temperature dependent, since resistivity is temperature dependent too and compensatory strategies are applied to solve the problem. It corresponds to sensor relative sensibility:

- Absolute sensitivity is defined as:
$$S = \frac{dR}{d\varepsilon} = R_0 G \tag{3.10}$$

- Relative sensitivity becomes:

$$\frac{S}{R_0} = G \tag{3.11}$$

In current situation forces are exerted in the three space directions. Basing on reference system adopted forces generated on x direction produce tensile stresses, while those generated on y and z directions exercise bending stresses.

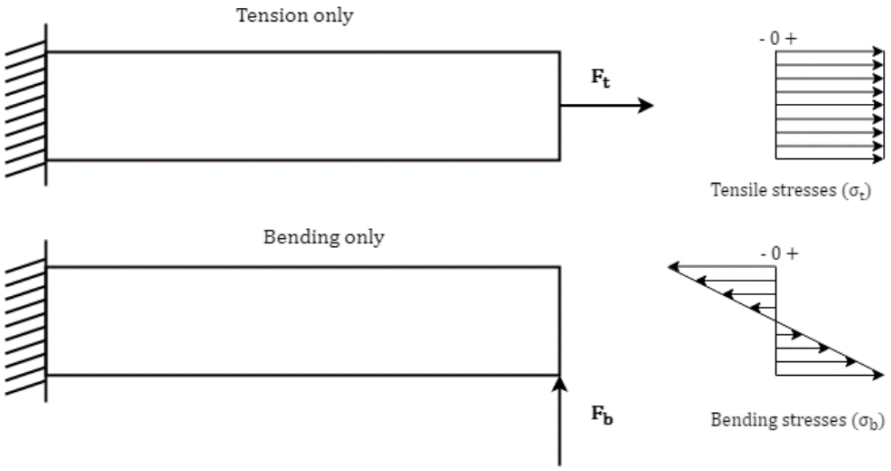

Figure 3.5: Stresses typologies [49].

Conditioning circuit which permit to measure the voltage variations (subchapter 3.2) is composed by four strain gauges for each force component. The reference configuration is call "Wheatston full-bridge" circuit (figure 3.6) and it allows a temperature compensation and has a quadrupled sensitivity.

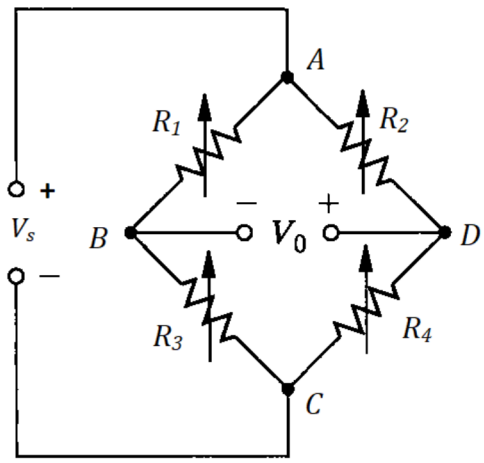

Figure 3.6: Wheatstone full-bridge electrical scheme [49].

Every strain gauge undergoes to a ΔR variation, which carries out to a bridge unbalance, which can be detected by a voltage measurement of V_0:

$$V_0 = \frac{V_s R_2 R_4}{(R_2 + R_4)^2} \left(\frac{\Delta R_4}{R_4} + \frac{\Delta R_1}{R_1} - \frac{\Delta R_2}{R_2} - \frac{\Delta R_3}{R_3} \right) \tag{3.12}$$

From the equation 3.12 it is clear the compensation temperature strategy exposed previously in section 3.2.3.

3.2.4 Out-of-plane forces conditioning circuit

Out-of-plane forces are only tensile type. In order to detect just tensile stresses and to avoid errors due to bending moment a similar to "diagonal bridge" configuration were adopted. Similar because two strain gauges (R_2 and R_3 referring to figure 3.6) were located on a unloading structure section with the aim to compensate thermal influences, since this structure is not able to obviate them.

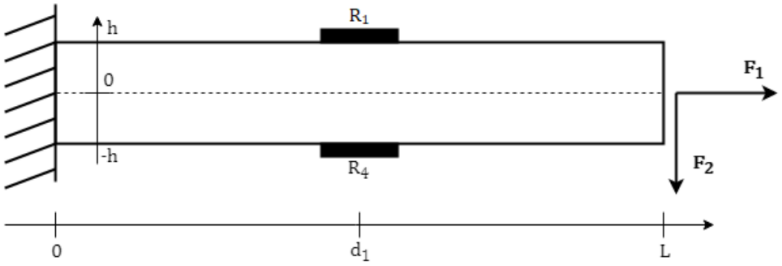

Figure 3.7: Wheatstone diagonal-bridge disposition [49].

Let's analyze stresses generated on the structure when it is subjected to a F_1 tensile force and to a F_2 bending force:

$$R_1 : \sigma_1 = \frac{F_1}{A} + \frac{F_2(L-d_1)h}{J} \tag{3.13}$$

$$R_2 : \sigma_2 = 0 \tag{3.14}$$

$$R_3 : \sigma_3 = 0 \tag{3.15}$$

$$R_4 : \sigma_1 = \frac{F_1}{A} - \frac{F_2(L-d_1)h}{J} \tag{3.16}$$

Where A is the beam section and J is the area moment of inertia.

Finded relations, replaced in equation 3.12 and combined with Hooke's law (equation 3.1 and gauge factor definition, allow to reach the following relationship:

$$\begin{aligned} V_0 &= \frac{V_s R_2 R_4}{(R_2+R_4)^2}\frac{GF}{E}\left[\frac{F_1}{A} + \frac{F_2(L-d_1)h}{J} + \frac{F_1}{A} - \frac{F_2(L-d_1)h}{J}\right] \\ &= 2\frac{V_s R_2 R_4}{(R_2+R_4)^2}\frac{GF}{EA}F_1 \end{aligned} \tag{3.17}$$

Thus, V_0 is directly proportional to F_1 by the γ scaling coefficient:

$$\gamma = 2\frac{V_s R_2 R_4}{(R_2+R_4)^2}\frac{GF}{EA} \tag{3.18}$$

$$V_0 = \gamma F_1 \tag{3.19}$$

3.2.5 In-plane forces conditioning circuit

In-plane forces turn out to have tensile and bending components, since body weight application on hold generate a wall normal and parallel component due to body COM[1] location outside the yz plane. Lateral displacements on the wall surface also generate force, which help to generate the same effects.

Thus, total stress results a two components sum:

$$\sigma_{\mathrm{TOT}} = \sigma_{\mathrm{b}} + \sigma_{\mathrm{t}} \tag{3.20}$$

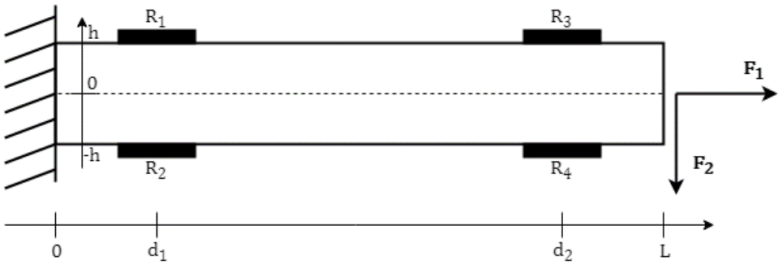

Figure 3.8: Wheatstone full-bridge disposition [49].

Present measurement was made adopting a Wheatstone full-bridge configuration (figure 3.8) with four strain gauges placed on beam opposite edges and at distinct locations from fixed side.

By subjecting the hold to a bending and to a tensile force, the following stresses are arise on the beam near the strain gauges location:

$$R_1 : \sigma_1 = \frac{F_1}{A} + \frac{F_2(L-d_1)h}{J} \tag{3.21}$$

$$R_2 : \sigma_2 = \frac{F_1}{A} - \frac{F_2(L-d_1)h}{J} \tag{3.22}$$

$$R_3 : \sigma_3 = \frac{F_1}{A} + \frac{F_2(L-d_1)h}{J} \tag{3.23}$$

$$R_4 : \sigma_4 = \frac{F_1}{A} - \frac{F_2(L-d_1)h}{J} \tag{3.24}$$

Adopting the same procedure explained in the previous section, previous relations, substituted in equation 3.12, allow to obtain:

$$\begin{aligned} V_0 = {} & \frac{V_{\mathrm{s}} R_2 R_4}{(R_2+R_4)^2} \frac{GF}{E} \left[\frac{F_1}{A} - \frac{F_2(L-d_1)h}{J} + \frac{F_1}{A} + \frac{F_2(L-d_1)h}{J} + \right. \\ & \left. - \frac{F_1}{A} + \frac{F_2(L-d_1)h}{J} - \frac{F_1}{A} - \frac{F_2(L-d_1)h}{J} \right] = \\ = {} & \frac{V_{\mathrm{s}} R_2 R_4}{(R_2+R_4)^2} \frac{GF}{E} \frac{h}{J} F_2(-L+d_2+L-d_1+L-d_1-L+d_2) = \\ = {} & 2\frac{V_{\mathrm{s}} R_2 R_4}{(R_2+R_4)^2} \frac{GF}{E} \frac{h}{J} (d_2-d_1) F_2 \end{aligned} \tag{3.25}$$

[1] COM: Center of Mass

Even here a direct proportion between voltage and force applied is shown, specifically:

$$V_0 = \beta F_2 \tag{3.26}$$

Where β represents the scaling coefficient and is equal to:

$$\beta = 2\frac{V_s R_2 R_4}{(R_2 + R_4)^2}\frac{GF}{E}\frac{h}{J}(d_2 - d_1) \tag{3.27}$$

By this way just a yz plane component was found. In order to found the remaining plane component, four other strain gauge are necessary. Thus, totally eight strain gauges are necessary to obtained the two in-plane forces.

3.3 Entire wall cabling

After illustrating in the previous chapters the single hold functionality, starting from the general principles that regulate the systems for taking forces and then associating them in the specific case of the patented hold used [47], in this section will be describe the conformation of the climbing wall used.

The wall used was wired with 3 sockets, named *2001*, *2002* and *2003* and arranged as shown in figure 3.9a.

(a) The top right hold correspond to *2001*, the top left one is the *2002* and the one below is the *2003*.

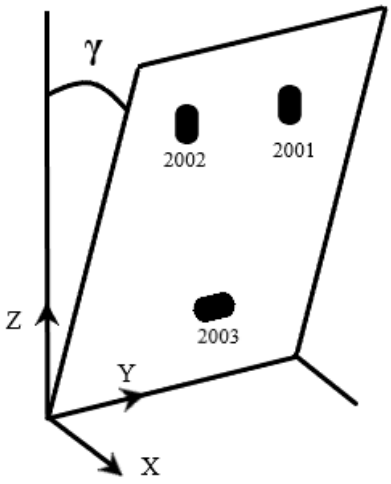

(b) Reference system adopted.

Figure 3.9: Testing wall. On the left is reported a photo of actual adopted wall in this thesis work. On right side is shown a scheme of used reference system.

The reference system has been set as in figure 3.9b: the origin was represented in the lower left corner but in reality it is only an indicative representation since

the system only serves to axes identification on which the forces obtained from the measurements will be projected. It should also be noted that the wall is inclined at a γ angle equal to 7° with respect to the vertical.

By this way, antero-posterior forces (F_x) are positive when pointing outside the wall, medio-lateral forces (F_y) are positive rightwards and vertical ones (F_z) are positive upwards.

3.3.1 Data acquisition system

The computerised Data Acquisition (DAQ) system, contained on patent previous exposed [47], is composed of three different parts:

- force transducers: placed on each hold of the instrumented wall, they produce as output an analog voltage signal proportional to the sensed force;
- acquisition hardware: this part is realised using Arduino® boards. For each hold transducers are connected to a board, which performs discrete sampling at a set frequency, analog to digital conversion of the signal and preprocessing;
- controller and data logger: the Arduino® boards are connected through cables to a Raspberry Pi®. The communication exploits a Controller Area Network (CAN) protocol purposely developed. Since the Raspberry Pi® is a computer, from its shell it is possible to operate the complete DAQ system.

Every time an analysis is performed, data are logged in the memory storage of the Raspberry Pi ®. Then, they are transferred on a PC where they are processed using scripts written in Matlab® and Python R® programming languages.

A block diagram of the wall DAQ system is shown in figure 3.10 on page 50.

3.3.2 Signal Pre-processing

For each hold, the output voltages of the three Wheatstone bridges associated are read by three 24-bit A/D converters, connected to an Arduino® Uno board. The continually running code loaded in the board flash memory reads the voltage values at a sampling frequency of 80 Hz and scales them to the force value in N by dividing each channel for the correct scaling value, stored in the board mass memory.

The coefficients are obtained in the initial set-up of the instrumented wall. During this phase each hold acquisition boards are connected to a PC through a USB cable and a different code is loaded in their flash memory. Then, applying known loads along different directions on the hold while running a purposely developed Matlab® script on the PC the three scaling parameters are extracted.

Data transmission is allow by a CAN protocol previous developed and implemented. The CAN interface mounted on the Raspberry Pi ® receives all data coming from the three Arduino® boards of the three holds. Operating from the command line of the computer, by launching a Python® script, data are logged in the mass memory.

Output file

An extract of the *file.txt* in which data are wrote and which is saved in mass memory are reported below:

.
.
.
2001, -157 -3 0 31200
2002, -60 134 0 35393
2003, -19 -357 0 24508
2001, -158 -3 0 31213
2002, -61 138 0 35405
2003, -18 -349 0 24520
.
.
.

Where, the first row element corresponds to the hold name, the elements from second to fourth represent the force detected in a orthogonal reference system in space and the fifth column is the instant in milliseconds since the system was turned on. In particular, in accordance with what will be illustrated in chapter 4.1.3 , second column correspond to F_1 value, third column corresponds to F_2 value and fourth column corresponds to F_e value.

In order to simplify the following data elaboration in Matlab, output file, which have "*.txt*" extension, was transformed into a "*.xlsx*" one and it was given as input on scripts reported in appendix A.1, A.2 and A.3.

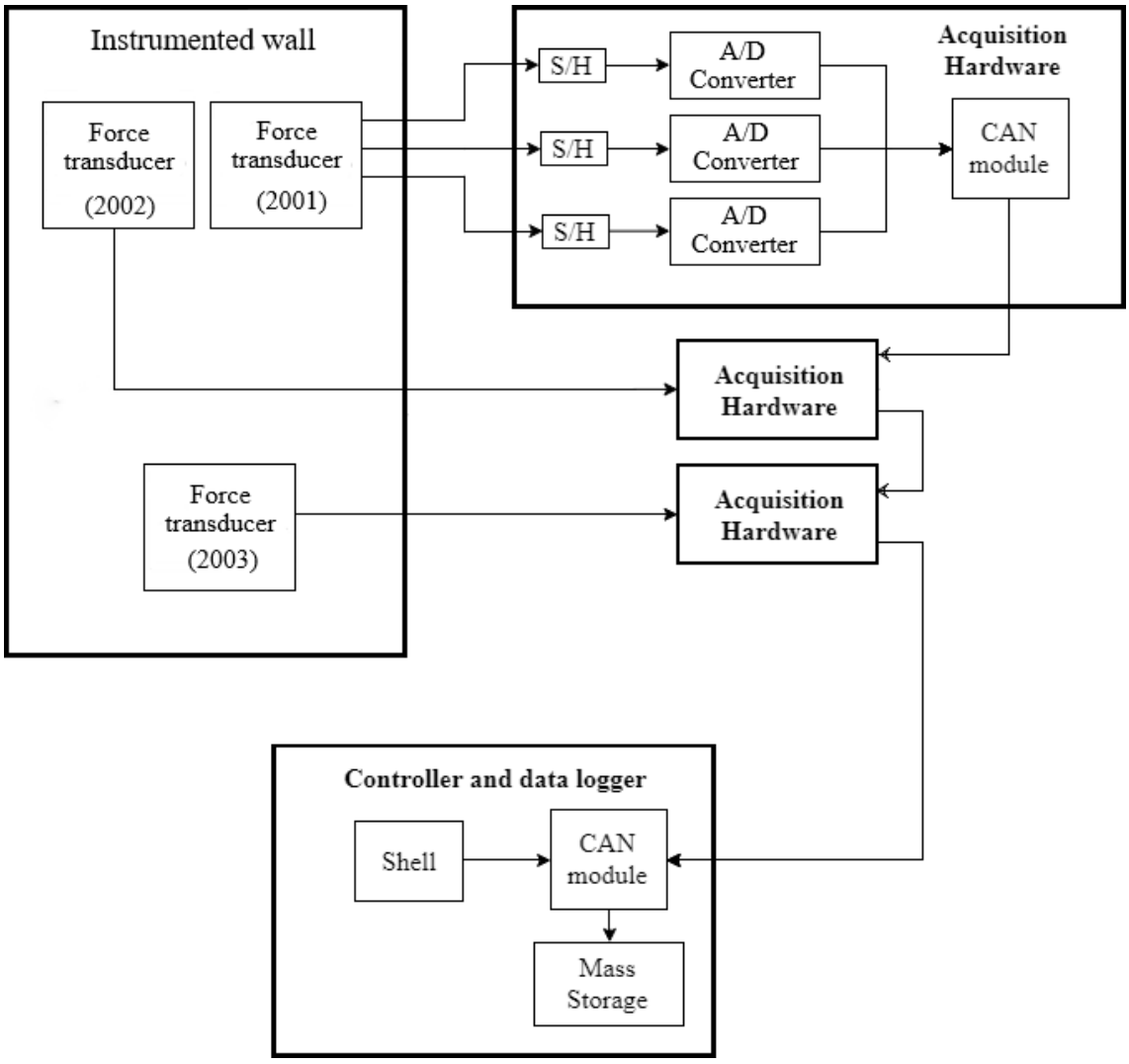

Figure 3.10: Block diagram of wall DAQ system. Adapted from [49]

Chapter 4

Experimental tests

This chapter starts with the actual practical phase executed directly on the previous introduced climbing wall.
It explains calibration process carried out in order to assess and provides sufficient stability and accuracy of the following acquisition step.
Then, will be illustrated the conceived experimental protocol which subjects performed in order to simulate as much as really possible climbing movements.
Follow a theoretical explanation concerning rotation matrix calculation with the aim of transform force detected on sensor coordinate to tridimensional cartesian reference system. In particular, Tait - Bryan angles was adopted for conversion.
Next a brief explanation regarding indexes choose for a preliminary climbing performance analysis was conducted. Theoretic notions, computation performed and results obtained are explained for each factor examined, that are "Hausdorff dimension", "Smoothness factor" and "Friction coefficient".

4.1 Introduction

After the previous chapters, in which the state of the art, concerning researches conducted about sport climbing, were evaluated combined to an explanation about force measurement devices with particular attention to instrumentation used in the current thesis work, the current chapter is intended to present the experimental tests done. This phase has been carried out at "Dipartimento di elettronica, informazione e bioingegneria (DEIB)" of Politecnico di Milano, where the wall, which is shown in figure 3.9a on page 47, is currently located.

4.1.1 Calibration process

The first phase dealt with was to calibrate the wall used for the measurements. Calibration process, as previous illustrated in chapter 3.3.2, was conducted for each hold individually through the use of a test weight of 10 kg.

The calibration program was loaded on each DAQ hold individually and scaling coefficient has been calculated by the cited software. Then, scaling factor has been passed to the specific hold's DAQ making hold ready for measurement.

Next, test mass was hung on the calibrated hold and the correspondence between test mass knowed weight and measured value and has been verified. The procedure was carried out three time for each hold and data concerning force recorded are shown in picture 4.1a on page 54, picture 4.2b on page 55 and picture 4.3a on page 56, while mass detected for each cycle is reported on figure 4.1b on page 54, figure 4.2a on page 55, and figure 4.3b on page 56. Notice that, in figure 4.1 and in first calibration cycle on figure 4.3, is evident the presence of a jump during the starter phase, when hold is unloaded. This reset is due to "auto-offset" function, loaded on each DAQ hold, able to delete any noise on canal acquisition.

Finally, the test mass was loaded twice in a row on each single hold and the signals recorded was verified. They are reported on page 57, where figure 4.4a shows forces measured on each hold, and in figure 4.4b mass detected for each hold is displayed.

All the graphics reported have been obtained by the developed software explained in chapter 5, which allows a graphical representation of signal recorded and wrote on output file.

Scaling coefficient, having measurement units equal to (1/N) obtained on each calibration process carried out for each holds are reported on table 4.1.

Cycle	2001 [1/N]	2002 [1/N]	2003 [1/N]
1	379,0087	379,0087	284,4713
2	362,8138	371,5707	267,8417
3	368,5354	372,4332	263,2158
Mean	370,1193	374,0025	271,8429
SD	8,2128	3,4918	11,1784

Table 4.1: Scaling coefficients and their mean and standard deviation for each hold.

Shown values don't vary significantly over time. Hold "2002", in particular, presents the lowest variance, while hold "2003" demonstrates the highest variance.

RMS noise measured in Newton and observed on the channels in subsequent calibrations is reported on following tables, in which mean and standard deviation values for each measuring channel is also calculated. Each table is specific for one of the three holds.

Cycle	F1 [N]	F2[N]	F3[N]
1	1,9355	0,733	0,6482
2	3,7142	0,7999	0,6962
3	2,1067	0,7417	0,6952
Mean	2,5855	0,7582	0,6799
SD	0,9813	0,0364	0,0274

Table 4.2: RMS noise (N) for hold "2001".

Cycle	F1 [N]	F2 [N]	F3 [N]
1	0,7953	0,9289	0,7173
2	0,8123	1,209	0,7342
3	0,8319	1,0433	0,7168
Mean	0,8132	1,0604	0,7228
SD	0,0183	0,1408	0,0099

Table 4.3: RMS noise (N) for hold "2002".

Cycle	F1 [N]	F2 [N]	F3 [N]
1	0,8955	1,0987	0
2	1,0246	1,8684	0
3	1,0625	1,8503	0
Mean	0,9942	1,6058	0
SD	0,0876	0,4393	0

Table 4.4: RMS noise (N) for hold "2003".

It is immediate to notice that hold "2001" has the highest noise values and this turns into bad performance compared to remaining hold. However, it is clear that the better performance and highest accuracy is demonstrated by hold "2002" (it can be, also, confirmed observing figure 4.4a and figure 4.4b), which have a mean noise RMS about 0.8 N among the three canals, contrary to more than 1 N present on hold "2001". Particular behavior shows hold "2003", where noise RMS, mediated on the three channels is consistent to hold "2002", but it results to be null on F3 channel and, consequently, equal to more than 1 N if compared on average between F1 and F2 channels. However, entire system accuracy can be assessed about 1 N and it can allows to conduct proposed study, since it is coherent to previous realized works executed with the same instrumentation. The RMS value of registered noise depends on the choice to use a low cost equipment and therefore the non-low value is thus justified.

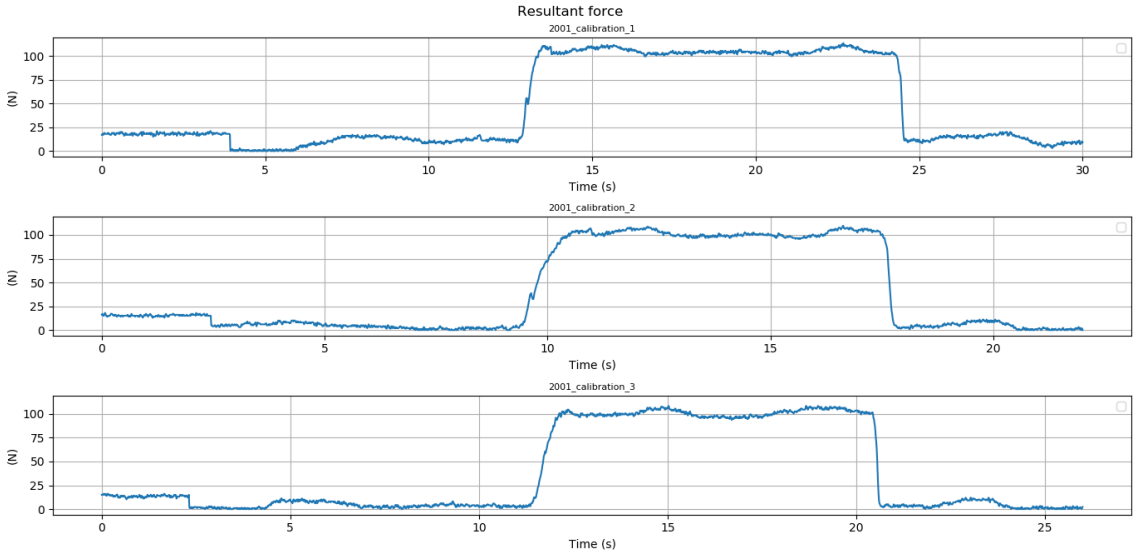

(a) Total force recorded.

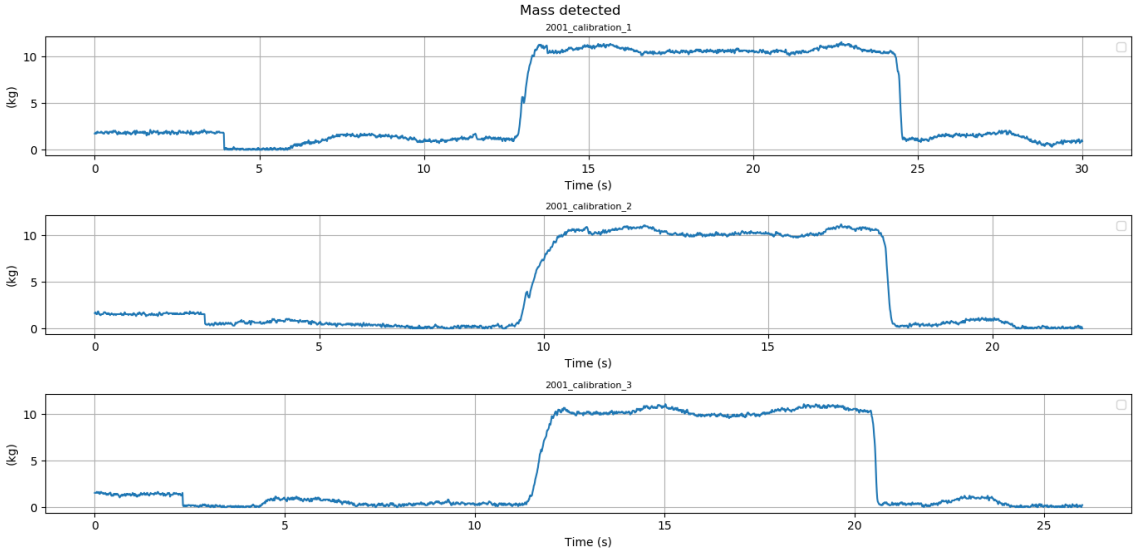

(b) Mass detected.

Figure 4.1: Force recorded and mass detected on "2001" hold.

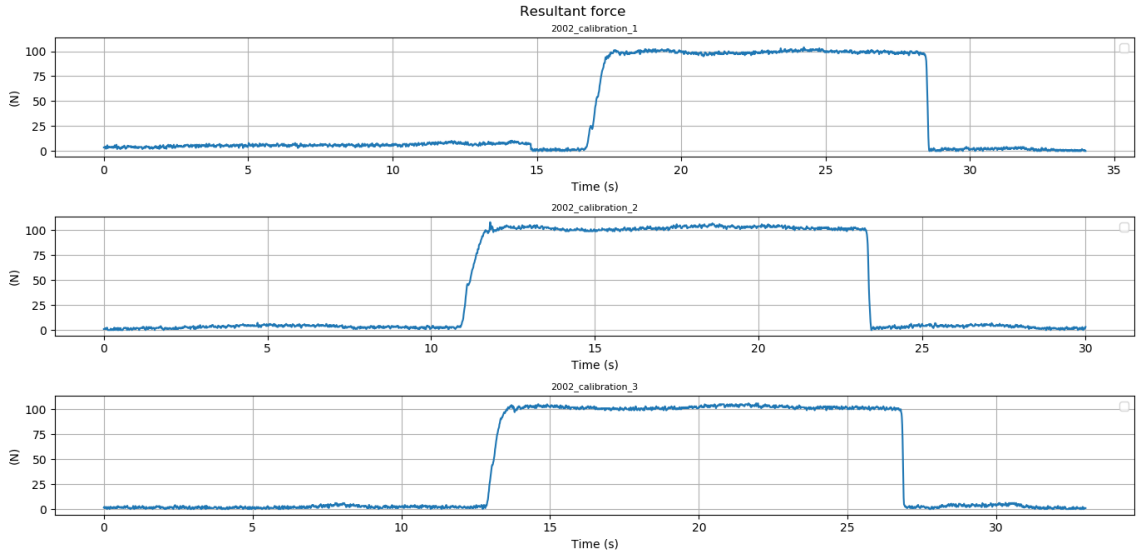

(a) Total force recorded.

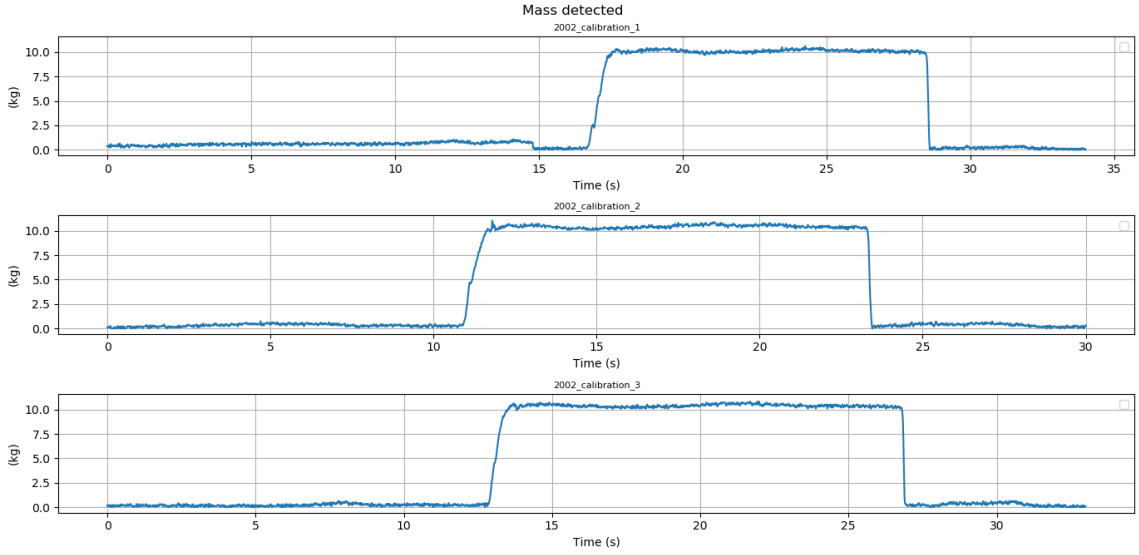

(b) Mass detected.

Figure 4.2: Force recorded and mass detected on "2002" hold.

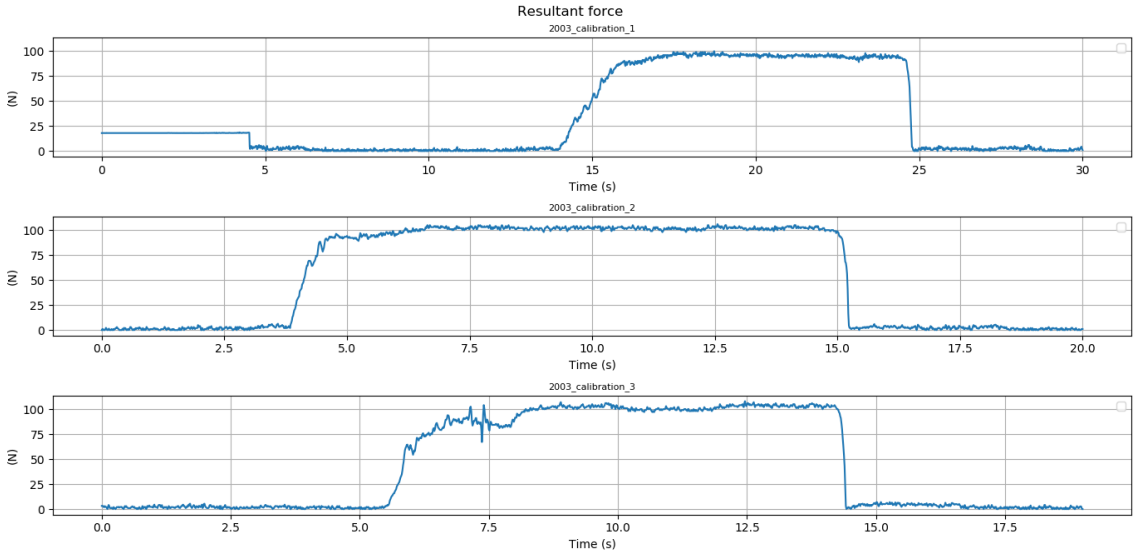

(a) Total force recorded.

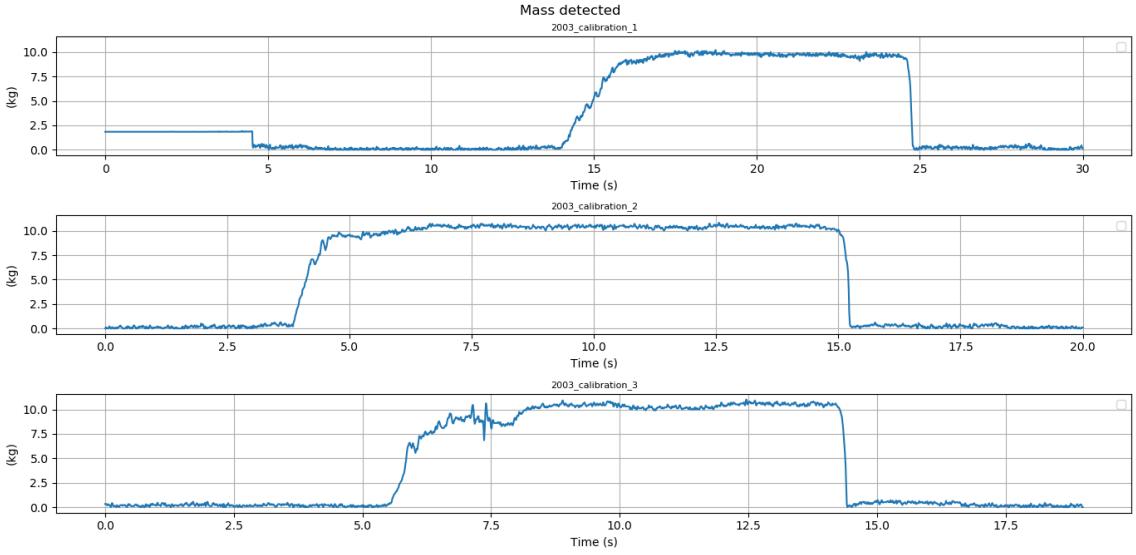

(b) Mass detected.

Figure 4.3: Force recorded and mass detected on "2003" hold.

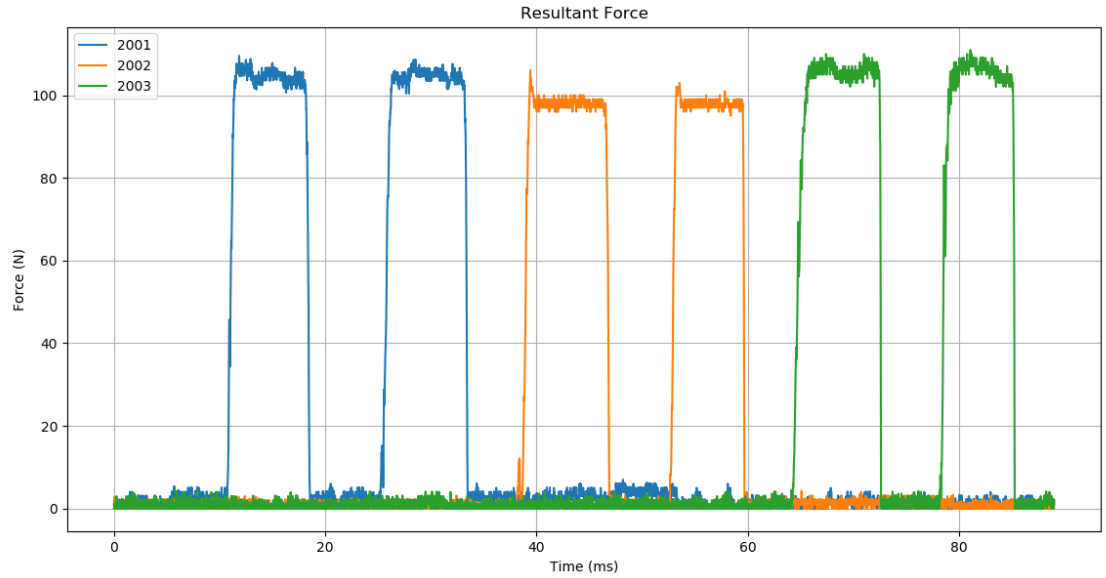

(a) Total force recorded.

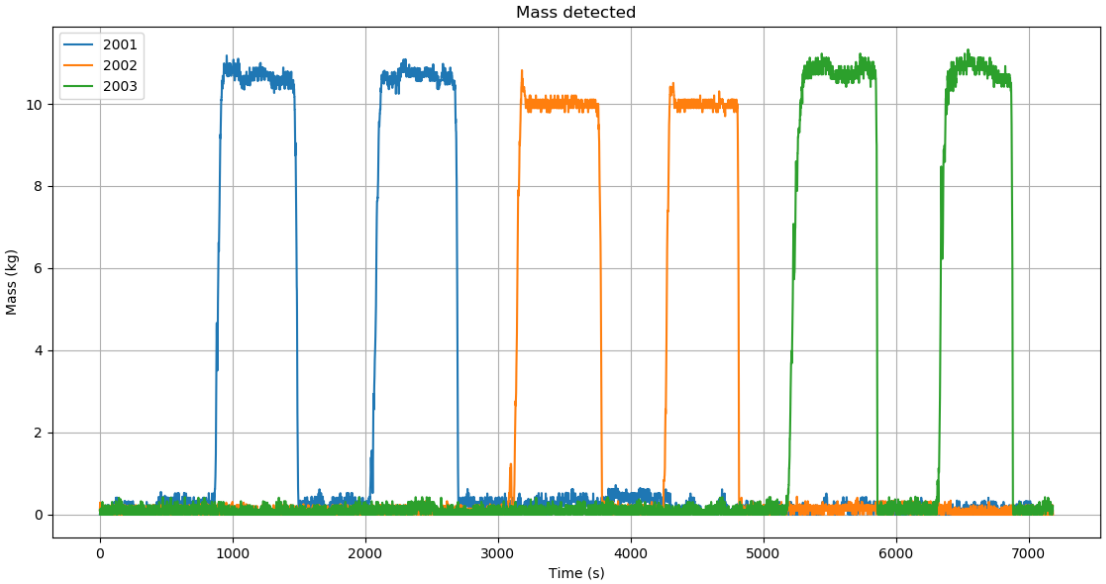

(b) Mass detected.

Figure 4.4: Force recorded and mass detected on each hold by moving test mass among the three holds.

4.1.2 Exercise performed

The following step concerns to the actual measurement phase simulating a realistic situation. The phase aim was to execute a simple exercise to imitate as much as possible a practical movement sequence executable by a climber during its ascent. The exercise consists into 7 steps:

- S1: subject grabs *2002* hold with the two hands;
- S2: subject places right foot on the *2003* hold while continues to grabs *2002* hold with the two hands;
- S3: subject grabs *2001* hold with right hand while continues to grabs *2002* hold with left hand and while maintain right foot on the *2003* hold;
- S4: subject standing as in S3 but places left foot on *2003* hold instead of right one;
- S5: subject grabs *2001* hold with the two hands while continues to places left foot on *2003* hold;
- S6: subject unloads *2003* hold and continues to grab *2001* hold with the two hands;
- S7: subject unloads *2001* hold and ends the exercise.

Two subjects were available for the measurements: an expert climber and a non climber one. Each subject performed the illustrated exercise twice.

A schematic drawing series is reported in figure 4.5 (p. 59) in order to propose a simplified view of the previous proposed exercised.

4.1.3 Tait-Bryan Angles

Each holds detect three component mof the total force along three orthogonal directions with unknown orientation except for the fact that two components are contained in the plane of the wall and that the third is orthogonal to it. A graphical view about previous exposed is reported in figure 4.6 on page 60.

In order to decompose forces and orient the axes according to the horizontal and vertical directions, orientation matrix was found adopting "Tait-Bryan Angles". After defining α as the unknown rotation angle around the X axis and γ as the known rotation angle around Y axis which is 7°, total rotation matrix was found as explained below. The transformation described was conducted analyzing the output file resulting from the calibration process during which a 10 kg test mass has been hung at each hold and supposing that its influence was exactly on vertical direction.

Firstly, the three rotation matrices around each axis have been calculated:

$$R_x = \begin{vmatrix} 1 & 0 & 0 \\ 0 & cos(\alpha) & -sin(\alpha) \\ 0 & sin(\alpha) & cos(\alpha) \end{vmatrix} \tag{4.1}$$

$$R_y = \begin{vmatrix} cos(\gamma) & 0 & sin(\gamma) \\ 0 & 1 & 0 \\ -sin(\gamma) & 0 & cos(\gamma) \end{vmatrix} \tag{4.2}$$

Figure 4.5: Schematic drawing series reporting executed exercise phases. Where: "RF" stands for tight foot, "LF" for left foot, "RH" for right hand and "LH" for left hand.

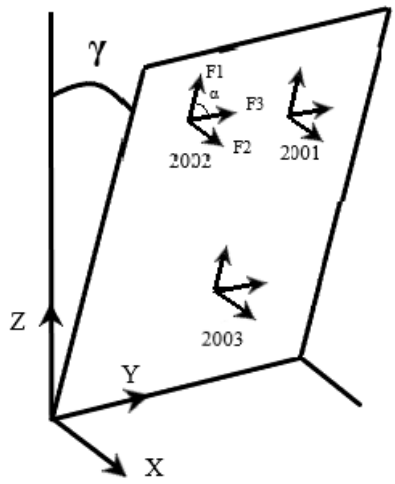

Figure 4.6: Reference systems orientation.

$$R_z = 0 \tag{4.3}$$

Then, 3D space rotation matrix has been calculated as:

$$R_{TOT} = R_z R_y R_x = \begin{vmatrix} cos(\gamma) & sin(\gamma)sin(\alpha) & sin(\gamma)cos(\alpha) \\ 0 & cos(\alpha) & -sin(\alpha) \\ -sin(\gamma) & cos(\gamma)sin(\alpha) & cos(\gamma)cos(\alpha) \end{vmatrix} \tag{4.4}$$

Finally, the following transformation was applied:

$$\begin{vmatrix} F_x \\ F_y \\ F_z \end{vmatrix} = R_{TOT} \begin{vmatrix} F_2 \\ F_3 \\ F_1 \end{vmatrix} \tag{4.5}$$

And the resulting system has been found:

$$\begin{cases} F_x = cos(\gamma)F_2 + sin(\gamma)sin(\alpha)F_3 + sin(\gamma)cos(\alpha)F_1 \\ F_y = cos(\alpha)F_3 - sin(\alpha)F_1 \\ F_{TOT} = -sin(\gamma)F_2 + cos(\gamma)sin(\alpha)F_3 + cos(\gamma)cos(\alpha)F_1 \end{cases} \tag{4.6}$$

In conclusion, α angle was found knowing that $F_x = F_y = 0$, since testing mass generates a component exactly along the vertical axis.

Thus, the following system was solved:

$$\begin{cases} 0 = cos(\gamma)F_2 + sin(\gamma)sin(\alpha)F_3 + sin(\gamma)cos(\alpha)F_1 \\ 0 = cos(\alpha)F_3 - sin(\alpha)F_1 \\ F_{TOT} = -sin(\gamma)F_2 + cos(\gamma)sin(\alpha)F_3 + cos(\gamma)cos(\alpha)F_1 \end{cases} \tag{4.7}$$

Clearly, once calculated α angle during the calibration process, transformation reported on equation 4.5 can be applied for every time step, i.e. for every line in output file, which a simplified preview is shown on chapter 3.3.2).

4.1.4 Indexes calculated

Once calculated α angle, the force's three components referred to orthogonal system chosen has been calculated.

Subsequently, the actual calculation phase was executed and the performance indexes, previous illustrated in chapters 2.4.4, 2.4.5 and 2.4.6, were elaborated. In particular, *Hausdorff Dimension*, *Smoothness Factor* and *Friction coefficient* are the chosen indexes for computation. This can be considered as the starter point of a more detailed analysis that can leads to a complete evaluation of climbers performance, which can be carried out with a larger climbing wall equipped with a greater number of holds.

4.2 Hausdorff Dimension

4.2.1 Theoretical introduction

Before reaching an Hausdorff dimension explanation, the chapter begins by explaining some concepts useful for its definition and its comprehension.

Starter point is the fractal definition, even if giving a satisfactory definition is an hard work. Intuitively, a fractal is a geometric figure in which a single pattern is repeated on different decreasing scales. Thus, is an object with homothety features: it repeats itself form in the same way on different scales, consequently a figure like the original is obtained zooming the initial one in any its portion. For a visual explanation and a more intuitive idea about previous reported notions, in figure 4.7 is shown a fractal object.

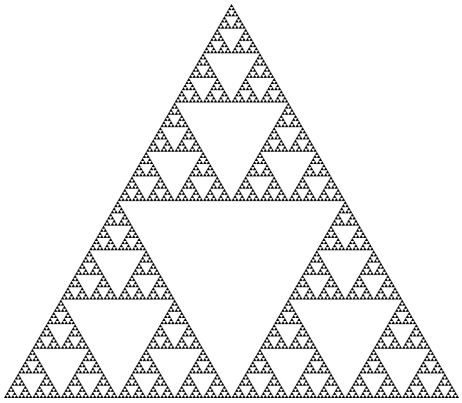

Figure 4.7: The Sierpinski triangle: basic fractal object.

The "irregularity degree" of a fractal object is explained by the fractal dimension parameter. It is commonly denoted by "D" letter and it is a statistical measure of complexity. It compares how feature changes in a pattern with the scale at which it is measured. The most important are *Hausdorff dimension* and *Minkowski - Bouligand dimension* which results strictly bounded to the first one. Both are necessary in order to describe fractal dimension which can't be, alternatively, explained by topological dimension [1].

[1]Intuitive dimension concept which assigns a dimension equal to one by one straight line, a dimension equal to two by a plane and a dimension equal to three by three-dimensional space

Hausdorff dimension is a chaos and irregularity measure which refines topological dimension concept and relates it to other space properties, such as area and volume. Starting from a geometric object X, consider the number *N(r)* of balls, with radius at most r, necessary to cover object entirely. Clearly, *N(r)* has a decreasing trend as r increasing and it follow the *1/r* polynomial law. The Hausdorff dimension is the d number such that N(r) grows as $1/r^d$ as r approaches zero.

The fractal dimension, in addition to the definition proposed by the mathematician Felix Hausdorff, can be explained by several other notions that are highly related to each other. Of all, Minkowski - Bouligand's is reported. It expresses a concept quite similar to that proposed by Hausdorff but turns the counting from square elements to spherical ones. This is also called *Box - counting method* and corresponds to a technique for calculating Hausdorff dimension.

Turning focus on main topic of current thesis work , Hausdorff dimension can be considered as the geometric entropy of a signal and it can applied to force - time signal. It was calculated adopting the previous enunciated "Box - counting method" on a two dimensional scatter plot, where vertical force is plotted on the abscissa and the total force on the ordinate. It turns out to be dependent by mean force applied, contact time and smoothness factor [45]. Particularly, it can distinguish between an efficient climbing style and a non-efficient one, keeping in mind that a good climbing performance is characterized by short contact time, smaller force applied and high smoothness on force-time signal. Hence, as exposed on chapter 2.4.4, smaller the Hausdorff dimension value greater the climber performance.

4.2.2 Computation

After a brief theoretical introduction about fractals primary concepts and their application on current work thesis, the actual calculation steps will be explained.

The calculation script has been written in Matlab® and it is reported in appendix A.1 on page 81. Script needs ".xlsx" file as input and starts correcting axes orientation, because some holds have inverted axes and they weren't correctly oriented (line 25). After the following orientation matrix calculation (line 32), data extraction for each hold was elaborated (line 39). In these code lines there was implemented the axes correction, there was extracted x, y and z components and there was estimated the resultant force applied to hold. Computing was executed instant by instant, thus for each output file line.

Follows the scatter plot creation (figure 4.8 on p. 64 and figure 4.10 on p. 66) on which the Hausdorff dimension will be find (line 78). This step starting with the scatter plot creation for each hold (line 86): it reports vertical force on the abscissa and total force on the ordinate. The scatter plot obtained is RGB encoded but it must be transformed into logical type. Hence, it has to be converted into greyscale format (line 98) and then converting it into a logical object (line 99). Finally, since Matlab® "box - counting" routine counts the boxes needed to cover the nonzero elements of input data, the scatter plot bits must to be complement. In conclusion, Hausdorff dimension was computed by the *Box counting method* which can be expressed by the following equation:

$$D = \lim_{R \to 0} \frac{logN}{logR} \tag{4.8}$$

Where N is the number of boxes of size R to cover completely the graph.

The local slope as function of radius was represented (line 110) and it will be reported in figure 4.9 (p. 65) for expert climber and in figure 4.11 (p. 67) for the beginner subject. Local slope is defined as:

$$DF = -\frac{\mathrm{d}ln(N)}{\mathrm{d}ln(R)} \tag{4.9}$$

4.2.3 Results

Once the scatter plot is generated and the relative local slope is represented, the actual Hausdorff Dimension is found observing the "slop" representation: if DF shows a constant segment in a certain range of r, then DF is the fractal dimension of the pertinent scatter plot.

In the following pages scatter plots obtained from a single acquisition per subject are reported for comparison. On page 64 are reported those relative to the expert climber from which is clearly denoted a different trend between holds grasped by hands and the only hold grasped by feet. The first ones (fig. 4.8a and fig. 4.8b) show a straight-like course from which is evident that force vertical component represents almost entirely the total force exchanged by the subject. This is obviously explained by the performed exercise: climber body appears to weight entirely on the upper holds ("2001" and "2003") through his arms.

Totally different turns out to be climber body weight action on lower hold and it is clear from figure 4.8c and figure 4.10c, which show a chaotic trend, which leads to not establish if a certain force component is preponderant on resultant force.

The difference in scatter plot trend between holds grasped by feet and those grasped by hands is confirmed by both subjects. Hands and feet turn out to produce distinct influence and their scatter plot are clearly distinguishable.

Some considerations concerning force levels between the two subject can be done. From literature and climbers experience, an efficient climbing style proves to have a greater lower limbs use than the upper ones. Legs muscles, in fact, are more extensive than the upper limbs muscle groups. As a consequence, upper muscles reach fatigue status faster than lower ones preventing climber from achieving lasting performance. This differentiates an expert climber from a beginner one and this is confirmed observing maximum force level exerted by the expert subject (fig. 4.8c on p. 64), which is more than 400 N, contrarily to just more than 350 N deployed by beginner climber. This reflection was conducted considering the maximum levels of strength achievable by both subjects with the upper limbs.

Concerning the Hausdorff dimension values, they turn out to have the same values for both kind of limbs between subjects. Upper limbs turn out to have a value equal to among 1.2 and lower limbs equal to among 1.6.

Hausdorff values dependences expressed by Fuss and Niegl [45] are partly confirmed. Increasing trend by contact time (fig. 4.12) is confirmed by the beginner subject but not for the expert one. Moreover, its raise with level force applied is observed in a "intra-subject" condition and is unproved in the "inter-subjects" condition. Finally, as subsequently introduced and explained, decreasing trend with smoothness level is shown for just one out of two expert climber acquisitions but it is always confirmed comparing hold "2002" and hold "2003".

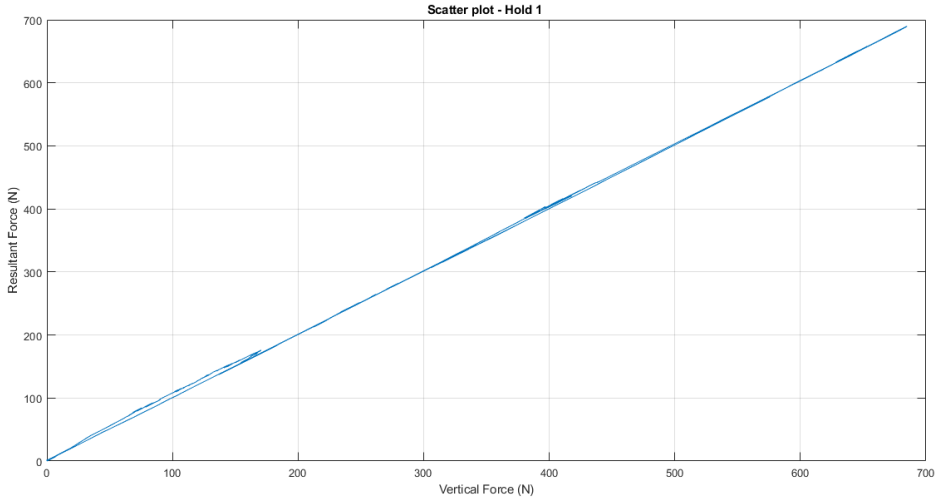

(a) Hold grasped by hands.

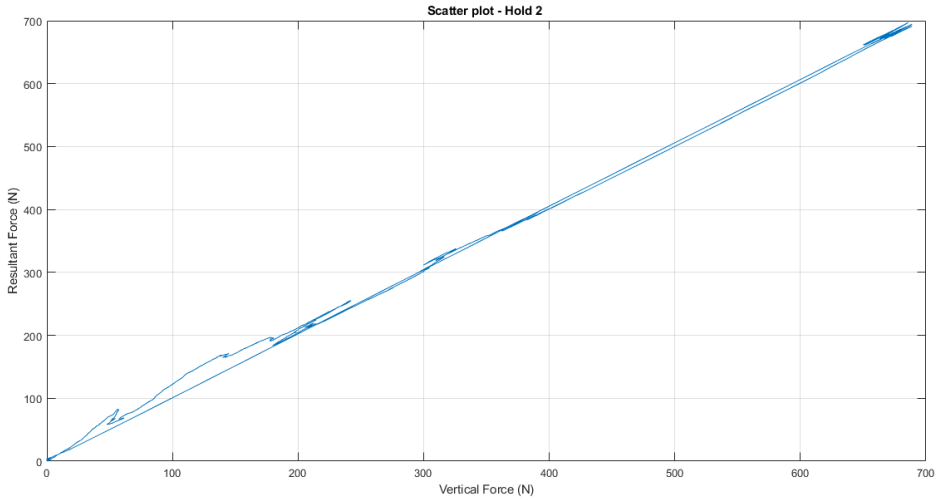

(b) Hold grasped by hands.

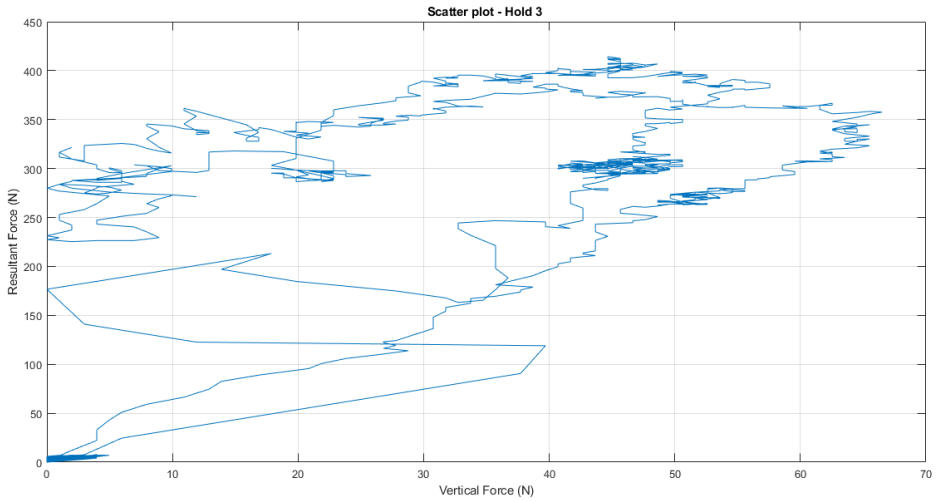

(c) Hold grasped by feet.

Figure 4.8: Scatter plot obtained from expert climber.

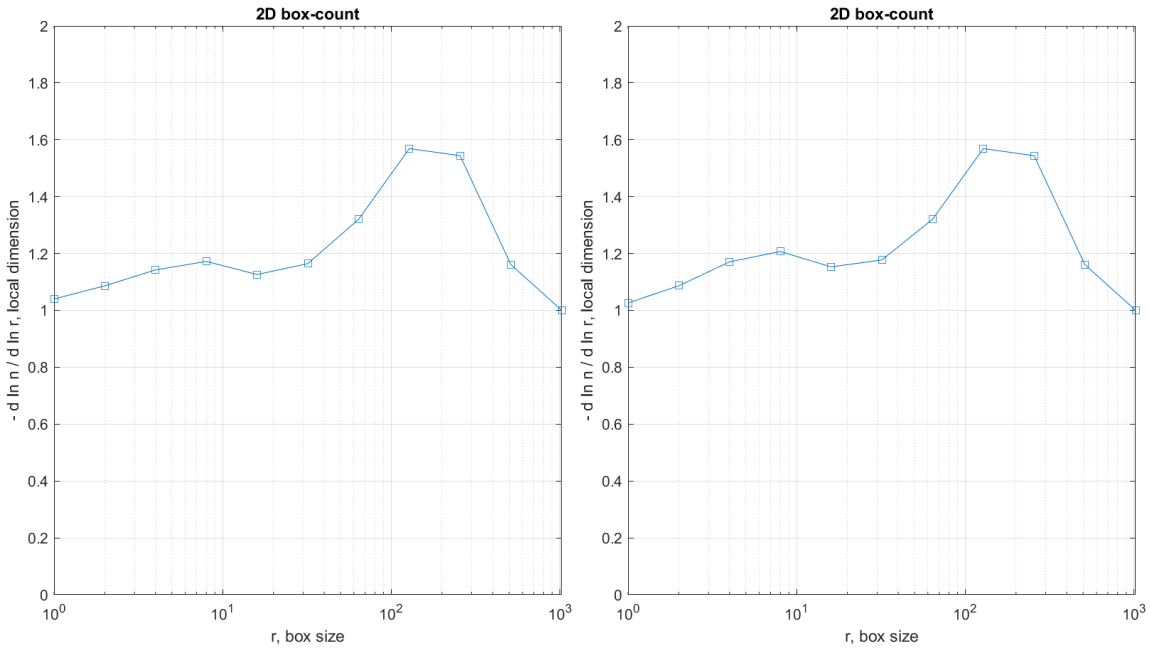

(a) Slope of "2001" scatter plot.

(b) Slope of "2002" scatter plot.

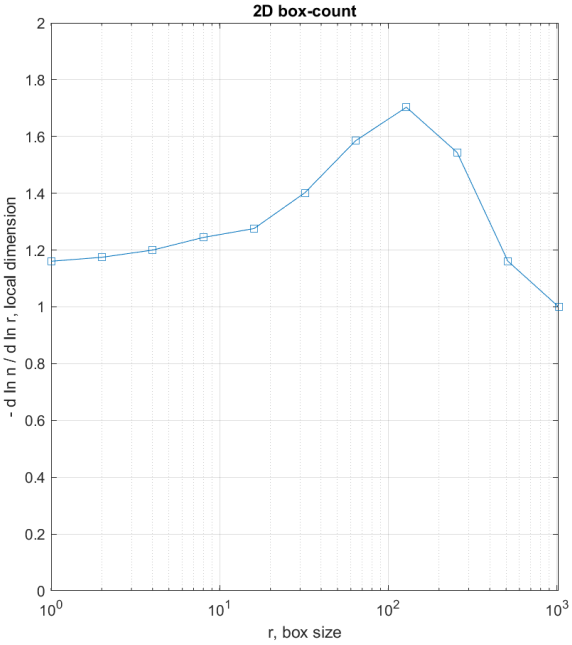

(c) Slope of "2003" scatter plot.

Figure 4.9: Semi-log plot of the local slope as a function of r for expert climber

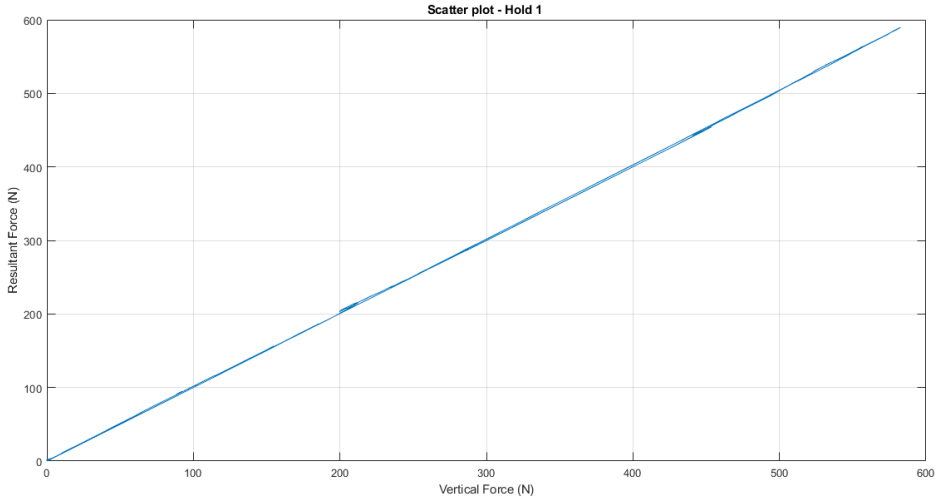

(a) Hold grasped by hands.

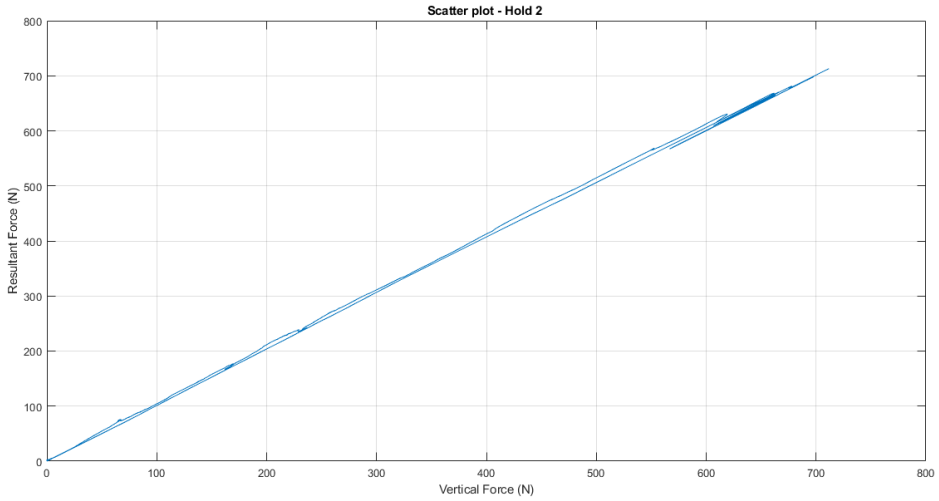

(b) Hold grasped by hands.

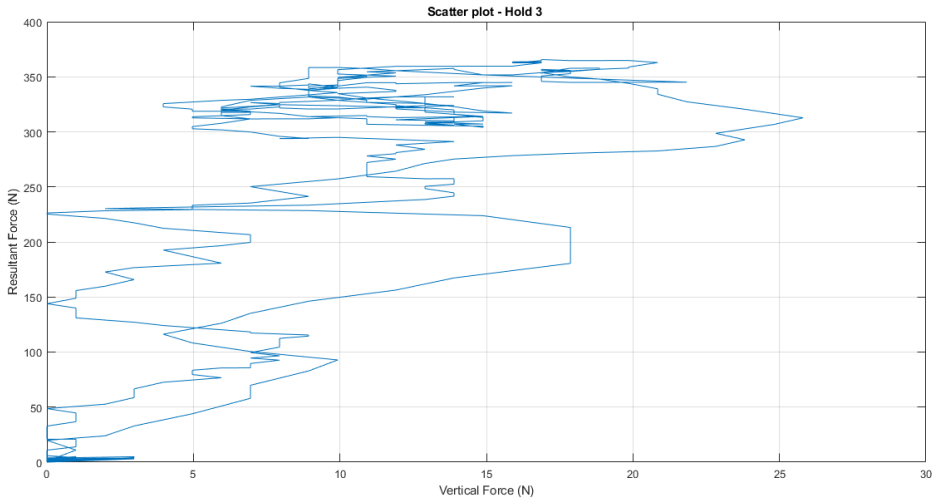

(c) Hold grasped by feet.

Figure 4.10: Scatter plot obtained from beginner climber.

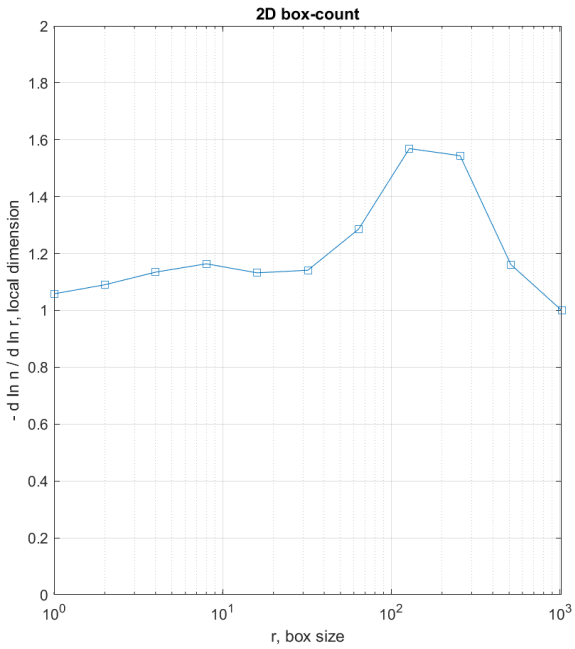

(a) Slope of "2001" scatter plot.

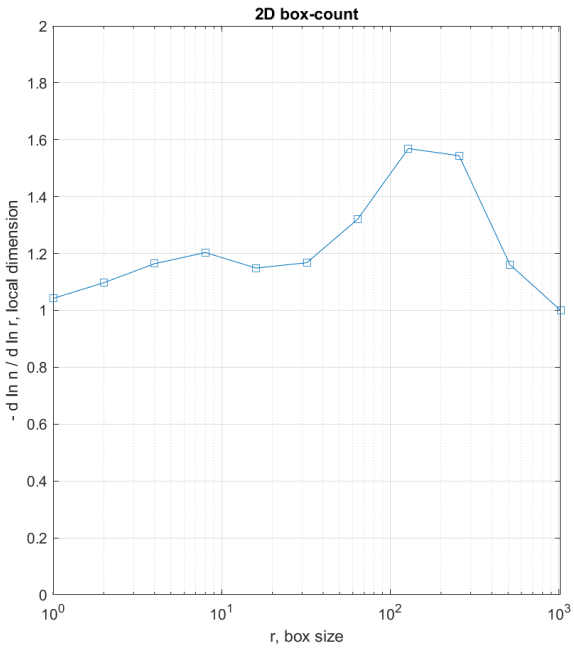

(b) Slope of "2002" scatter plot.

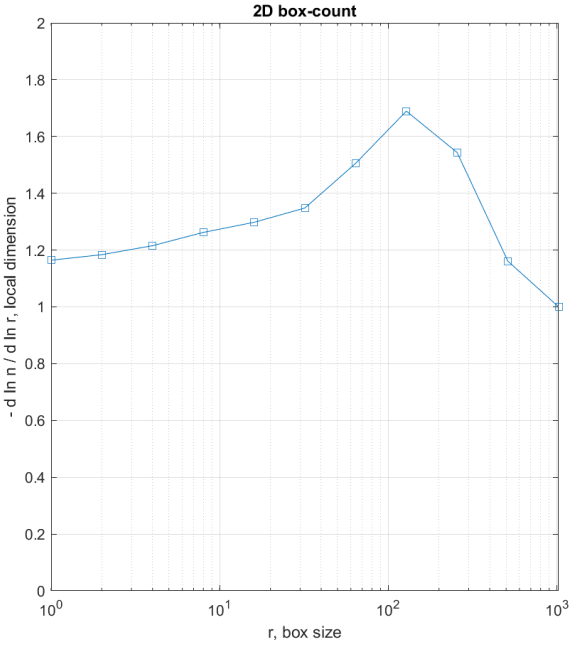

(c) Slope of "2003" scatter plot.

Figure 4.11: Semi-log plot of the local slope as a function of r for beginner climber

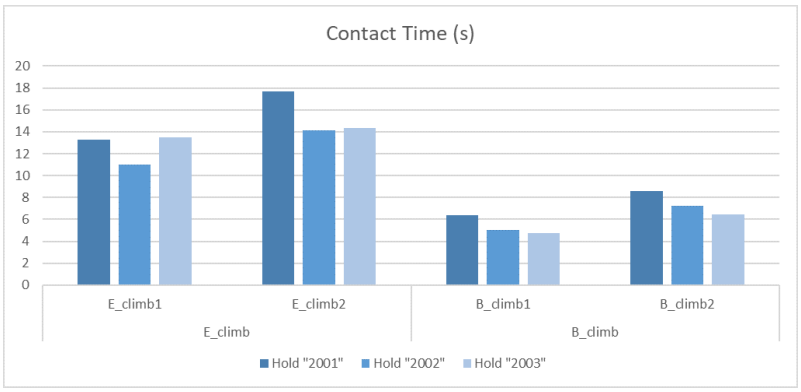

Figure 4.12: Contact time. Expert climber is denoted by "E_climb" and beginner climber by "B_climb". Contact times for each hold and for each subject record respectively are shown.

4.3 Smoothness Factor

4.3.1 Theoretical introduction

Studies conducted [45] propose some other parameters in order to describe mechanical measures of climbing performance as also suggests the shared climbing experience. In addition to the geometric entropy measurement proposed on previous section, an index concerning application force smoothness can be extrapolated from resultant force signal. An experienced climber charges the hold as smoothly as possible: he just grabs hold and shifts fluidly to following hold. Thus, the more expertise a climber, the better the smoothness factor.

4.3.2 Computation

As previous explained on chapter 4.2.2 on page 62, even for smoothness factor the calculation script has been written in Matlab® and it is reported in appendix A.2 on page 85. Script needs ".xlsx" file as input and starts correcting axes orientation, because some holds have inverted axes and they weren't correctly oriented (line 25). After the following orientation matrix calculation (line 32), data extraction for each hold was elaborated (line 39). In these code lines there was implemented the axes correction, there was extracted x, y and z components and there was estimated the resultant force applied for each hold. Computing was executed instant by instant, thus for each output file line. Then, subject body weight are requested in order to calculate the following final factor (line 81) and the phase concerning the actual smoothness factor calculation starts. Firstly, the real signal segment contained the climber application interval is extracted for each hold (line 110), then contact time T (line 116) was retrieved and resultant force impulse J is executed by a trapezoidal numerical integration (line 126). Then parabolic curve (line 131) for each hold is estimated following equation reported below:

$$F_{\mathrm{t}} = \left[\frac{t}{T} - \left(\frac{t}{T}\right)^2\right]\left(\frac{6J}{T}\right) \tag{4.10}$$

Moreover, absolute difference between resultant force and parabolic curve (line

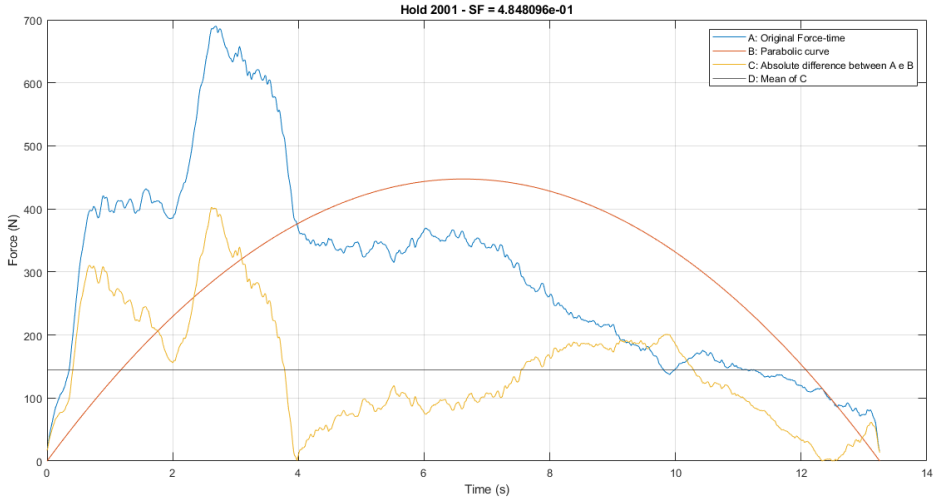

(a) Hold grasped by hands.

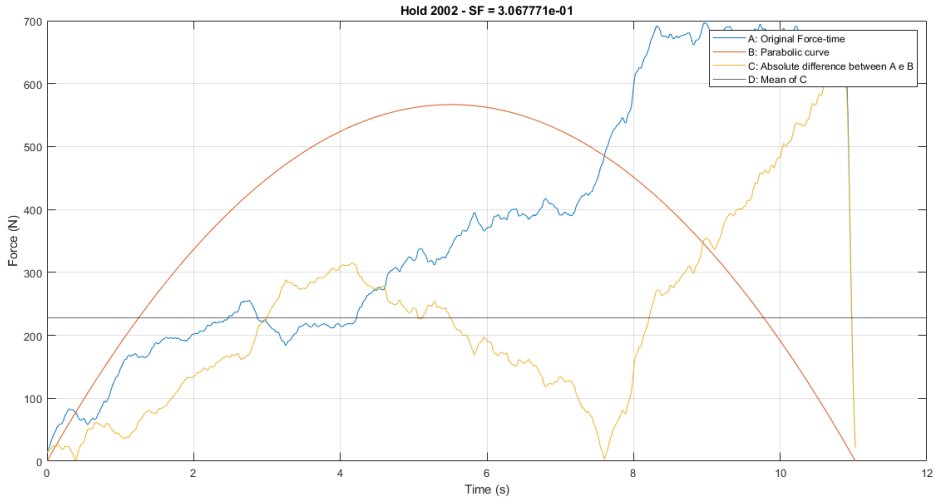

(b) Hold grasped by hands.

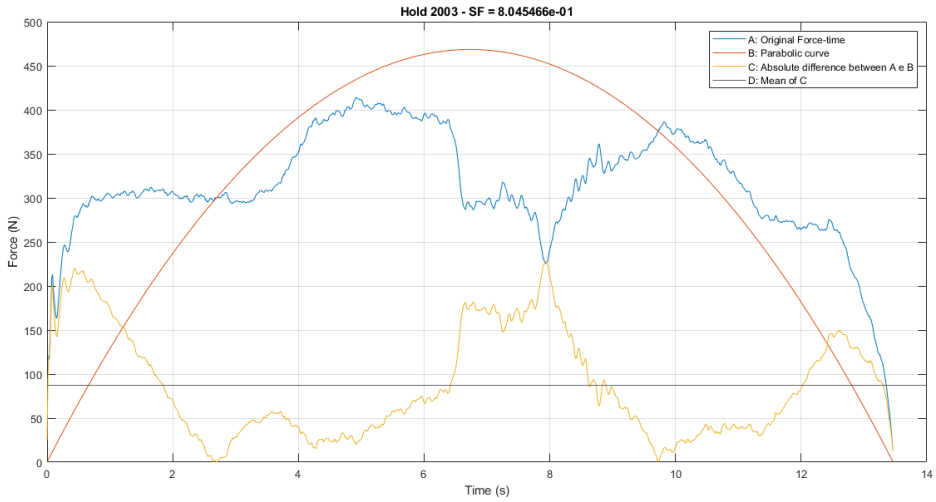

(c) Hold grasped by feet.

Figure 4.13: Smoothness factor for expert climber.

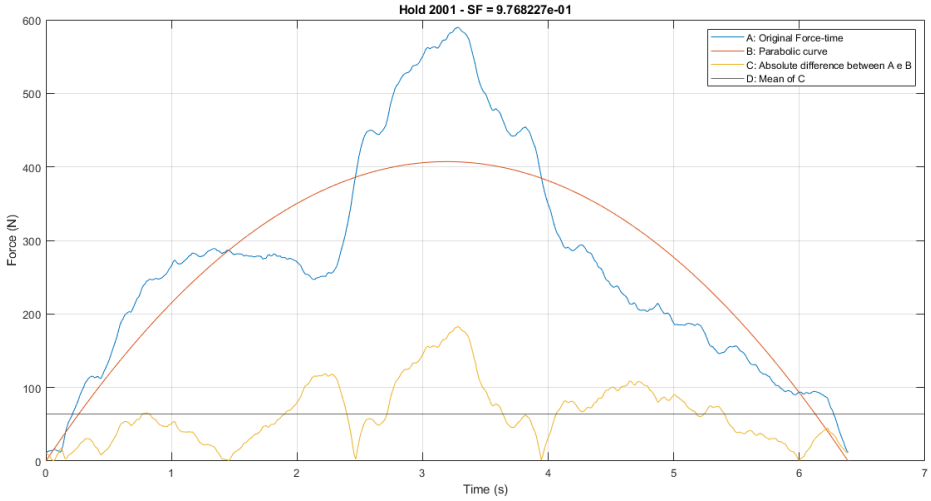

(a) Hold grasped by hands.

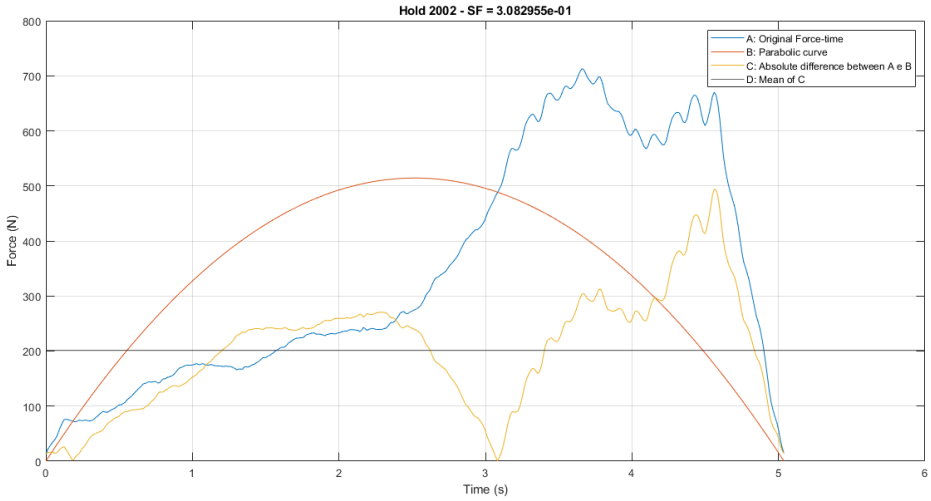

(b) Hold grasped by hands.

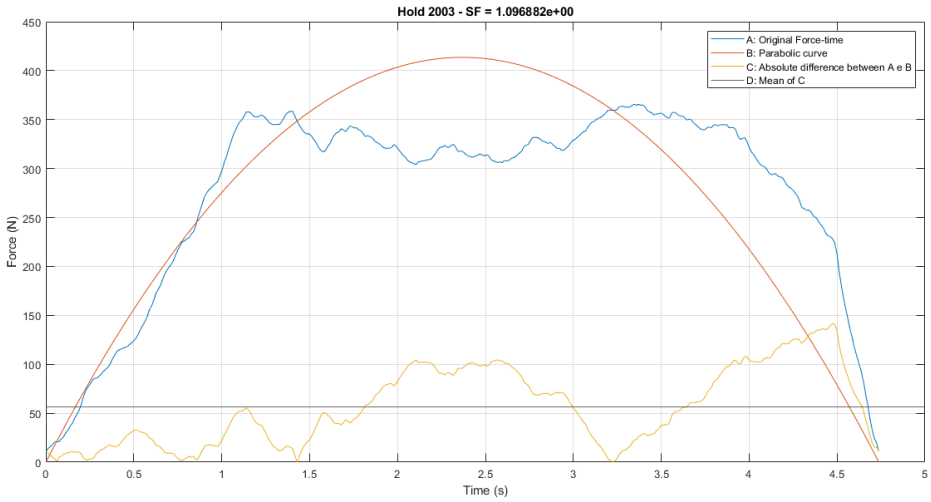

(c) Hold grasped by feet.

Figure 4.14: Smoothness factor for beginner climber.

137) and its mean value was calculated. Finally, smoothness factor was found as the ratio between climber body weight and absolute difference mean value.

4.3.3 Results

For a better comprehension of all preceding steps refer to figures on pages 69 and 70, where are reported the three smoothness factor calculated for each hold and for the two subjects respectively. Each graph shows all the processes executed up to smoothness factor calculation which is figured by a straight line parallel to the abscissas. Finally, on bar diagram on figure 4.15 (p. 71) are reported smoothness factor obtained on each hold and for each subject acquisition.

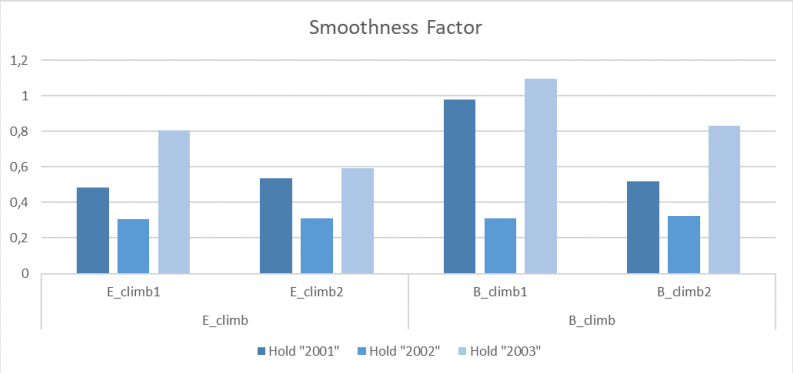

Figure 4.15: Smoothness factor comparison among each execution. Expert climber is denoted by "E_climb" and beginner climber by "B_climb".

For both subjects, can be always noticed a reduction comparing the two holds grasped by hands, in particular continuing on performed exercise, thus passing from the first hold (hold "2001") to the second one (hold "2002").

In addition, resultant force impulse was investigated and its values are indicated on bar diagram reported on figure 4.16 (p. 71). Moreover, in order to evaluate it objectively between the two subjects, it was normalized to the corresponding climber body weight and these values are shown on figure 4.17 (p. 72). It is remarkable that expert climber shows higher impulse values related to the beginner one, even if a standardized trend between subjects can't be observed among the different holds.

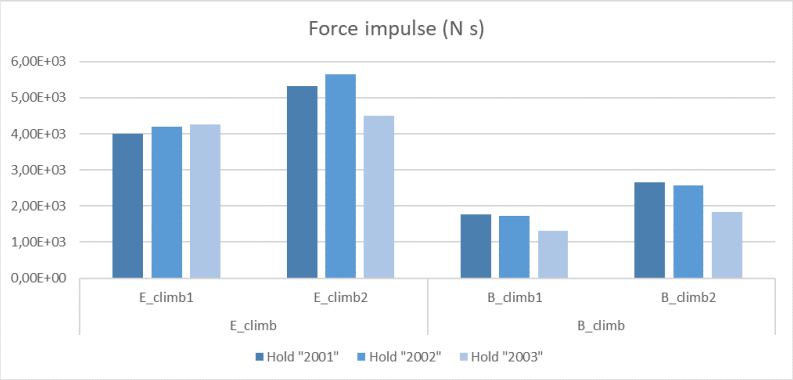

Figure 4.16: Resultant force impulse. Expert climber is denoted by "E_climb" and beginner climber by "B_climb".

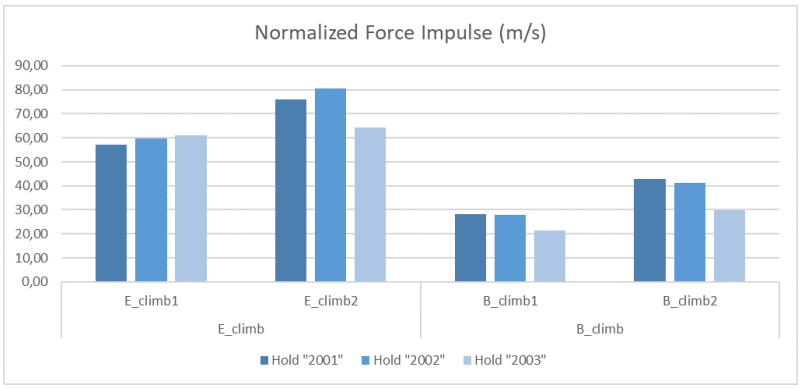

Figure 4.17: Normalized resultant force impulse. Expert climber is denoted by "E_climb" and beginner climber by "B_climb".

4.4 Friction coefficient

4.4.1 Theoretical introduction

As reported on chapter 2.4.6, an estimation concerning the amount of force component useful to climbing path prosecution was carried out. It corresponds to ratio of tangential to normal force, where the first represent the motion advantageous component, which in current case (see fig. 4.6 on p. 60) coincides with the resultant between Y component and Z component, and the second one is related to force quantity used by the athlete in a route not optimal direction and corresponds to Z component. Hence, it was calculated as in equation 4.11 and it was weighted to resultant force.

$$FC = \left(\frac{\sqrt{F_Y^2 + F_Z^2}}{|F_X|} \right) \tag{4.11}$$

$$FC_{\text{weighted}} = \frac{FC}{\sqrt{F_X^2 + F_Y^2 + F_Z^2}} \tag{4.12}$$

Since an expert climber has the ability to use most of its power upon ascent's useful directions and to avoid energy expenditure on other directions, it can be considered as a performance evaluation index. Thus, a good performance in indoor climbing has greater forces exchanged tangentially to the wall than forces exchanged orthogonally.

4.4.2 Computation

As previous stated in chapter 4.3.2 on page 68, even Friction coefficient calculation was executed on Matlab® and script is reported in appendix A.3 on page 90. Script needs ".xlsx" file as input and starts correcting axes orientation(line 25) and computing orientation matrix (line 32), until data extraction for each hold elaboration (line 39). In these code lines there was implemented the axes correction, there was extracted x, y and z components and there was estimated the resultant force applied on each hold. Computing was executed instant by instant,thus for each output file line. Suddenly, samples concerning the actual contact time was extracted (line 96) and rows containing "Inf" elements were deleted. This element type results from

executed ratio on line 73, when denominator, i.e. force along x axis , is zero. Finally, mean and maximum values was calculated for each hold and and they was averaged over the whole climber performance.

4.4.3 Results

The resulting values averaged on entire performed exercise and specific for each hold are shown on bar diagrams reported on figure 4.18. It is evident that a significant difference marks friction coefficients obtained on holds used by hands (fig. 4.18a) from numbers obtained on the unique hold loaded by feet (fig. 4.18b). Conclusions carried out on preceding researches [45], according to which an efficient climbing style is characterized by high friction coefficient values, are confirmed just for the hold used by lower limbs. While, on holds used by upper limbs, the suggests trend is found just for the beginner climber contrarily to the expert one.

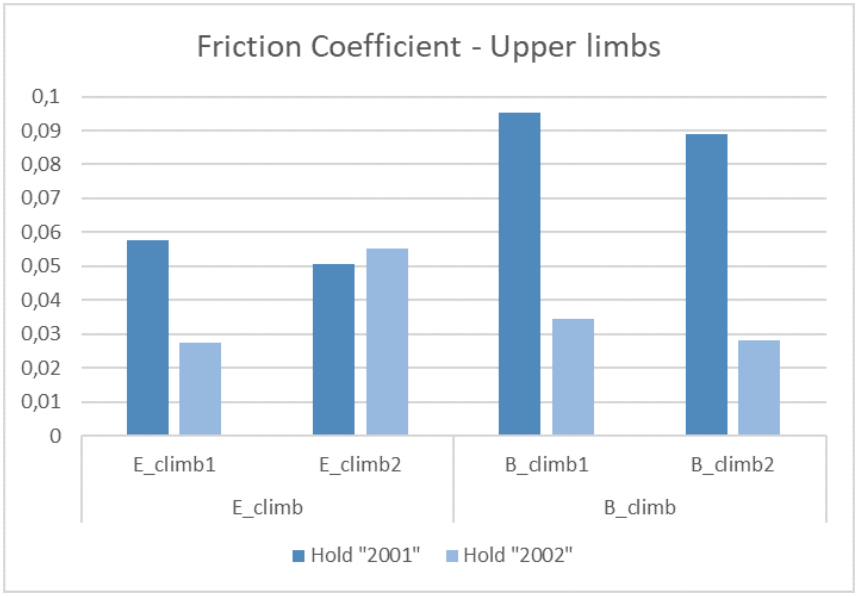

(a) Holds grasped by hands.

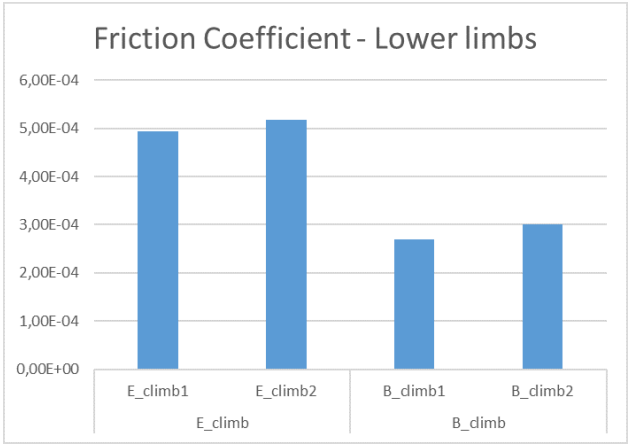

(b) Hold "2003", grasped by feet.

Figure 4.18: Friction coefficients obtained. Data are categorized in two groups, i.e. the two exercise repetition, for each subject.

According previously explained in the chapter 2.4.6, greater friction coefficient

values was found for hold used by hands than those grasped by feet. This confirms the body centre of mass distance from the wall. This great difference between upper and lower limbs values could describes a beginner climber but in current case *A_climb* represents an expert one. The higher climbing level of *A_climb* subject can be explained by the smaller difference between hands and foot friction coefficients than difference in *M_climb* subject.

4.5 Results

Obtained results for the three calculated indexes will now reported. Concerning *Hausdorff Dimension*, two distinct values were obtained: about 1.2 for both holds grasped by hands and about 1.6 for the hold used by feet. These two values were found to be the same for both climbers.

Regarding instead *Smoothness Factor* values, they turned out to be equal to 0.50 for expert climber and equal to 0.67 for the beginner one. Values have been obtained by averaging, for each subject, the 6 (2 for each hold) obtained.

Lastly, *Friction coefficient* values will be illustrated dividing them between foot values and hands values. For the first, $5.05*10^{-04}$ was found for the expert climber and $2{,}85*10^{-04}$ for the beginner one. These values have been obtained by averaging, for each subject, the 2 (1 for each hold) coefficient obtained. While, the seconds were equal to 0,048 for the expert climber and equal to 0,062 for the beginner one. Lasts values have been obtained by averaging, for each subject, the 4 (2 for each hold) coefficient obtained.

Chapter 5

GUI

In order to have a visual idea about data recorded by each wall hold, a graphical representation of data recorded was developed.
Force and mass variations during the performed exercise for each hold used by the athlete will be shown.
Furthermore, with the aim of making representation easy to perform, a graphical user interface was developed and all the functions needed were integrated into it. In such a way an intuitive and usable execution mode on a large scale is provided.

5.1 Introduction

The output file explained on chapter 3.3.2 gives just a numerical conception about data recorded but visualizing them can be very useful for better understand holds functioning and performance, as well as providing a quick forces trend representation in order to better understand climber movement during time.

For this reason, it was decided to implement a window capable of representing the detected resultant force trend for each individual hold and the consequent mass measurement. The code was developed in Python object oriented language using "Tkinter", which represents one of the most used libraries for the graphical interface implementation using Python programming language. The choice to develop a graphical interface was carried out in order to make the viewing process easier, intuitive and repeatable by any user who will find himself working with such instrumentation in the future.

The code necessary for the purpose is articulated into two scripts: one contains the graphical interface layout and the arising actions from each buttons activation and the second one includes all the functions that have to be perform in order to elaborate data contained in output file and visualize them. Practically, the first one represents the *Front - end* code program and will be described on following chapter 5.2 and the second one corresponds to the *Back - end* code side and will be explained on chapter 5.3.

5.2 Front - end

The graphical interface, which layout is shown on figure 5.1 and its relative code is reported on appendix A.4 on page 94, allows user to make the necessary choices for the type of representation who wants to obtained. Basically, user must do two choices: the first inherent to the number of files to be displayed and the second one related to representing data relating to a single hold or not. The input data must be in *.txt* format.

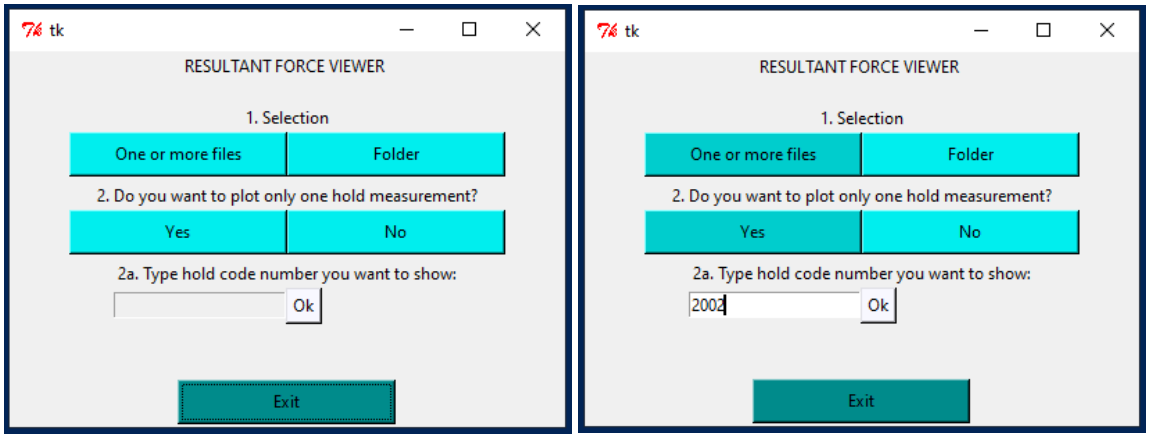

(a) Graphical user interface layout.

(b) GUI post "more files" selection.

Figure 5.1: GUI different details.

As far as the first selection is concerned, possible choices are:

- "One or more files" buttons allows to chose one or more than one file for the subsequent visualizing;
- "Folder" buttons executed a sort of batch-mode which generate an illustration for each file contained into selected folder.

The user is then asked to choose whether represent the acquisition data for a single specific hold (see figure 5.2) or for all connected holds (see figure 5.3). This choice must be made using the "Yes" or "No" buttons.

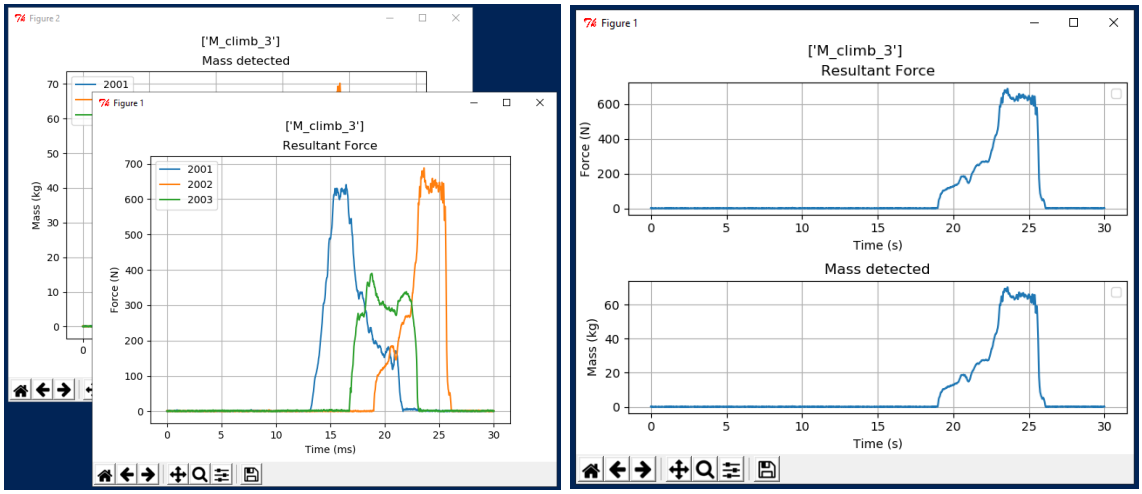

(a) All the holds acquisitions showed. (b) Just one hold acquisition showed.

Figure 5.2: Final representations with one input file.

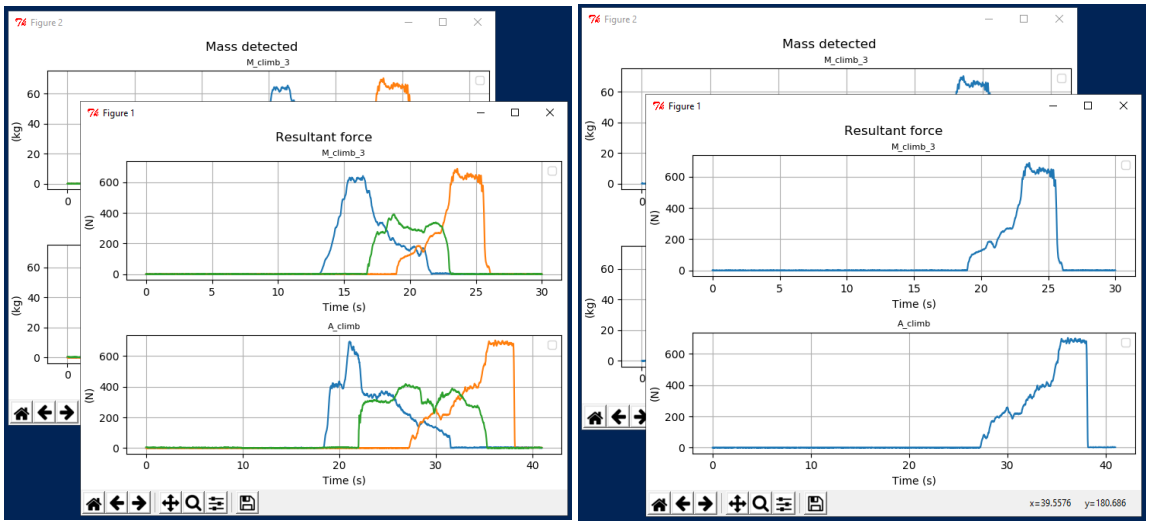

(a) All the holds acquisitions showed. (b) Just one hold acquisition showed.

Figure 5.3: Final representations with more than one input files.

Clicking on the "yes" button, widget in which the user must enter the name of the hold to be displayed is enabled allowing user typing the hold identification numeric code. This returns a single representation, if only one file has been before selected, or multiple representations, each containing only the selected hold, if multiple files or an entire folder have been chosen. The name to be inserted in the input widget

(see figure 5.1b) corresponds to the hold identification numeric code which appears to be contained in the first column of output file, which was previously explained in chapter 3.3.2.

On the other hand, if all the holds acquisitions have to be represented, "No" button must by clicked. Even here a single representation is generated, if only one file has been previously selected, or more representations, if multiple files or an entire folder were chosen.

To terminate and close the interface, the user can click on the "Exit" button.

5.3 Back - end

All the back-end side processes are contained into *GUI_functions.py* script, which are reported in appendix A.5 on page 100. It can be considered a list of functions useful for the acquired raw data processing in order to transform them into a format suitable for their visualization. The developed functions are explained in detail in the next lines and they were integrated into GUI button (A.4).

- *read_folder*: takes path folder as input (line 99 on A.4) and return a list containing the folder files reading (*files_read*) and a list containing their file name (*files_name*);
- *read_file*: takes the split list containing chosen files names (just one if a single file is chose) (line 83 on A.4) and return a list containing the reading files (*files_read*) and a list containing their file name (*files_name*);
- *total_force_mass*: takes the two preceding functions output (*files_read* and *files_name*) as input, calculates resultant force and mass for each line and returns, as well as the files name (*files_name_passed*), a list of lists, called *summary_tot*, in which every line is made as follow: *[hold_serial_number, resultant_force, mass]*;
- *force_mass_extraction*: functions that, taken last two outputs (*summary_tot* and *files_name_passed*) as input, extracts data for each hold and return the forces and mass data divided for each hold. Current functions was developed based on the actual number of holds used;
- *select_hold*: receive the forces and mass data specific for each hold, files name list and hold identification numeric code, which are asked to the user by the *entry* widget, and returns just data about hold selected;
- *represent_single*: visualizing actions when one file is selected and all the three holds signals want to be shown;
- *represent_single_selected*: representing actions when one file is selected and just one hold signal wants to be shown;
- *represent_multi*: functions for representing all the three holds signals for more than one file;
- *represent_multi_selected*: functions for representing just one holds signal extracted from more than one selected file.

Chapter 6

Conclusions

This work was thought as a preliminary study concerning performance evaluation in indoor sport climbing, since subjects available to conduct analysis do not constitute a statistically significant samples and a wider climbing wall is necessary for conducting a complete climbing performance analysis and better understand how the chosen indexes vary on a wider temporal window.

As previous reported, calibration process reveals an overall noise threshold about 1 N averaged among the three holds. The better accuracy was found on "2002" hold and the worse one in terms of accuracy appears to be "2001" hold. This noise value, although not particularly low, is consistent among the acquisitions made and therefore is an indicator of reliability in the measurements even if are not highly accurate. Thus, even if is not particularly low, it can be a good trade-off between costs and expected measure result.

Performed exercise, although sufficient enough for a preliminary analysis, reflects the limited size of the wall used. In view of an improved research, a higher climbing wall may be needed in order to avoid that the vertical force totally influences the resulting force on the grips grasped by the hands. In this way, climber will overstep the hold and will performs a more realistic movement.

As described above, obtained results for the three calculated indexes show a particularly marked difference trend between hold grasped by foot and those used by hands. Some difference are shown between expert and beginner climber and results are now shown in detail.
Concerning *Hausdorff Dimension*, two distinct values were obtained: about 1.2 for both holds grasped by hands and about 1.6 for the hold used by feet. These two values were found to be the same for both climbers.
Regarding instead *Smoothness Factor* values, they turned out to be equal to 0.50 for expert climber and equal to 0.67 for the beginner one. Values have been obtained by averaging, for each subject, the 6 (2 for each hold) obtained.
Lastly, *Friction coefficient* values will be illustrated dividing them between foot values and hands values. For the first, $5.05*10^{-04}$ was found for the expert climber and $2{,}85*10^{-04}$ for the beginner one. These values have been obtained by averaging, for each subject, the 2 (1 for each hold) coefficient obtained. While, the seconds were equal to 0,048 for the expert climber and equal to 0,062 for the beginner one. Lasts values have been obtained by averaging, for each subject, the 4 (2 for each hold) coefficient obtained.

Literature shows that an efficient climbing style is distinguished by a greater

lower limbs use than that made by a beginner one. Thus, found differences in the three calculated indexes between holds used by hands and foot can be considered as a starter point for carrying out an investigation in this direction.

In order to achieve very strong statistically significant effect, a number of subjects as large as possible should be necessary. Moreover, with a view to assessing performance between expert and beginner climbers, the group should consist of both these types of climbers. This make it possible to perform statistical analysis using statistical software package, such as Stata ®.

Concerning graphical user interface, it can be considered as a beginning step for a fuller and more detailed interface. At the moment it allow to perform just representation actions concerning the signal of resultant force in time but, in the future, it may include a performance parameter evaluation section, which can be obtained integrating Matlab scripts developed on it.

Appendix A

Code Listings

A.1 Hausdorff Dimension Calculation

```
clear all
close all
clc

%% Load acquisition file
[file,path]=uigetfile('*.xlsx','Load acquisition file');
filename_pos=sprintf('%s%s',path,file);
content = readmatrix(filename_pos);
num_holds = length(unique(content(:,1)));

%% Initialization

h1 = 1;
h2 = h1;
h3 = h1;

hold1=[];
hold2=[];
hold3=[];

force_mat_h1 = [];
force_mat_h2 = [];
force_mat_h3 = [];

%% Correct orientation (optional)
% Some holds might have inverted axes and may not be
    correctly oriented
% Second and third colomns must be positive and first
    colomn must be negative
axis_mat_h1 = [1 -1 1];
axis_mat_h2 = [-1 -1 1];
axis_mat_h3 = [1 -1 1];

```

```
32 %% Rotation matrix calculation
33 alpha = deg2rad(0); % X axis rotation angle
34 gamma = deg2rad(7); % Y axis rotation angle
35 x_rotation = [1 0 0; 0 cos(alpha) -sin(alpha); 0 sin(
       alpha) cos(alpha)];
36 y_rotation = [cos(gamma) 0 sin(gamma); 0 1 0; -sin(gamma)
        0 cos(gamma)];
37 rot_mat = x_rotation .* y_rotation;
38
39 %% Data extraction for each hold
40 for i=1:length(content)
41     if content(i,1) == 2001
42         % Data extraction
43         hold1(h1,:) = [content(i,2), content(i,3),
               content(i,4)];
44         % Correct orientation
45         hold1(h1,:) = hold1(h1,:) .* axis_mat_h1;
46         % X, Y and Z components
47         force_mat_h1(h1,1:3) = rot_mat * [hold1(h1,2)
               hold1(h1,3) hold1(h1,1)].';
48         % Resultant force
49         force_mat_h1(h1,4) = sqrt((force_mat_h1(h1,1).^2)
               +(force_mat_h1(h1,2).^2)+(force_mat_h1(h1,3)
               .^2));
50         h1 = h1 + 1;
51     elseif content(i,1) == 2002
52         % Swapping second and third columns
53         save2 = content(i,2);
54         content(i,2) = content(i,3);
55         content(i,3) = save2;
56         % Data extraction
57         hold2(h2,:) = [content(i,2), content(i,3),
               content(i,4)];
58         % Correct orientation
59         hold2(h2,:) = hold2(h2,:) .* axis_mat_h2;
60         % X, Y and Z components
61         force_mat_h2(h2,1:3) = rot_mat * [hold2(h2,2)
               hold2(h2,3) hold2(h2,1)].';
62         % Resultant force
63         force_mat_h2(h2,4) = sqrt((force_mat_h2(h2,1).^2)
               +(force_mat_h2(h2,2).^2)+(force_mat_h2(h2,3)
               .^2));
64         h2 = h2 + 1;
65     elseif content(i,1) == 2003
66         % Data extraction
67         hold3(h3,:) = [content(i,2), content(i,3),
               content(i,4)];
68         % Correct orientation
```

```
69          hold3(h3,:) = hold3(h3,:) .* axis_mat_h3;
70          % X, Y and Z components
71          force_mat_h3(h3,1:3) = rot_mat * [hold3(h3,2)
               hold3(h3,3) hold3(h3,1)].';
72          % Resultant force
73          force_mat_h3(h3,4) = sqrt((force_mat_h3(h3,1).^2)
               +(force_mat_h3(h3,2).^2)+(force_mat_h3(h3,3)
               .^2));
74          h3 = h3 + 1;
75      end
76  end
77
78  %% Hausdorff Dimension
79
80  % 3D matrix creation
81  force_mat = cat(3, force_mat_h1, force_mat_h2,
       force_mat_h3);
82
83  % Scatter plot creation
84  newpath = fullfile(pwd,'Scatterplot - Total');
85  mkdir(newpath);
86  for t=1:num_holds
87      fig=figure(2*t-1)
88      scatter_plot(t)=plot(abs(force_mat(:,3,t)),force_mat
           (:,4,t));
89      title(sprintf('Scatter plot - Hold %d ', t))
90      xlabel('Vertical Force (N)')
91      ylabel('Resultant Force (N)')
92      grid on
93      filename=sprintf('scatter_plot_tot%d.png',t);
94      saveas(fig,fullfile(newpath,filename),'png');
95      scatter_frame(t)=getframe(fig);
96
97      % Convert RGB Scatter plot to Gray Double Scatter
           plot
98      scatter_gray(:,:,t) = rgb2gray(scatter_frame(t).cdata
           );
99      scatter_double(:,:,t) = imbinarize(scatter_gray(:,:,t
           ));
100     scatter_complement(:,:,t) = imcomplement(
           scatter_double(:,:,t));
101
102     % Hausdorff dimension
103     [n(t,:), r(t,:)] = boxcount(scatter_complement(:,:,t)
           );
104
105     figure(2*t)
106     subplot(1,2,1)
```

```
107         boxcount(scatter_complement(:,:,t),'plot')
108         grid on
109         subplot(1,2,2)
110         boxcount(scatter_complement(:,:,t),'slope')
111         grid on
112         sgtitle(sprintf('Hold %d ', t))
113     end
```

A.2 Smoothness Factor Calculation

```
clear all
close all
clc

%% Load acquisition file
[file,path]=uigetfile('*.xlsx','Load acquisition file');
filename_pos=sprintf('%s%s',path,file);
content = readmatrix(filename_pos);
num_holds = length(unique(content(:,1)));

%% Initialization

h1 = 1;
h2 = h1;
h3 = h1;

hold1=[];
hold2=[];
hold3=[];

force_mat_h1 = [];
force_mat_h2 = [];
force_mat_h3 = [];

%% Correct orientation (optional)
% Some holds might have inverted axes and may not be
    correctly oriented
% Second and third colomns must be positive and first
    colomn must be negative
axis_mat_h1 = [1 -1 1];
axis_mat_h2 = [-1 -1 1];
axis_mat_h3 = [1 -1 1];

%% Rotation matrix calculation
alpha = deg2rad(0); % X axis rotation angle
gamma = deg2rad(7); % Y axis rotation angle
x_rotation = [1 0 0; 0 cos(alpha) -sin(alpha); 0 sin(
    alpha) cos(alpha)];
y_rotation = [cos(gamma) 0 sin(gamma); 0 1 0; -sin(gamma)
     0 cos(gamma)];
rot_mat = x_rotation .* y_rotation;

%% Data extraction for each hold
for i=1:length(content)
    if content(i,1) == 2001
        % Data extraction
```

```
43          hold1(h1,:) = [content(i,2), content(i,3),
                content(i,4)];
44          % Correct orientation
45          hold1(h1,:) = hold1(h1,:) .* axis_mat_h1;
46          % X, Y and Z components
47          force_mat_h1(h1,1:3) = rot_mat * [hold1(h1,2)
                hold1(h1,3) hold1(h1,1)].';
48          % Resultant force
49          force_mat_h1(h1,4) = sqrt((force_mat_h1(h1,1).^2)
                +(force_mat_h1(h1,2).^2)+(force_mat_h1(h1,3)
                .^2));
50          h1 = h1 + 1;
51      elseif content(i,1) == 2002
52          % Swapping second and third columns
53          save2 = content(i,2);
54          content(i,2) = content(i,3);
55          content(i,3) = save2;
56          % Data extraction
57          hold2(h2,:) = [content(i,2), content(i,3),
                content(i,4)];
58          % Correct orientation
59          hold2(h2,:) = hold2(h2,:) .* axis_mat_h2;
60          % X, Y and Z components
61          force_mat_h2(h2,1:3) = rot_mat * [hold2(h2,2)
                hold2(h2,3) hold2(h2,1)].';
62          % Resultant force
63          force_mat_h2(h2,4) = sqrt((force_mat_h2(h2,1).^2)
                +(force_mat_h2(h2,2).^2)+(force_mat_h2(h2,3)
                .^2));
64          h2 = h2 + 1;
65      elseif content(i,1) == 2003
66          % Data extraction
67          hold3(h3,:) = [content(i,2), content(i,3),
                content(i,4)];
68          % Correct orientation
69          hold3(h3,:) = hold3(h3,:) .* axis_mat_h3;
70          % X, Y and Z components
71          force_mat_h3(h3,1:3) = rot_mat * [hold3(h3,2)
                hold3(h3,3) hold3(h3,1)].';
72          % Resultant force
73          force_mat_h3(h3,4) = sqrt((force_mat_h3(h3,1).^2)
                +(force_mat_h3(h3,2).^2)+(force_mat_h3(h3,3)
                .^2));
74          h3 = h3 + 1;
75      end
76  end
77
78  % 3D matrix creation
```

```
79 force_mat = cat(3, force_mat_h1, force_mat_h2,
       force_mat_h3);
80
81 % Body weight request
82 prompt = 'Type your body weight... ';
83 body_weight = input(prompt);
84
85 %Force_mat Dimensions
86 [time_step, force_type, num_holds] = size(force_mat);
87
88 %Time series creation
89 Fs = 80; %Hz
90 Ts = 1/Fs;
91 time = linspace(0,Ts*time_step,time_step);
92
93 % Resultant force - Time plot
94 newpath = fullfile(pwd,'Smoothness_Factor');
95 mkdir(newpath);
96 for t=1:num_holds
97     fig=figure(t)
98     scatter_plot(t)=plot(time,force_mat(:,4,t));
99     title(sprintf('Resultant Force - Hold %d ', t))
100    xlabel('Time')
101    ylabel('Resultant Force')
102    filename=sprintf('resultant_force_plot_%d.png',t);
103    saveas(fig,fullfile(newpath,filename),'png');
104 end
105
106 % Calculation of force signal maximum and minumum peaks
107 F_max = max(max(force_mat(:,4,:), 3));
108 F_min = min(min(force_mat(:,4,:), 3));
109
110 %% Samples extraction
111 % Contact-time steps number extraction
112 contact_force_mat_h1 = force_mat_h1((force_mat_h1(:,4)
       >10),4);
113 contact_force_mat_h2 = force_mat_h2((force_mat_h2(:,4)
       >10),4);
114 contact_force_mat_h3 = force_mat_h3((force_mat_h3(:,4)
       >10),4);
115
116 % Time to contact for each hold
117 T1 = length(contact_force_mat_h1).*Ts;
118 T2 = length(contact_force_mat_h2).*Ts;
119 T3 = length(contact_force_mat_h3).*Ts;
120
121 % Time series in contact time for each hold
122 time1 = linspace(0,T1,length(contact_force_mat_h1));
```

```
123 time2 = linspace(0,T2,length(contact_force_mat_h2));
124 time3 = linspace(0,T3,length(contact_force_mat_h3));
125
126 % Force impulse
127 J_1=trapz(time1, contact_force_mat_h1);
128 J_2=trapz(time2, contact_force_mat_h2);
129 J_3=trapz(time3, contact_force_mat_h3);
130
131 % Parabolic curve equation
132 Ft_1 = ((time1./T1)-(time1./T1).^2).*((6*J_1)./T1);
133 Ft_1 = Ft_1.';
134 Ft_2 = ((time2./T2)-(time2./T2).^2).*((6*J_2)./T2);
135 Ft_2 = Ft_2.';
136 Ft_3 = ((time3./T3)-(time3./T3).^2).*((6*J_3)./T3);
137 Ft_3 = Ft_3.';
138
139 % Absolute difference between Resultant force and
      Parabolic curve equation
140 c1 = abs(Ft_1 - contact_force_mat_h1);
141 c2 = abs(Ft_2 - contact_force_mat_h2);
142 c3 = abs(Ft_3 - contact_force_mat_h3);
143
144 % Absolute difference mean
145 d1 = mean(c1);
146 d2 = mean(c2);
147 d3 = mean(c3);
148
149 % Smoothness Factor
150 SF_1 = body_weight ./ d1;
151 SF_2 = body_weight ./ d2;
152 SF_3 = body_weight ./ d3;
153
154 % Generate figure
155 figure
156 plot(time1,contact_force_mat_h1)
157 hold on
158 plot(time1,Ft_1)
159 hold on
160 plot(time1,c1)
161 hold on
162 yline(d1)
163 title(sprintf('Hold 2001 - SF = %d', SF_1))
164 grid on
165 ylabel('Force (N)')
166 xlabel('Time (s)')
167 legend('A: Original Force-time','B: Parabolic curve','C:
      Absolute difference between A e B','D: Mean of C')
168
```

```
169 figure
170 plot(time2,contact_force_mat_h2)
171 hold on
172 plot(time2,Ft_2)
173 hold on
174 plot(time2,c2)
175 hold on
176 yline(d2)
177 title(sprintf('Hold 2002 - SF = %d', SF_2))
178 grid on
179 ylabel('Force (N)')
180 xlabel('Time (s)')
181 legend('A: Original Force-time','B: Parabolic curve','C:
    Absolute difference between A e B','D: Mean of C')
182
183 figure
184 plot(time3,contact_force_mat_h3)
185 hold on
186 plot(time3,Ft_3)
187 hold on
188 plot(time3,c3)
189 hold on
190 yline(d3)
191 title(sprintf('Hold 2003 - SF = %d', SF_3))
192 grid on
193 ylabel('Force (N)')
194 xlabel('Time (s)')
195 legend('A: Original Force-time','B: Parabolic curve','C:
    Absolute difference between A e B','D: Mean of C')
```

A.3 Friction Coefficient Calculation

```
clear all
close all
clc

%% Load acquisition file
[file,path]=uigetfile('*.xlsx','Load acquisition file');
filename_pos=sprintf('%s%s',path,file);
content = readmatrix(filename_pos);
num_holds = length(unique(content(:,1)));

%% Initialization

h1 = 1;
h2 = h1;
h3 = h1;

hold1=[];
hold2=[];
hold3=[];

force_mat_h1 = [];
force_mat_h2 = [];
force_mat_h3 = [];

%% Correct orientation (optional)
% Some holds might have inverted axes and may not be
    correctly oriented
% Second and third colomns must be positive and first
    colomn must be negative
axis_mat_h1 = [1 -1 1];
axis_mat_h2 = [-1 -1 1];
axis_mat_h3 = [1 -1 1];

%% Rotation matrix calculation
alpha = deg2rad(0); % X axis rotation angle
gamma = deg2rad(7); % Y axis rotation angle
x_rotation = [1 0 0; 0 cos(alpha) -sin(alpha); 0 sin(
    alpha) cos(alpha)];
y_rotation = [cos(gamma) 0 sin(gamma); 0 1 0; -sin(gamma)
     0 cos(gamma)];
rot_mat = x_rotation .* y_rotation;

%% Data extraction for each hold
for i=1:length(content)
    if content(i,1) == 2001
        % Data extraction
```

```
43          hold1(h1,:) = [content(i,2), content(i,3),
                content(i,4)];
44          % Correct orientation
45          hold1(h1,:) = hold1(h1,:) .* axis_mat_h1;
46          % X, Y and Z components
47          force_mat_h1(h1,1:3) = rot_mat * [hold1(h1,2)
                hold1(h1,3) hold1(h1,1)].';
48          % Resultant force
49          force_mat_h1(h1,4) = sqrt((force_mat_h1(h1,1).^2)
                +(force_mat_h1(h1,2).^2)+(force_mat_h1(h1,3)
                .^2));
50          % Tangential force
51          force_mat_h1(h1,5) = sqrt((force_mat_h1(h1,2).^2)
                +(force_mat_h1(h1,3).^2));
52          % Friction Coefficient
53          force_mat_h1(h1,6) = force_mat_h1(h1,5)./abs(
                force_mat_h1(h1,1));
54          % Weighted Friction Coefficient
55          force_mat_h1(h1,7) = force_mat_h1(h1,6)./
                force_mat_h1(h1,4);
56          h1 = h1 + 1;
57      elseif content(i,1) == 2002
58          % Swapping second and third columns
59          save2 = content(i,2);
60          content(i,2) = content(i,3);
61          content(i,3) = save2;
62          % Data extraction
63          hold2(h2,:) = [content(i,2), content(i,3),
                content(i,4)];
64          % Correct orientation
65          hold2(h2,:) = hold2(h2,:) .* axis_mat_h2;
66          % X, Y and Z components
67          force_mat_h2(h2,1:3) = rot_mat * [hold2(h2,2)
                hold2(h2,3) hold2(h2,1)].';
68          % Resultant force
69          force_mat_h2(h2,4) = sqrt((force_mat_h2(h2,1).^2)
                +(force_mat_h2(h2,2).^2)+(force_mat_h2(h2,3)
                .^2));
70          % Tangential force
71          force_mat_h2(h2,5) = sqrt((force_mat_h2(h2,2).^2)
                +(force_mat_h2(h2,3).^2));
72          % Friction Coefficient
73          force_mat_h2(h2,6) = force_mat_h2(h2,5)./abs(
                force_mat_h2(h2,1));
74          % Weighted Friction Coefficient
75          force_mat_h2(h2,7) = force_mat_h2(h2,6)./
                force_mat_h2(h2,4);
76          h2 = h2 + 1;
```

```
77      elseif content(i,1) == 2003
78          % Data extraction
79          hold3(h3,:) = [content(i,2), content(i,3),
                content(i,4)];
80          % Correct orientation
81          hold3(h3,:) = hold3(h3,:) .* axis_mat_h3;
82          % X, Y and Z components
83          force_mat_h3(h3,1:3) = rot_mat * [hold3(h3,2)
                hold3(h3,3) hold3(h3,1)].';
84          % Resultant force
85          force_mat_h3(h3,4) = sqrt((force_mat_h3(h3,1).^2)
                +(force_mat_h3(h3,2).^2)+(force_mat_h3(h3,3)
                .^2));
86          % Tangential force
87          force_mat_h3(h3,5) = sqrt((force_mat_h3(h3,2).^2)
                +(force_mat_h3(h3,3).^2));
88          % Friction Coefficient
89          force_mat_h3(h3,6) = force_mat_h3(h3,5)./abs(
                force_mat_h3(h3,1));
90          % Weighted Friction Coefficient
91          force_mat_h3(h3,7) = force_mat_h3(h3,6)./
                force_mat_h3(h3,4);
92          h3 = h3 + 1;
93      end
94  end
95
96  %% Samples extraction
97  % Contact-time steps number extraction
98  contact_force_mat_h1 = force_mat_h1((force_mat_h1(:,4)
        >10),:);
99  contact_force_mat_h2 = force_mat_h2((force_mat_h2(:,4)
        >10),:);
100 contact_force_mat_h3 = force_mat_h3((force_mat_h3(:,4)
        >10),:);
101
102 % Delete rows with Inf element
103 contact_force_mat_h1(any(isinf(contact_force_mat_h1),2)
        ,:) = [];
104 contact_force_mat_h2(any(isinf(contact_force_mat_h2),2)
        ,:) = [];
105 contact_force_mat_h3(any(isinf(contact_force_mat_h3),2)
        ,:) = [];
106
107 %% Mean and MAX Friction coefficient for each hold
108 % Hold 2001
109 MAX_FC_1 = max(contact_force_mat_h1);
110 mean_FC_1 = mean(contact_force_mat_h1);
111
```

```
112 % Hold 2002
113 MAX_FC_2 = max(contact_force_mat_h2);
114 mean_FC_2 = mean(contact_force_mat_h2);
115
116 % Hold 2003
117 MAX_FC_3 = max(contact_force_mat_h3);
118 mean_FC_3 = mean(contact_force_mat_h3);
119
120 % 3D matrices creation
121 MAX_FC = cat(1, MAX_FC_1, MAX_FC_2, MAX_FC_3);
122 mean_FC = cat(1, mean_FC_1, mean_FC_2, mean_FC_3);
123
124 %% Mean and MAX Friction coefficient avereged over total
        performance
125 MAX_performance = mean(MAX_FC);
126 mean_performance = mean(mean_FC);
```

A.4 Graphical User Interface

```
1  from Tkinter import *
2  import tkFileDialog
3  import GUI_functions
4  class MyApp:
5
6          def __init__(self, parent):
7                  #------ constants for controlling layout
                       ------
8                  button_width = 19
9
10                 button_padx = "2m"
11                 button_pady = "1m"
12
13                 buttons_frame_padx =  "1m"
14                 buttons_frame_pady =  "2m"
15                 buttons_frame_ipadx = "3m"
16                 buttons_frame_ipady = "1m"
17                 #---------------- end constants
                       ----------------
18
19                 self.myParent = parent
20
21                 self.myContainer1 = Frame(parent)
22                 self.myContainer1.pack(expand=YES, fill=
                       BOTH)
23                 myMessage="RESULTANT FORCE VIEWER \n"
24                 Label(self.myContainer1, text=myMessage,
                       justify=CENTER).pack(side=TOP, anchor=
                       CENTER)
25
26                 self.buttons_frame = Frame(self.
                       myContainer1)
27                 self.buttons_frame.pack(side=TOP, expand=
                       YES)
28                 Label(self.buttons_frame, text = "1. 
                       Selection", justify=CENTER).pack(side=
                       TOP, anchor=CENTER)
29
30                 self.buttons_frame_sel = Frame(self.
                       myContainer1)
31                 self.buttons_frame_sel.pack(side=TOP,
                       expand=YES)
32                 Label(self.buttons_frame_sel, text = "2. 
                       Do you want to plot only one hold 
                       measurement?", justify=CENTER).pack(
                       side=TOP, anchor=CENTER)
```

```
33
34                  self.entry_frame= Frame(self.myContainer1
                        )
35                  self.entry_frame.pack(side=TOP, expand =
                        YES)
36                  Label(self.entry_frame, text = "2a. Type
                        hold code number you want to show:",
                        justify=CENTER).pack(side=TOP, anchor=
                        CENTER)
37
38                  self.buttons_exit= Frame(self.
                        myContainer1)
39                  self.buttons_exit.pack(side=BOTTOM,
                        expand = YES)
40                  Label(self.buttons_exit, text = "\n",
                        justify=CENTER).pack(side=TOP, anchor=
                        CENTER)
41
42                  self.button1 = Button(self.buttons_frame,
                         command=self.button1Click)
43                  self.button1.configure(text="One or more
                        files", width=button_width, padx=
                        button_padx, pady=button_pady,
                        background = "cyan2")
44                  self.button1.focus_force()
45                  self.button1.pack(side=LEFT)
46
47                  self.button3 = Button(self.buttons_frame,
                         command=self.button3Click)
48                  self.button3.configure(text="Folder",
                        width=button_width, padx=button_padx,
                        pady=button_pady)
49                  self.button3.focus_force()
50                  self.button3.configure(width=button_width
                        , padx=button_padx, pady=button_pady,
                        background = "cyan2")
51                  self.button3.pack(side=LEFT)
52
53                  self.button5 = Button(self.
                        buttons_frame_sel, command=self.
                        button5Click)
54                  self.button5.configure(text="Yes")
55                  self.button5.focus_force()
56                  self.button5.configure(width=button_width
                        , padx=button_padx, pady=button_pady,
                        background = "cyan2")
57                  self.button5.pack(side=LEFT)
58
```

```
59                  self.button6 = Button(self.
                        buttons_frame_sel, command=self.
                        button6Click)
60                  self.button6.configure(text="No")
61                  self.button6.focus_force()
62                  self.button6.configure(width=button_width
                        , padx=button_padx, pady=button_pady,
                        background = "cyan2")
63                  self.button6.pack(side=LEFT)
64
65                  self.entry1 = Entry(self.entry_frame,
                        width = 20, state=DISABLED)
66                  self.entry1.pack(side = LEFT)
67
68                  self.button7 = Button(self.entry_frame,
                        command=self.button7Click)
69                  self.button7.configure(text="Ok")
70                  self.button7.focus_force()
71                  self.button7.configure(background = "
                        ghostwhite")
72                  self.button7.pack(side=LEFT)
73
74                  self.button4 = Button(self.buttons_exit,
                        command=self.button4Click)
75                  self.button4.configure(text="Exit")
76                  self.button4.focus_force()
77                  self.button4.configure(width=button_width
                        , padx=button_padx, pady=button_pady,
                        background = "cyan4")
78                  self.button4.pack(side=RIGHT)
79
80          def button1Click(self):          # One or more
                files selected
81                  if self.button1["background"] == "cyan2":
82                          self.button1["background"] = "
                                cyan3"
83                          self.file_list = tkFileDialog.
                                askopenfilenames(parent=root,
                                title='Choose one or more
                                files')
84                          self.file_list = root.tk.
                                splitlist(self.file_list)
85                          self.file_list_passed, self.
                                file_name_passed =
                                GUI_functions.read_file(self.
                                file_list)
86                          if len(self.file_list_passed) ==
                                1:
```

```
87                                  self.plot_flag = 1      # Only one file selected
88                              else:
89                                  self.plot_flag = 2      # More than one file selected
90                              self.summary_passed, self.file_name_passed = GUI_functions.total_force_mass(self.file_list_passed, self.file_name_passed)
91                              self.f1, self.f2, self.f3, self.m1, self.m2, self.m3, self.file_name_passed = GUI_functions.force_mass_extraction(self.summary_passed, self.file_name_passed)
92                      else:
93                              self.button1["background"] = "cyan2"
94
95          def button3Click(self):         # Folder selected
96                  if self.button3["background"] == "cyan2":
97                              self.button3["background"] = "cyan3"
98                              self.plot_flag = 2              # More files selected
99                              self.path = tkFileDialog.askdirectory(title='Select folder')
100                             self.file_list_passed, self.file_name_passed = GUI_functions.read_folder(self.path)
101                             self.summary_passed, self.file_name_passed = GUI_functions.total_force_mass(self.file_list_passed, self.file_name_passed)
102                             self.f1, self.f2, self.f3, self.m1, self.m2, self.m3, self.file_name_passed = GUI_functions.force_mass_extraction(self.summary_passed, self.file_name_passed)
```

```
103                 else:
104                         self.button3["background"] = "
                                cyan2"
105
106         def button5Click(self):             # YES
107                 if self.button5["background"] == "cyan2":
108                         self.button5["background"] = "
                                cyan3"
109                         self.entry1.configure(state =
                                NORMAL)
110                 else:
111                         self.button5["background"] = "
                                cyan2"
112
113         def button6Click(self):             #NO
114                 if self.button6["background"] == "cyan2":
115                         self.button6["background"] = "
                                cyan3"
116                         if self.plot_flag == 1:
117                                 GUI_functions.
                                        represent_single(self.
                                        f1, self.f2, self.f3,
                                        self.m1, self.m2, self
                                        .m3, self.
                                        file_name_passed)
118                                 del self.plot_flag
119                         elif self.plot_flag == 2:
120                                 GUI_functions.
                                        represent_multi(self.
                                        f1, self.f2, self.f3,
                                        self.m1, self.m2, self
                                        .m3, self.
                                        file_name_passed)
121                                 del self.plot_flag
122                 else:
123                         self.button6["background"] = "
                                cyan2"
124
125         def button4Click(self):
126                 self.myParent.destroy()
127
128         def button7Click(self):             # Ok
129                 self.hold_user = self.entry1.get()
130                 self.hold_user = int(self.hold_user)
131                 self.entry1.delete(0, 'end')
132                 self.f_s, self.m_s, self.
                        file_name_passed_s = GUI_functions.
                        select_hold(self.f1, self.f2, self.f3,
```

```
                        self.m1, self.m2, self.m3, self.
                        file_name_passed, self.hold_user)
133                 if self.plot_flag == 1:
134                         GUI_functions.
                                represent_single_selected(self
                                .f_s, self.m_s, self.
                                file_name_passed_s)
135                 elif self.plot_flag == 2:
136                         GUI_functions.
                                represent_multi_selected(self.
                                f_s, self.m_s, self.
                                file_name_passed_s)
137                 del self.plot_flag
138
139 root = Tk()
140 root.geometry("400x270")
141 myapp = MyApp(root)
142 root.mainloop()
```

A.5 Graphical User Interface - Functions

```
1  import os
2  import glob
3  import math
4  import matplotlib.pyplot as plt
5  import numpy as np
6  from Tkinter import *
7  import tkFileDialog
8
9  def read_folder(path_passed):
10     path_passed = path_passed + "\*.txt"
11     file_list = glob.glob(path_passed)
12     file_list = [str(item) for item in file_list] #list
          of string indicating names of all files contained
          in the folder selected
13     files_name = []
14     files_read = [] #list of list containing files
          reading
15     for file in file_list:
16         base = os.path.basename(file)
17         name = os.path.splitext(base)[0]
18         files_name.append(name)
19         f = open(file, 'r')
20         line = f.readlines()
21         files_read.append(line)
22         f.close()
23     return files_read, files_name
24
25 def read_file(file_list_passed):
26     file_list_passed = list(file_list_passed)
27     file_list_passed = [str(item) for item in
          file_list_passed] #list of string indicating names
           of files selected
28     files_name = []
29     file_read = [] #list of list containing files reading
30     for file in file_list_passed:
31         # File name extraction and saving from path name
32         base = os.path.basename(file)
33         name = os.path.splitext(base)[0]
34         files_name.append(name)
35         # File openinig
36         f = open(file, 'r')
37         line = f.readlines()
38         file_read.append(line)
39         f.close()
40     return file_read, files_name
41
```

```
42 def total_force_mass(file_list_passed, file_name_passed):
43 # Calculate resultant force and mass for each line and
       return a list of lists in which every line is made up
       as follow: [hold_serial_number, resultant_force, mass]
44     summary = [[] for _ in range(len(file_list_passed))]
45     summary_tot = []
46     for c in range(len(file_list_passed)):
47         for hold in range(len(file_list_passed[c])):
48             new_line = file_list_passed[c][hold].split(",
                   ")
49             hold = new_line[0]
50             force_time = new_line[1]
51             force_time = force_time.split("\t")
52             force = (int(force_time[1]), int(force_time
                   [2]), int(force_time[3]))
53             force_tot_line = math.sqrt(pow(force[0],2) +
                   pow(force[1],2) + pow(force[2],2))
54             kg_line = force_tot_line / 9.8
55             line = hold + "\t" + str(force_tot_line) + "\
                   t" + str(kg_line)
56             line = line.split("\t")
57             line = [int(line[0]), float(line[1]), float(
                   line[2])]
58             summary[c].append(line)
59         summary_tot.append(summary[c])
60     return summary_tot, file_name_passed
61
62 def force_mass_extraction(summary_passed,
       file_name_passed):
63 #   Function developed based on the actual number of
       using holds
64 #   Modify it if you use more than 3 holds paying
       attention to the hold serial number (In this case:
       "2001", "2002", "2003").
65     force_2001 = [[] for _ in range(len(summary_passed))]
66     force_2001_tot = []
67     force_2002 = [[] for _ in range(len(summary_passed))]
68     force_2002_tot = []
69     force_2003 = [[] for _ in range(len(summary_passed))]
70     force_2003_tot = []
71     mass_2001 = [[] for _ in range(len(summary_passed))]
72     mass_2001_tot = []
73     mass_2002 = [[] for _ in range(len(summary_passed))]
74     mass_2002_tot = []
75     mass_2003 = [[] for _ in range(len(summary_passed))]
76     mass_2003_tot = []
77     for c in range(len(summary_passed)):
78         for hold in range(len(summary_passed[c])):
```

```
79                 if summary_passed[c][hold][0] == 2001:
80                     force_2001[c].append(summary_passed[c][
                           hold][1])
81                     mass_2001[c].append(summary_passed[c][
                           hold][2])
82                 elif summary_passed[c][hold][0] == 2002:
83                     force_2002[c].append(summary_passed[c][
                           hold][1])
84                     mass_2002[c].append(summary_passed[c][
                           hold][2])
85                 elif summary_passed[c][hold][0] == 2003:
86                     force_2003[c].append(summary_passed[c][
                           hold][1])
87                     mass_2003[c].append(summary_passed[c][
                           hold][2])
88             force_2001_tot.append(force_2001[c])
89             force_2002_tot.append(force_2002[c])
90             force_2003_tot.append(force_2003[c])
91             mass_2001_tot.append(mass_2001[c])
92             mass_2002_tot.append(mass_2002[c])
93             mass_2003_tot.append(mass_2003[c])
94
95         return force_2001_tot, force_2002_tot, force_2003_tot
               , mass_2001_tot, mass_2002_tot, mass_2003_tot,
               file_name_passed
96
97 def select_hold(force_2001_tot_passed,
       force_2002_tot_passed, force_2003_tot_passed,
       mass_2001_tot_passed, mass_2002_tot_passed,
       mass_2003_tot_passed, file_name_passed,
       hold_user_passed):
98 # Function to select the hold data that you have chosen
       to view
99     if hold_user_passed == 2001:
100        return force_2001_tot_passed,
               mass_2001_tot_passed, file_name_passed
101    elif hold_user_passed == 2002:
102        return force_2002_tot_passed,
               mass_2002_tot_passed, file_name_passed
103    elif hold_user_passed == 2003:
104        return force_2003_tot_passed,
               mass_2003_tot_passed, file_name_passed
105
106 def represent_single(force_2001_tot_passed,
       force_2002_tot_passed, force_2003_tot_passed,
       mass_2001_tot_passed, mass_2002_tot_passed,
       mass_2003_tot_passed, file_name_passed):
107 # Function for represent all the three holds signals for
```

```
        just one file
108
109     f1_time = np.linspace(0, round(len(
            force_2001_tot_passed[0])/80), num=len(
            force_2001_tot_passed[0]))
110     f2_time = np.linspace(0, round(len(
            force_2002_tot_passed[0])/80), num=len(
            force_2002_tot_passed[0]))
111     f3_time = np.linspace(0, round(len(
            force_2003_tot_passed[0])/80), num=len(
            force_2003_tot_passed[0]))
112
113     m1_time = np.linspace(0, round(len(
            mass_2001_tot_passed[0])/80), num=len(
            force_2001_tot_passed[0]))
114     m2_time = np.linspace(0, round(len(
            mass_2002_tot_passed[0])/80), num=len(
            force_2002_tot_passed[0]))
115     m3_time = np.linspace(0, round(len(
            mass_2003_tot_passed[0])/80), num=len(
            force_2003_tot_passed[0]))
116
117     figf, axesf = plt.subplots()
118     figf.suptitle(file_name_passed)
119     axesf.plot(f1_time, force_2001_tot_passed[0], label='
            2001')
120     axesf.plot(f2_time, force_2002_tot_passed[0], label='
            2002')
121     axesf.plot(f3_time, force_2003_tot_passed[0], label='
            2003')
122     axesf.set_title('Resultant Force')
123     axesf.set_xlabel('Time (ms)')
124     axesf.set_ylabel('Force (N)')
125     axesf.legend()
126     axesf.grid(True)
127
128     figm, axesm = plt.subplots()
129     figm.suptitle(file_name_passed)
130     axesm.plot(mass_2001_tot_passed[0], label='2001')
131     axesm.plot(mass_2002_tot_passed[0], label='2002')
132     axesm.plot(mass_2003_tot_passed[0], label='2003')
133     axesm.set_title('Mass detected')
134     axesm.set_xlabel('Time (s)')
135     axesm.set_ylabel('Mass (kg)')
136     axesm.legend()
137     axesm.grid(True)
138
139     plt.show()
```

```
140
141 def represent_single_selected(force_tot_passed,
        mass_tot_passed, file_name_passed):
142 # Function for represent just one hold signal extracted
        from a single chosen file
143
144     f_time = np.linspace(0, round(len(force_tot_passed
            [0])/80), num=len(force_tot_passed[0]))
145
146     m_time = np.linspace(0, round(len(mass_tot_passed[0])
            /80), num=len(mass_tot_passed[0]))
147
148     fig, axes = plt.subplots(2, 1, constrained_layout=
            True)
149     axes[0].plot(f_time, force_tot_passed[0])
150     axes[0].set_title('Resultant Force')
151     axes[0].set_xlabel('Time (s)')
152     axes[0].set_ylabel('Force (N)')
153     axes[0].legend()
154     axes[0].grid(True)
155     fig.suptitle(file_name_passed)
156
157     axes[1].plot(m_time, mass_tot_passed[0])
158     axes[1].set_title('Mass detected')
159     axes[1].set_xlabel('Time (s)')
160     axes[1].set_ylabel('Mass (kg)')
161     axes[1].legend()
162     axes[1].grid(True)
163     plt.show()
164
165 def represent_multi(force_2001_tot_passed,
        force_2002_tot_passed, force_2003_tot_passed,
        mass_2001_tot_passed, mass_2002_tot_passed,
        mass_2003_tot_passed, file_name_passed):
166 # Function for represent all the three holds signals for
        more than one file
167
168     nrows = len(force_2001_tot_passed)
169     figf, axesf = plt.subplots(nrows, 1, sharey = True,
            constrained_layout=True)
170     figm, axesm = plt.subplots(nrows, 1, sharey = True,
            constrained_layout=True)
171     f = 0
172     for row in axesf:
173
174         f1_time = np.linspace(0, round(len(
                force_2001_tot_passed[f])/80), num=len(
                force_2001_tot_passed[f]))
```

```
175             f2_time = np.linspace(0, round(len(
                    force_2002_tot_passed[f])/80), num=len(
                    force_2002_tot_passed[f]))
176             f3_time = np.linspace(0, round(len(
                    force_2003_tot_passed[f])/80), num=len(
                    force_2003_tot_passed[f]))
177
178             row.plot(f1_time, force_2001_tot_passed[f])
179             row.plot(f2_time, force_2002_tot_passed[f])
180             row.plot(f3_time, force_2003_tot_passed[f])
181             row.set_title(file_name_passed[f], fontsize=8)
182             row.set_xlabel('Time (s)')
183             row.set_ylabel('(N)')
184             row.legend()
185             row.grid(True)
186             f = f + 1
187         figf.suptitle('Resultant force')
188         m = 0
189         for row in axesm:
190
191             m1_time = np.linspace(0, round(len(
                    mass_2001_tot_passed[m])/80), num=len(
                    force_2001_tot_passed[m]))
192             m2_time = np.linspace(0, round(len(
                    mass_2002_tot_passed[m])/80), num=len(
                    force_2002_tot_passed[m]))
193             m3_time = np.linspace(0, round(len(
                    mass_2003_tot_passed[m])/80), num=len(
                    force_2003_tot_passed[m]))
194
195             row.plot(m1_time, mass_2001_tot_passed[m])
196             row.plot(m2_time, mass_2002_tot_passed[m])
197             row.plot(m3_time, mass_2003_tot_passed[m])
198             row.set_title(file_name_passed[m], fontsize=8)
199             row.set_xlabel('Time (s)')
200             row.set_ylabel('(kg)')
201             row.legend()
202             row.grid(True)
203             m = m + 1
204         figm.suptitle('Mass detected')
205         plt.show()
206
207 def represent_multi_selected(force_tot_passed,
        mass_tot_passed, file_name_passed):
208 # Function for represent just one hold signal extracted
        from each chosen files
209
210         nrows = len(force_tot_passed)
```

```
211     figf, axesf = plt.subplots(nrows, 1, sharey = True,
            constrained_layout=True)
212     figm, axesm = plt.subplots(nrows, 1, sharey = True,
            constrained_layout=True)
213     f = 0
214     for row in axesf:
215         f_time = np.linspace(0, round(len(
                force_tot_passed[f])/80), num=len(
                force_tot_passed[f]))
216         row.plot(f_time, force_tot_passed[f])
217         row.set_title(file_name_passed[f], fontsize=8)
218         row.set_xlabel('Time (s)')
219         row.set_ylabel('(N)')
220         row.legend()
221         row.grid(True)
222         f = f + 1
223     figf.suptitle('Resultant force')
224     m = 0
225     for row in axesm:
226         m_time = np.linspace(0, round(len(mass_tot_passed
                [m])/80), num=len(mass_tot_passed[m]))
227         row.plot(m_time, mass_tot_passed[m])
228         row.set_title(file_name_passed[m], fontsize=8)
229         row.set_xlabel('Time (s)')
230         row.set_ylabel('(kg)')
231         row.legend()
232         row.grid(True)
233         m = m + 1
234     figm.suptitle('Mass detected')
235     plt.show()
```

Bibliography

[1] Kevin Phillips, Joseph Sassaman, and James Smoliga. "Optimizing Rock Climbing Performance Through Sport-Specific Strength and Conditioning". In: *Strength and Conditioning Journal* 34 (June 2012), pp. 1–18. DOI: 10.1519/SSC.0b013e318255f012.

[2] J. Monroe Thorington. "The Story Of Mont Aiguille". In: (1965).

[3] Laura Amato. *Mont Blanc First Ascent: 5 Fast Facts You Need to Know*. Aug 8, 2015. URL: https://heavy.com/news/2015/08/mont-blanc-first-ascent-google-doodle-anniversary-august-8-1786-michel-gabriel-paccard-jacques-balmat/.

[4] *Storia dell'Arrampicata Sportiva*. URL: http://www.federclimb.it/l-arrampicata-sportiva/storia.html.

[5] *International Federation of Sport Climbing website*. URL: https://www.ifsc-climbing.org/index.php/about-us/key-figures.

[6] François Leonardon Tim Hatch. "IFSC Rules 2019". In: (March 2019).

[7] Marco Di Marco. *L'arrampicata sportiva tra Boulder, Speed e Lead*. July 10, 2019. URL: https://www.sciaremag.it/notiziesci/larrampicata-sportiva-tra-boulder-speed-e-lead/.

[8] *Sport Climbing*. December 1, 2018. URL: https://tokyo2020.org/en/games/sport/olympic/sport-climbing/.

[9] *Understanding Climbing Grades*. August 18, 2017. URL: https://sportrock.com/understanding-climbing-grades/.

[10] *UIAA Grades for Rock Climbing*. URL: https://www.theuiaa.org/mountaineering/uiaa-grades-for-rock-climbing/.

[11] Brad Lane. *The Yosemite Decimal System*. URL: https://blog.theclymb.com/out-there/the-yosemite-decimal-system/.

[12] Niall Grimes. *A brief explanation of UK traditional climbing grades*. February 28, 2016. URL: https://www.thebmc.co.uk/a-brief-explanation-of-uk-traditional-climbing-grades.

[13] *Guide To Climbing Grades: Everything You Need To Know*. URL: https://climbthatrock.com/climbing-grades-guide/.

[14] *Rock climbing grades*. URL: https://www.guidedolomiti.com/en/rock-climbing-grades/.

[15] Alex Beale. *Bouldering Grades: The Complete Guide*. URL: https://www.99boulders.com/bouldering-grades.

[16] Alexander de Bree. *Everything You Need to Know About Bouldering Grades*. September 10, 2019. URL: https://climbingblogger.com/bouldering-grades/.

[17] Alex Beale. *The Hardest Boulder Problems in the World*. URL: https://www.99boulders.com/hardest-boulder-problems.

[18] L. Martin F. Quaine. "A biomechanical study of equilibrium in sport rock climbing". In: *Gait and Posture 10* (1999).

[19] Whittaker A et al Grant S Hynes V. "Anthropometric,strength, endurance and flexibility characteristics of elite and recreational climbers". In: *J Sports Sci* (1996).

[20] Masaaki Sakamoto Daichi Asakawa. "Characteristics of counter-movements in sport climbing: a comparison between experienced climbers and beginners". In: *The Journal of Physical Therapy Science* (2019).

[21] Soňa Jandová Jiří Baláš Michaela Panáčková. "The Effect of Climbing Ability and Slope Inclination on Vertical Foot Loading Using a Novel Force Sensor Instrumentation System". In: *Journal of Human Kinetics* (2014).

[22] A W Sheel. "Physiology of sport rock climbing". In: *Br J Sports Med* (2004).

[23] Ansorge EJ O'Leary DS Augustyniak RA. "Muscle metaboreflex improves O_2 delivery to ischemic active skeletal muscle". In: *Am J Physiol* (1999).

[24] A K Lish et al. P B Watts L M Joubert. "Anthropometry of young competitive sport rock climbers". In: *Br J Sports Med* (2003).

[25] Phillip B. Watts. "Physiology of difficult rock climbing". In: *J Appl Physiol* (2004).

[26] Gebert W Werner I. "Blood lactate responses to competitive climbing". In: *The science of climbing and mountaineering* (2000).

[27] Ewa Sadowska-Krepa Artur Magiera Robert Roczniok. "Changes in Performance and Morning-Measured Responses in Sport Rock Climbers". In: *Journal of Human Kinetics* (2019).

[28] Busschaert B et al. Meeusen R Piacentini MF. "Hormonal responses in athletes: the use of a two bout exercise protocol to detect subtle differences in (over)training status." In: *Eur J Appl Physiol* (2004).

[29] Nassis GP Papacosta E. "Saliva as a tool for monitoring steroid, peptide and immune markers in sport and exercise science". In: *J Sci Med Sport* (2011).

[30] Haff GG Bompa TO. "Periodization. Theory and Methodology of Training". In: *Champaign: Human Kinetics* (2009).

[31] Ch Hill et al. John Booth Frank Marino. "Energy cost of sport climbing in elite performers". In: *British Journal of Sports Medicine* (1999).

[32] Energy system contributions in indoor rock climbing. "Bertuzzi, Franchini, Kokubun et al." In: *Eur J Appl Physiol* (2007).

[33] T. Muller M. Philippe D. Wegst. "Climbing-specific finger flexor performance and forearm muscle oxygenation in elite male and female sport climbers". In: *Eur J Appl. Physiology* (2011).

[34] Robert Hudek Andreas Schweizer. "Kinetics of Crimp and Slope Grip in Rock Climbing". In: *Journal of applied biomechanics* (2011).

[35] Fryer et al. "Forearm oxygenation and blood flow kinetics during a sustained contraction in multiple ability groups of rock climbers". In: *J Sports Sci* (2015).

[36] Andreas Schweizer. "Sport climbing from a medical point of view". In: *Swiss Medical Weekly* (2012).

[37] Rufibach K et al. Allenspach P Saupe N. "A. Radiological changes and signs of osteoarthritis in the fingers of male performance sport climbers". In: *J Sports Med Phys Fitness* (2011).

[38] Isabelle Schöffl Volker Rainer Schöffl. "Injuries to the Finger Flexor Pulley System". In: *The Journal of Hand Surgery* (2006).

[39] Serdar Arıtan M. Amca Laurent Vigouroux. "Effect of hold depth and grip technique on maximal finger forces in rock climbing". In: *Journal of Sports Sciences* (2012).

[40] T. Woodman et al. Xavier Sanchez M. Torregrossa. "Identification of Parameters That Predict Sport Climbing Performance". In: *Frontiers in Psychology* (2019).

[41] Douglas G. McIlwraith et al. Julien Pansiot Rachel C. King. "ClimBSN: Climber Performance Monitoring with BSN". In: (2008).

[42] F. Schena et al. F. Sibella I. Frosio. "3D analysis of the body center of mass in rock climbing". In: *Human Movement Science* (2007).

[43] Pierre LEGRENEUR. "Body mass center optimization in sport climbing". In: (2018).

[44] F.K. Fuss G. Niegl. "The fully instrumented climbing wall: performance analysis, route grading and vector diagrams - a preliminary studt". In: (2008).

[45] F.K. Fuss G. Niegl. "Instrumented climbing holds and performance analysis in sport climbing". In: *Sports Technology* (2009).

[46] F.K. Fuss G. Niegl. "The importance of friction between hand and hold in rock climbing". In: *Sports Technology* (2012).

[47] A. Colombo et al. R. Sesana D. Maffiodo. "Dispositivo sensorizzato di fissaggio di presa per arrampicata sportiva dotato di sensore di forza triassiale". Patent (IT). June 2019.

[48] Akihiro Kawamura Hitomi Iguma and Ryo Kurazume. "A New 3D Motion and Force Measurement System for Sport Climbing". In: ().

[49] Stefano Gabetti. "Instrumented Holds: Hardware Refinement and Software Development for the Quantitative Study of Sport Climbing". MA thesis. Politecnico di Torino, Sept. 2018.